THE INFLUENCE OF ANGULAR AND LINEAR ACCELERATION AND THERMAL STIMULATION ON THE HUMAN SEMICIRCULAR CANAL

by

ROBERT W. STEER, JR.

B.S., Merrimack College, 1960

S.M., Massachusetts Institute of Technology, 1963

SUBMITTED IN PARTIAL FULFILLMENT

OF THE REQUIREMENTS FOR THE

DEGREE OF DOCTOR OF SCIENCE

at the

MASSACHUSETTS INSTITUTE OF TECHNOLOGY

August 1967

Signature of Author _____

Department of Aeronautics and Astronautics, August 1967

Certified by _____

Thesis Supervisor

Certified by _____

Thesis Supervisor

Certified by _____

Thesis Supervisor

Certified by _____

Thesis Supervisor

Accepted by _____

Chairman, Departmental Committee on Graduate Students

THE INFLUENCE OF ANGULAR AND LINEAR ACCELERATION AND THERMAL STIMULATION ON THE HUMAN SEMICIRCULAR CANALS

by

Robert W. Steer, Jr.

Submitted to the Department of Aeronautics and Astronautics, Massachusetts Institute of Technology, on August 21, 1967, in partial fulfillment of the requirements for the degree of Doctor of Science.

ABSTRACT

The hydrodynamic properties of the human semicircular canal system were studied to determine its dynamic characteristics and their relationship to observed subjective and objective vestibular responses to various motion inputs. Four topics of particular importance in current vestibular research were examined in detail.

The density, coefficient of expansion, and viscosity of the labyrinthine fluids, endolymph and perilymph, have been measured to provide precise values for the coefficients of the dynamic models. A microviscometer was designed, built, calibrated, and used to measure the viscosity of 1-2 microliter samples of endolymph and perilymph. Density measurements were made via precision balance scales and accurate volume measurements and coefficients of expansion were made by microscopic measurements of the volume of the fluids at several temperatures.

The semicircular canal is modelled as a rigid torus of fluid, with the cupula acting as an elastic and viscous restraint. A system transfer function is evaluated for cupula displacement as a function of angular acceleration. It is shown that the cupula's effective inertia and viscous drag on the wall of the membranous labyrinth influence the dynamic performance of the system but do not resolve the disparity between previous

calculations of damping, which only considered hydrodynamic drag of endolymph in the canalicular duct, and experimentally measured damping coefficients.

Caloric stimulation of the vestibular apparatus is examined, and a model is proposed, based on the published measured time history of the temperature gradient across the lateral canal when the external auditory meatus is irrigated with water above or below body temperature. The presence of a thermal gradient across the lateral canal is shown to produce the physiological equivalent of an angular acceleration because of the torque which acts on the endolymph as a result of its thermal coefficient of expansion. Caloric experiments were performed which attest to the validity of the model.

The influence of linear acceleration on the semicircular canals was investigated. Human objective and subjective responses to rotation about a horizontal axis, to counter-rotation, and to stimulation by a rotating acceleration vector were examined. The observed responses of long duration nystagmus and continuous sensation of rotation are not in conformity with classical models of the vestibular system and there has developed a sizable body of experimental evidence which attributes a significant portion of these unusual responses to the semicircular canals. It is shown, through the distensibility of the canalicular duct under the influence of linear acceleration, that the observed bias component of nystagmus can be attributed to a first order nonlinearity of the semicircular canal dynamics. Experiments were performed on a centrifuge equipped with a rotating chair to show the relationship between the magnitude of the acceleration field, the rotation rate of the subject, and the slow phase velocity of vestibular nystagmus.

Thesis Supervisor: Laurence R. Young

Title: Associate Professor of Aeronautics and Astronautics

Thesis Supervisor: Yao Tzu Li

Title: Professor of Aeronautics and Astronautics

Thesis Supervisor: Erik L. Mollo-Christensen

Title: Professor of Meteorology

Thesis Supervisor: Jacob L. Meiry

Title: Assistant Professor of Aeronautics and Astronautics

TO MY WIFE

whose unbounded patience and forebearance
during the preparation of this
thesis and throughout my
doctoral program will always
be remembered and appreciated

ACKNOWLEDGMENTS

The author gratefully acknowledges the guidance, criticisms, and suggestions of his thesis committee, Professors L. R. Young, Y. T. Li, E. L. Mollo-Christensen, and J. L. Meiry, without whose assistance this thesis would have been impossible.

The author also expresses his special thanks to Dr. Alfred D. Weiss, Massachusetts General Hospital, for his advice and assistance in performing experiments for the Caloric Stimulation Model, and to Dr. Herbert Silverstein, formerly of the Massachusetts Eye and Ear Infirmary, for his advice and assistance in obtaining samples of cat and human endolymph and perilymph.

He is also grateful for the technical support provided by Mr. John Barley, Mr. John Buchanan and the staff at the M.I.T. Instrumentation Laboratory Special Test Facility, for the manuscript typing provided by Mrs. Damian J. Kulash, and for the students and staff who served as experimental subjects.

This research was supported by NASA Grant NGR 22-009-156.

TABLE OF CONTENTS

Chapter No.		Page No.
I	Introduction	1
	1.1 Objectives of the Research	2
	1.2 Application of the Research	8
II	The Anatomy and Physiology of the Human Vestibular System	10
	2.1 Gross Anatomical Description of the Vestibular System	10
	2.2 The Utricle and the Saccule	13
	2.3 The Semicircular Canals	15
	2.4 Nystagmus as a Measure of Vestibular Stimulation	24
III	The "Rigid Tube" Dynamic Characteristics of the Semicircular Canals	29
	3.1 Introduction	29
	3.2 A Physical Model of the Semicircular Canals	35
	3.3 The Hydrodynamic Drag of the Endolymph in the Membranous Canalicular Duct	38
	3.4 The Influence of Cupular Drag, Inertia, and Elasticity on the Responses of the Semicircular Canal	50

TABLE OF CONTENTS (cont.)

	3.5 A Dynamic Model for the Semicircular Canals	56
	3.6 Summary and Conclusions	61
IV	Response of the Semicircular Canals to Caloric Stimulation	63
	4.1 Introduction	63
	4.2 A Dynamic Model for Caloric Stimulation	64
	4.3 Experimental Verification of Caloric Model	75
	4.4 The "Caloric Latency Product"	80
V	The Response of the Semicircular Canals to Rotation in a Linear Acceleration Field	88
	5.1 Vestibular Responses to Constant Rotation in a Linear Acceleration Field	89
	5.2 The Flexible Nature of the Semicircular Canals	92
	5.3 The Flexible Torus as a "Roller Pump"	92
	5.4 A Model for Canalicular Response to Rotating Linear Acceleration Stimulation	95
	5.5 Experimental Verification of the Model	100
VI	Results, Conclusions, and Recommendations	101
	6.1 Results and Conclusions	101

TABLE OF CONTENTS (cont.)

	6.2 Recommendations for Further Research	113
APPENDIX A	Physical Properties of Labyrinthine Fluids	117
APPENDIX B	Instruments Used to Measure the Physical Properties of the Labyrinthine Fluids	120
REFERENCES		130
BIOGRAPHICAL SKETCH		143

LIST OF FIGURES

Figure No.	Title	Page No.
2.1	The membranous inner ear	12
2.2	Orientation of semicircular canals with respect to the skull	14
2.3	Schematic drawing of a cross section of an otolith and its macula	16
2.4	The three semicircular ducts of a guinea pig	17
2.5	Cross section of human bony and membranous lateral canals	19
2.6	A view of crista-cupula system of the horizontal semicircular canal from a squirrel monkey	21
2.7	Electrical discharge rate of the hair cells as a function of displacement of the sensory hairs	23
3.1	Schematic diagram of the semicircular canal	37
3.2	Schematic diagram for dynamics of the semicircular canal	39
3.3	Torus placement relative to a cylindrical coordinate system for calculation of its dynamics	41

LIST OF FIGURES (cont.)

3.4	System block diagram for the average endolymph velocity ($\bar{v}$) in the canalicular duct from an input F(s)	47
3.5	A physical model for the cupula	52
3.6	Schematic model for cupula displacement (θ_c) resulting from angular acceleration (α) inputs	57
4.1	Position of lateral semicircular canal with respect to skull	65
4.2	Time history of temperature across the lateral semicircular canal (ΔT) in response to caloric irrigation in the external auditory canal	68
4.3	Measured and calculated temperature differences (ΔT) across lateral semicircular canal for stimulus applied in fig. 4.2	70
4.4	Block diagram for caloric stimulation	73
4.5	Calculated cupula displacements for step and step-exponential caloric stimuli and slow phase nystagmus velocity from caloric irrigation	79
4.6	Latency time (t_L) vs. temperature T_i for four experimental subjects	83
4.7	Average latency times vs. temperature for hot and cold caloric stimuli	84

LIST OF FIGURES (cont.)

4.8	Latency times to onset of subjective sensation and nystagmus for angular acceleration stimulation	84
5.1	Slow phase velocity of vestibular nystagmus from constant velocity rotation about vertical and horizontal axes	91
5.2	Illustration of the pumping action of the distended duct when the linear acceleration field is rotated at a uniform angular velocity	94
5.3	The functional dependence of the flow of endolymph on the physical properties of the labyrinthine fluids and membranous ducts and the rotation rate in a linear acceleration field	99
5.4	Experimental set-up for rotation in a lateral acceleration field	101
5.5	Sample eye movement records for rotations in 0.3 g lateral field	103
5.6	Slow phase nystagmus velocities from rotation in 0.3 g field	104
5.7	Biase and sinusoidal amplitude of slow phase nystagmus from rotation in 0.3 g field	105

LIST OF FIGURES (cont.)

5.8	Average values of bias and sinusoidal amplitude ($\pm 1\sigma$) for rotation in 0.3 g field (6 subjects)	105
5.9	Magnitude of sinusoidal component	106
5.10	Summary of available data of normalized bias and sinusoidal amplitude of vestibular nystagmus from rotation in a 1 g field	106
6.1	Block diagram for cupula response to linear and angular acceleration and caloric stimuli	116
B.1	Close up vies of microviscometer	122
B.2	Viscosity test set up	124
B.3	Electrical schematic for micro-viscometer	125

CHAPTER 1

INTRODUCTION

With the advent of space flight and high speed air and marine vehicles, the desire to utilize man as a major control and decision element has imposed ever increasing demands on his sensory systems. It has become necessary to examine in detail the dynamic properties of these sensory systems and to establish their fundamental performance limitations, for only through such knowledge can their behavior outside their normal physiological environments be understood and, hopefully, predicted. Of paramount importance in such an investigation is the human's motion sensing system, the vestibular apparatus, for it is a very significant contributor to man's ability to live and work in unusual motion environments.

This thesis studies the human vestibular system with particular emphasis on the dynamic properties of the semicircular canals, which have classically been considered as angular motion sensors. Their dynamic characteristics are evaluated from their physical properties in the context of a control theory description of the system, and models for the system's responses to angular and linear accelerations and caloric stimulation are presented. The models are examined

in the light of published results of other researchers and several experiments have been performed to test their validity.

1.1 Objectives of the Research

The vestibularly induced motion sickness experienced by three of the Russian cosmonauts during space flight has stimulated a great deal of vestibular research and experimentation. In the past, subjects have been tested in many unusual motion environments and their objective and subjective responses to such stimuli often do not conform to the predictions of existing vestibular system describing functions. This thesis is primarily concerned with four topics of current interest in vestibular physiology in which existing descriptions of the vestibular apparatus are inadequate to explain observed experimental results. Each of these areas of investigation is outlined in the following sections.

1.1.1 The dynamic response of the semicircular canals to angular acceleration stimulation

A critical review of the literature on vestibular stimulation by angular acceleration shows that there is a large disparity between the observed dynamic responses of the human to angular motions and the calculated dynamic responses of the semicircular canals. The hypothesis of van Egmond, Groen, and Jongkees (1949) that the objective and subjective responses of the human to angular acceleration stimulation

ould be described by a second order differential equation has been verified by many researchers, and the coefficients of the equation have been experimentally evaluated. To date, all attempts to determine analytically the dynamic characteristics of the angular motion sensors, the semicircular canals, have used a wide variety of approximations and attributed the damping of the system to the viscous drag of the endolymph in the semicircular canals. Such analyses have shown the damping to inertia ratio of the system to differ significantly from experimentally observed values.

In Chapter 3 a detailed fluid dynamic analysis of the semicircular canals is carried out in an attempt to resolve the conflict between theoretical and experimental results. Unlike revious analytic evaluations, the influence of cupula inertia and viscous drag on the membranous ampulla are considered in addition to the hydrodynamic drag of the endolymph in the canalicular duct and are shown to be responsible for only a small portion of the dynamic response characteristics of the semicircular canals. It is concluded that the semicircular canals do in fact have a higher frequency response than has been experimentally evaluated.

1.1.2 Physical properties of the labyrinthine fluids, endolymph and perilymph

The labyrinthine fluids, endolymph and perilymph, are clear, colorless, relatively invicid fluids with physical appearances much like water. The total volume of endolymph in the human labyrinth is only a few microlitres, and the largest samples that can be obtained from humans are about 2

microlitres. The perilymph space is somewhat larger, and sample sizes up to 5 microlitres or more can be obtained.

The microtechniques that have evolved in the chemical analysis field have been applied to these fluids, and several studies have been conducted showing the variations of their chemical properties with functional disorders of the labyrinth. However, until recently, no attempt has been made to measure the physical properties of human endolymph and perilymph which are required to evaluate the coefficients of the dynamic performance of the end organs.

To measure viscosity and its variation with temperature, the author has designed a microviscometer to operate with 1-2 microlitre samples of fluids. The design details and sample handling techniques associated with this instrument are the subject of Appendix B, and the measured results of the viscosity and its variation with temperature, and the density and coefficient of expansion of human endolymph and perilymph are presented in table 1 of Appendix A.

The fluids used for these measurements were obtained through the cooperation of Dr. Herbert Silverstein at the Massachusetts Eye and Ear Infirmary, from patients undergoing surgery for a membranous labyrinthectomy for unilateral Meniere's disease. Before the fluids' properties were measured, a microchemical analysis was conducted to show that they were in fact normal endolymph and perilymph.

1.1.3 The dynamic response of the semicircular canals to caloric stimulation

Caloric irrigation of the external auditory canal has been used as a diagnostic tool for clinical evaluation of vestibular function since the early 1900's. It was hypothesized by Barany in 1906 that the mechanism of caloric vestibular stimulation was a convection current of endolymph in the lateral semicircular canal due to the temperature gradient across it when the external canal is irrigated with water above or below normal body temperature. With the exception of some preliminary analytic efforts by Schmalz in 1931, there has been no attempt to develop an analytic model for vestibular response to caloric stimulation. With the several significant advances that have been made in the past decade in the measurements of eye movements and vestibular neuron discharge rates, more refined caloric tests such as the Hallpike minimum caloric tests, caloric threshold tests, and small volume ice water stimulations, are now possible and are often used. Such refinements make a dynamic model, which can predict vestibular response to various amplitudes and durations of caloric stimulation, a useful tool for vestibular research and clinical examinations.

In Chapter 4, the measurements of Cawthorne and Cobb of the time history of the temperature gradient across the lateral semicircular canal and the coefficient of expansion of endolymph, measured by the author, are used to generate a dynamic model for vestibular response from caloric

stimulation.[20,146] Model predicted responses are compared to independent published data, and through the cooperation of Dr. Alfred Weiss at the Massachusetts Eye and Ear Infirmary, additional caloric experiments were performed to test further the validity of the model.

1.1.4 Response of the semicircular canals to rotation in a linear acceleration field

The recent works of Guedry, Benson, Jones, and others have shown that a continuous nystagmus response is elicited from humans and animals when they are rotated at a constant angular velocity in a linear acceleration field that is not colinear with the axis of rotation.[75,8,96] A sinusoidal component of vestibular nystagmus is observed along with a steady state bias component of nystagmus. Both components persist long after the usual response of the semicircular canals to the initial transient of acceleration and continue for as long as the subject is rotated at a constant angular velocity.

Substantial evidence has been collected which attributes the sinusoidal component of the observed nystagmus to the stimulation of the utricular otolith by the sinusoidal component of acceleration which is present in the frontal (left-right) plane of the subject. However, it has been shown, by direct neuron recordings from the vestibular stem in cats, that the bias component of the observed vestibular nystagmus originates from the semicircular canals. Classical

models of the semicircular canals which are based on the assumption of a rigid canal duct show them to be angular accelerometers cannot give rise to a steady state cupula displacement due to constant rotation of the labyrinth in a linear acceleration field.

In Chapter 5, the influence of linear acceleration on the flexible canalicular duct is shown to bring about a distension of the membranous canal due to the differences in the densities of the duct, the endolymph, and the perilymph. Rotation of the labyrinth in a linear acceleration field can then generate a "roller pump" action as a result of the constricted portion of the duct being "pushed along" the periphery of the bony canal by the rotating acceleration field. In this way the endolymph is pumped toward the cupula and effects a steady cupula deflection. The magnitude of the distension of the duct that is required to produce the observed bias component of nystagmus is calculated.

A model is proposed which quantifies the relationship between cupula displacement, the magnitude of the acceleration field, and the rate of rotation of the labyrinth. The model is examined in the light of published data and additional experiments are performed to evaluate the rotation rate above which the bias component of nystagmus can no longer be observed.

1.2 Application of the Research

The results of this research are applicable to the fields of physiological research, aerospace medicine and psychology, and human engineering.

1.2.1 A microviscometer as a research instrument

The microviscometer designed for measurements of the viscosities of the labyrinthine fluids is a useful tool for physiological research. Its capability to utilize 1-2 microlitre individual samples makes it particularly useful in performing correlation studies, compatible with microchemistry techniques, between changes in body fluid characteristics and malfunctions of the associated organs. It has been noted, for example, that there is some correlation between various degrees of some forms of deafness and the viscosity of perilymph, but until now the small volume of available perilymph has prohibited any quantitative evaluation of this observation.[155]

1.2.2 Applications of mathematical models of the vestibular apparatus

Mathematical descriptions of the dynamic responses of the sensory end organs provide researchers with a knowledge of the sensed motion information that is being transmitted to the central nervous system.

The proposed model of semicircular canal dynamics is useful in the field of aerospace medicine and psychology for it provides an analytic evaluation of the information output

of the canals for acceleration inputs and thus anticipated mission acceleration profiles can be investigated for situations which can result in disorientation and vertigo.

Physiological research leans heavily on such analytic models, for without knowledge of the transduction characteristics of the sensory end organs, the physiologist is severely handicapped in his attempt to describe associated body mechanisms. Control and human engineering research also demands an analytic description of the motion sensors, for in many cases the human's ability to control a vehicle or perform a presecribed task is significantly influenced by vestibularly received inputs.[126,159] In addition, the model of the dynamic response of the labyrinth to caloric irrigation is useful for physiological research and more refined clinical evaluation of functional disorders of the labyrinth.

CHAPTER 2

THE ANATOMY AND PHYSIOLOGY OF THE HUMAN VESTIBULAR SYSTEM

The vestibular system, man's motion sensing center, is the non-auditory portion of the inner ear. The information from it is used to assist him in his balance and body orientation relative to his environment. Considerable physiological research and histological study has been directed toward the vestibular system, and because of its implications on man's orientation in space, its properties and functions are currently under intense investigation.

In this chapter the gross anatomical features of the non-auditory labyrinth are reviewed. The construction and function of the utricle are discussed, and a detailed description of the semicircular canals is given. Finally, the phenomenon of nystagmus is considered from the viewpoint of its value as a measure of vestibular stimulation.

2.1 Gross Anatomical Description of the Vestibular System

The membranous labyrinth is enclosed in a cavity called the bony labyrinth in the temporal bone of the skull. It is functionally divided into an auditory transducer called the cochlea and the vestibular system which contains the organs

of equilibrium (fig. 2.1). As components of the vestibular system, there are three semicircular canals in each labyrinth. They originate at the utricle and are attached by fibrous connections to three hollow canals in the bony labyrinth. Two of the canals, the posterior and the anterior, have a common duct for about 15% of their length. At one end of each canal is an expanded section called the ampulla. It contains a gelatinous, elastically restrained "flapper valve" called the cupula, which is attached to the crista. The crista is a raised section of the inner wall of the ampulla and contains a layer of sensory hair cells which respond to motion of the cupula.

The utricle occupies the center portion of the bony labyrinth called the vestibule. At one end of the utricle is the utricular macula, an expanded section containing a bed of sensory cells. On the macula lies the otolith, a gelatinous substance which contains calcium carbonate grains and is supported by fibrous connections to the macula.

Attached to the utricle is the saccule, a smaller organ that is structurally the same as the utricle. However, the plane of its macula is perpendicular to that of the utricular macula. The endolymphatic sac is also attached to the utricle and the saccule and can best be described as the filter for used endolymph. It has no sensory function. The volume inside the utricle, the saccule, and the semicircular canals is filled with a fluid called endolymph, and the remainder of the volume between the membranous labyrinth and the bony

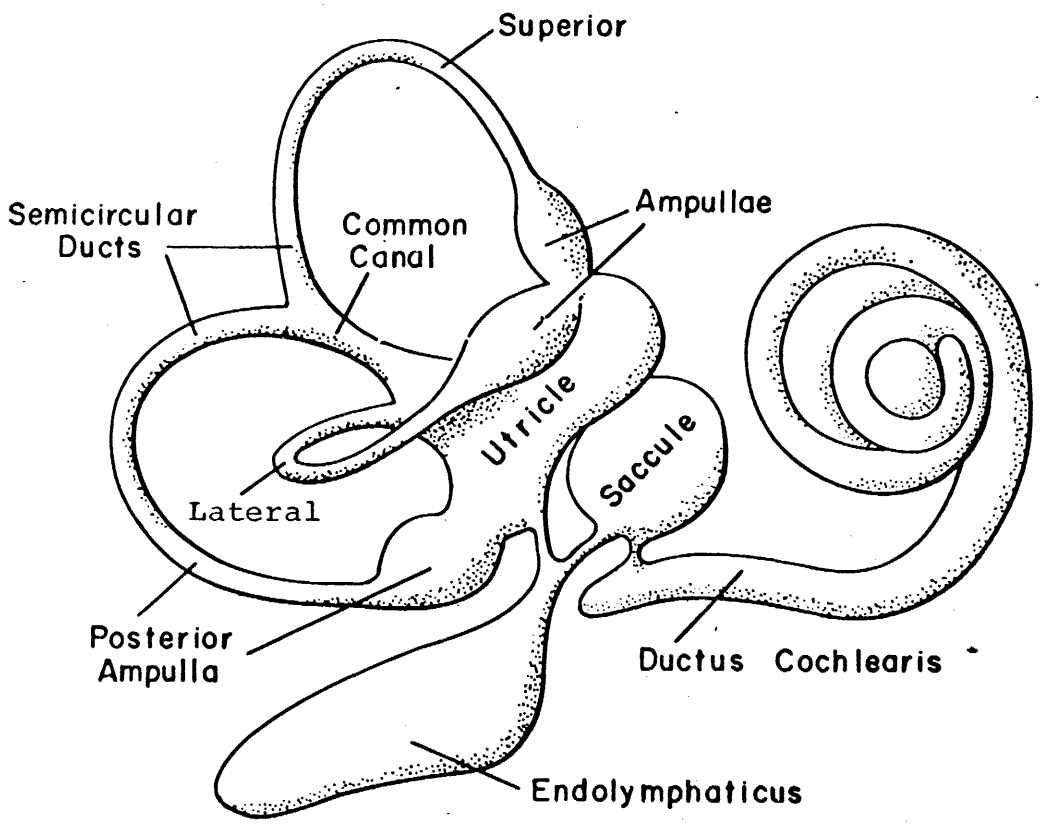


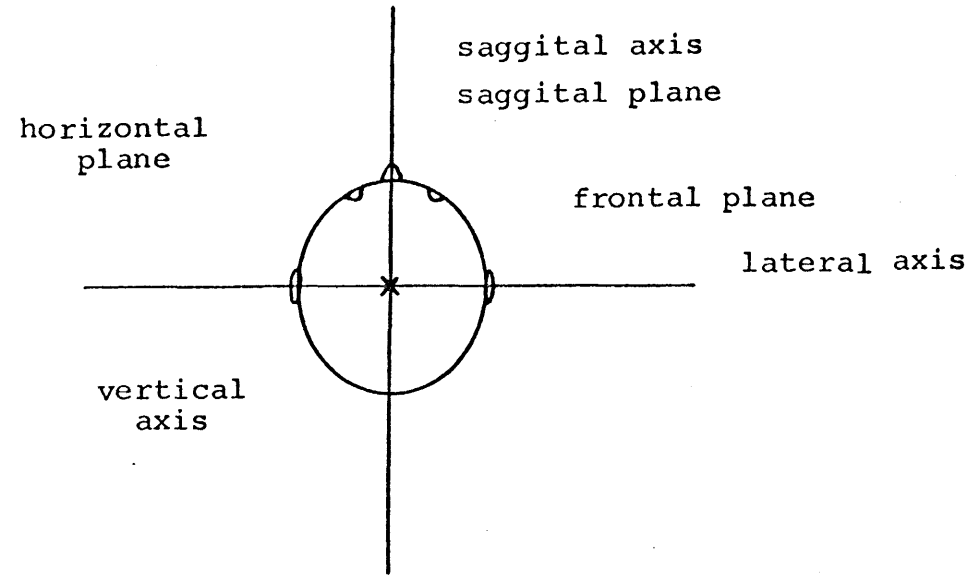
Fig. 2.1 The Membranous Inner Ear (Ref. 7)

labyrinth is filled with perilymph.

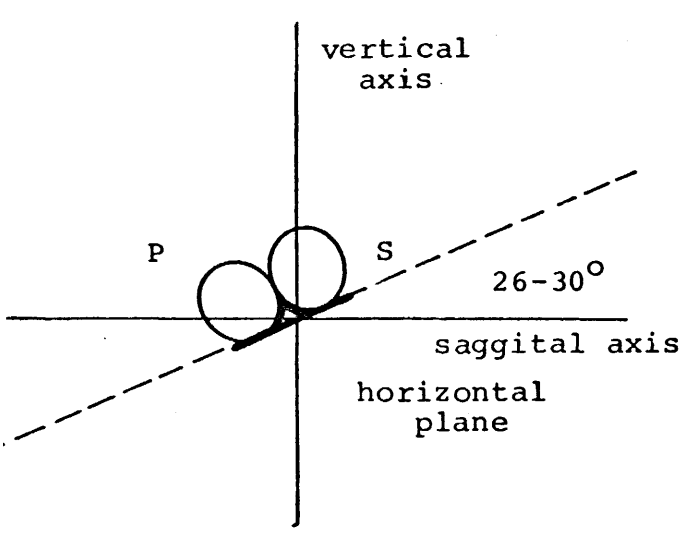
The orientation of the vestibular system with respect to the skull is shown in fig. 2.2b, c. The three semicircular canals of each labyrinth form a near orthogonal set and the plane of the lateral canals is tilted up from the horizontal plane by about 30^{o} and intersects the frontal plane in a line parallel to the lateral axis. The remaining canals are positioned as shown in fig. 2.2c with the superior canal of one labyrinth approximately parallel to the posterior canal of the other.

2.2 The Utricle and the Saccule

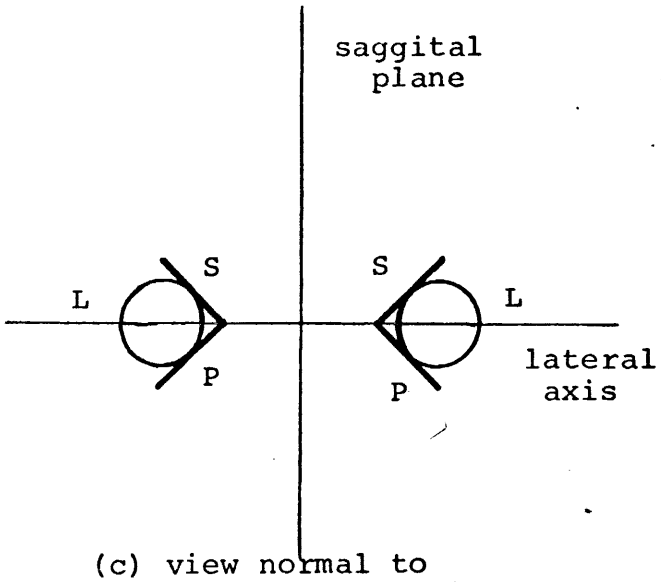
The utricular macula and its otolith, as shown schematically in fig. 2.3, are generally considered to be the linear acceleration sensors of the vestibular system. The macula is a bed of sensory hair cells upon which rests the otolith. The utricular macula is approximately a heart shaped structure with an elevated section at its back edge. The sensory epithelium of the macula has been studied and the orientation of its sensory cells has been mapped for some species of animals. The otolith is a gelatinous substance with a large number of suspended calcium carbonate grains called otoconia with a specific gravity of about 2.9 and ranging in size from 1 to 30 microns. It is suspended over the macula by supporting cells which allow the otolith to move over the surface of the macula, under the influence of inertial acceleration, for a distance of about 0.1 mm. The



(a)



(b) view into right ear



(c) view normal to lateral canal plane

Figure 2.2

Orientation of semicircular canals (lateral, L; superior, S; posterior, P) with respect to the skull.

sensory hair cells of the macula are thus stimulated by the movement of the otolith, and they transmit linear acceleration information to the central nervous system.

The macula of the saccule has a structure with striking similarity to the utricular macula. It too has an otolith with otoconia and supporting hair cells, and the types and distribution of its sensory hair cells are similar to those of the utricular macula. However, whereas researchers have shown the linear acceleration sensitivity of the utricular otolith by direct measurement of neural activity in animals, no such functional response has been observed from the macula of the saccule. The purpose of this organ is still a subject for debate with some researchers hypothesizing that it serves an auditory function, and others, a vestibular function.

In summary, the utricular otolith has been shown to be a two axis linear accelerometer, with other possible modes of stimulation, and the saccular otolith is a much studied but little understood organ. Intense research activity is now being focused on these organs to clarify their roles as motion receptors.

2.3 The Semicircular Canals

The human semicircular canals are a set of endolymph filled canals with origins at the utricular sac, extending through the canals of the bony labyrinth for about 2/3 of the circumference of a circle and each terminating on an enlarged portion of the duct called the ampulla. Within the ampulla are two structures, the cupula and its base, the crista,

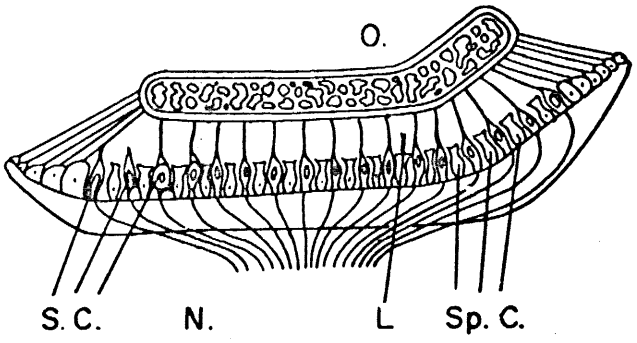


Figure 2.3

Schematic drawing of a cross section of an otolith and its macula. O is the Otolith, suspended by strands which run from the margins to the macula, consisting of supporting cells (Sp.C.) and sensory cells S.C. Between the otolith and the macula there is a thin layer (L) to allow the otolith to slide over the macula. N is the nerve (ref. 73)

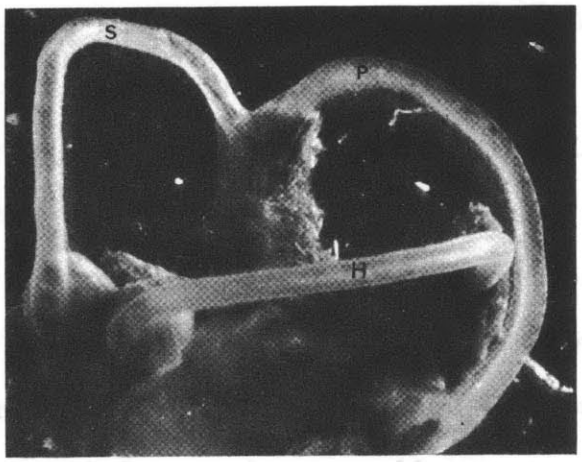


Figure 2.4
The three semicircular ducts of a guinea pig.
H = horizontal, S = superior, P = posterior (ref.49)

which contains sensory hair cells from which neural bundles project toward the central nervous system. The entire structure is immersed in the perilymph which fills the bony labyrinth. As background material for the next three chapters, each of these components will now be considered individually.

The three semicircular ducts of a guinea pig are shown in the photograph in fig. 2.4, from which the common duct of the superior and posterior canal, the ampullae of all three canals, and their entrance into the utricular sac can clearly be seen. The membranous duct itself is a tissue-like structure that is only a few cell layers thick and has an approximately circular cross section in most mammals. In man it is attached to the bony labyrinth along its outer periphery. A cross sectional view of the relative dimensions of the membranous and bony canal ducts is shown in fig. 2.5.

The membranous ampulla, as observed in fig. 2.4, is an enlarged area at the end of the canalicular duct as it enters the utricular sac. In man the ampulla is firmly attached by fibrous connections on all sides, and is thus fixed with respect to the skull. Within the ampulla is housed the cupula, a gelatinous substance which acts as a sliding, elastically restrained valve. When the canal is subjected to angular acceleration, the inertial reaction of the endolymph moves the cupula which in turn stimulates the sensory hair cells of the crista.

Lowenstein et al has shown by injection of india ink into the endolymph of the semicircular canal of a thornback

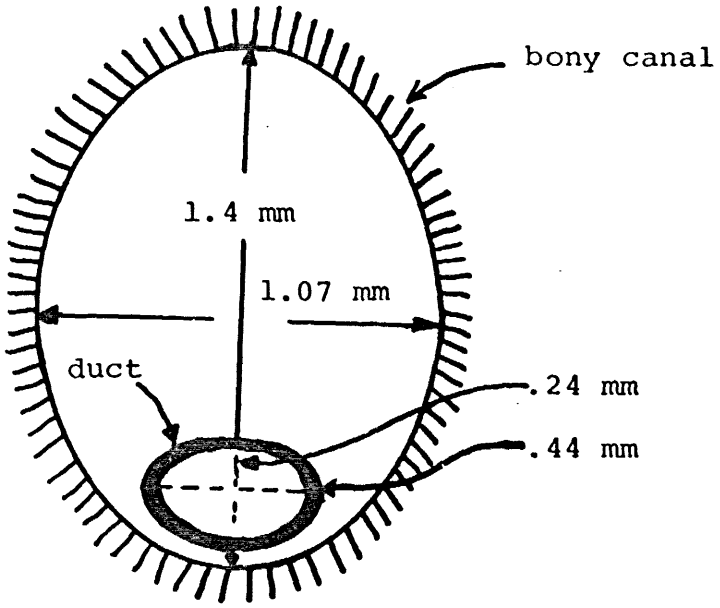


Figure 2.5
Cross section of human bony and membranous lateral canals
(ref. 91)

ray followed by stimulation of the canal with angular acceleration that the cupula forms a near hermetic seal at the wall of the membranous ampulla.[116] The photograph, from the histological studies of Igarashi, shown in fig. 2.6, which illustrates the cupula, on its crista in the ampulla of a squirrel monkey, shows a very close tolerance between the cupula and the ampulla wall, of the order of a few microns.[91] It will be shown in the next chapter that this close tolerance is responsible for much of the damping of the semicircular canal dynamics.

The studies of Crampton and others have shown that the canalicular neurons (of cats) are not significantly stimulated by linear acceleration and thus that the cupula must be neutrally buoyant in, and therefore of the same specific gravity as the endolymph that surrounds it.[44]

The base of the cupula is attached to the crista and the sensory cells from the crista's epithelial layer extend their hairs into the base of the cupula. The majority of sensory cells in the vestibular system exhibit a frequency modulated transfer characteristic between the position of their sensory hairs and the electrical outputs of their attached neurons. A carrier frequency of about ten action potentials per second is a typical resting discharge rate for vestibular neurons, and experiments using micro-manipulators and observation of cupula displacement have shown an increase in neural discharge rate for displacement of the cells' sensory hairs in one direction and a decrease for displacement in the opposite direction. The question of whether electrical or chemical

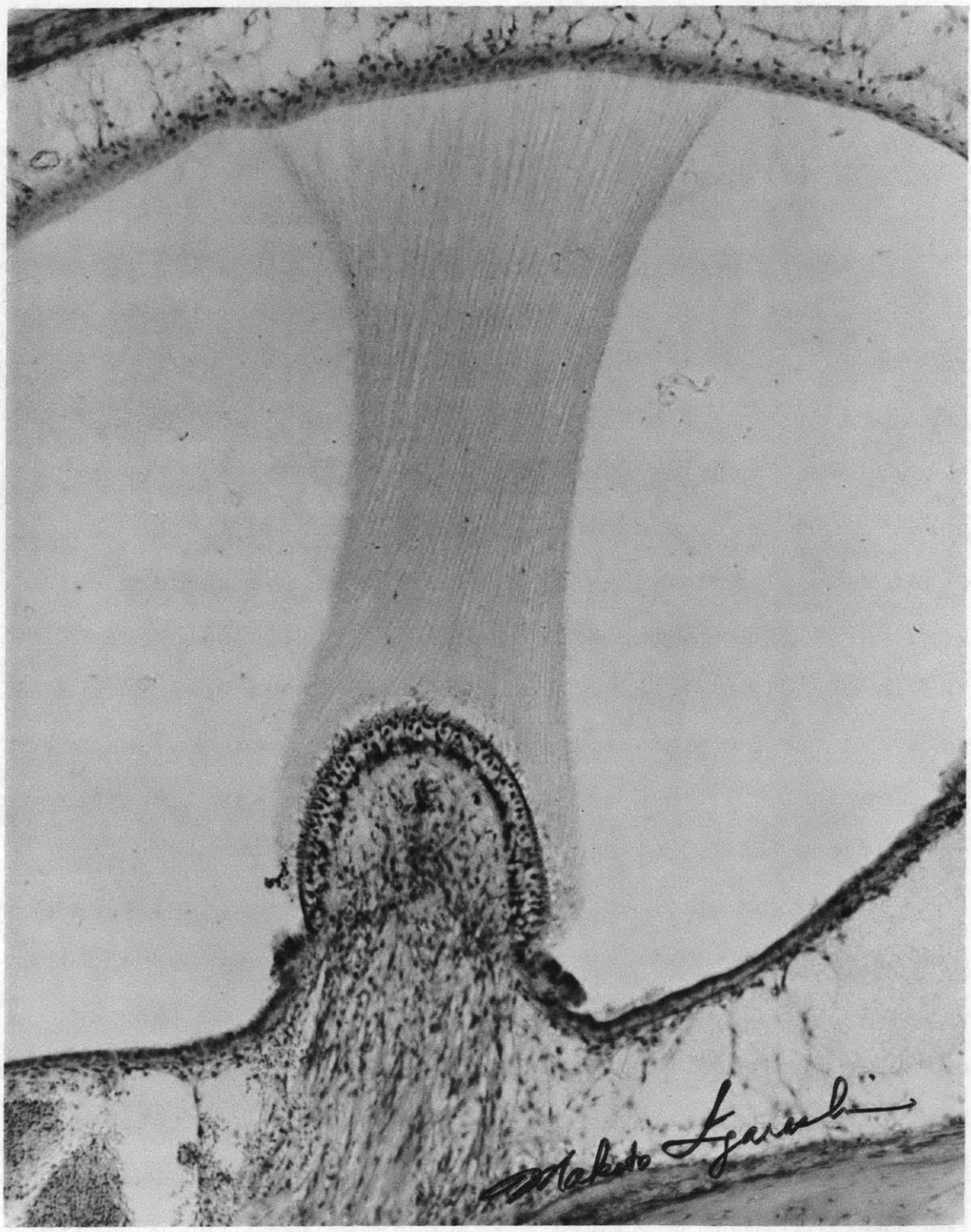


Figure 2.6
A view of crista-cupula system of the horizontal semicircular canal from a squirrel monkey (ref.91)

action is responsible for the transmission between sensory cells and nerve endings has not yet been resolved, and it is now one of the most investigated subjects of current vestibular research.

Engstrom, Wersall, and others have identified two basically different nerve endings on the sensory cells in the epithelium of the crista-ampullaris.[50,157] One such cell has efferent fibers going to the CNS, and the other has afferent fibers which appear to come from other sensory cells. As shown in fig. 2.7, these two nerve endings are different in the way they make contact with the sensory cell, with one nerve ending surrounding nearly the entire cell, and the other simply terminating on the bottom of the sensory cell. Both nerve endings terminate on sensory cells which have a bundle of hairs called stereocilia projecting upward from the cell and one larger stiffer hair called the kinocilium which is always the longest of the hairs and is always located on one side of the bundle of stereocilia.

The directional sensitivity of the sensory cells has been determined by studies of their population densities and the orientation of their kinocilia in the cristae of the semicircular canals. It has been found that in the crista of the horizontal (lateral) semicircular canal, the majority of the kinocilia are always oriented toward the utricle, where as for the vertical canals (posterior and superior), the majority of the kinocilia are always oriented away from the utricle. The experimental results of Lowenstein, Crampton, Jones, and others, have shown for several species of animals that the flow of

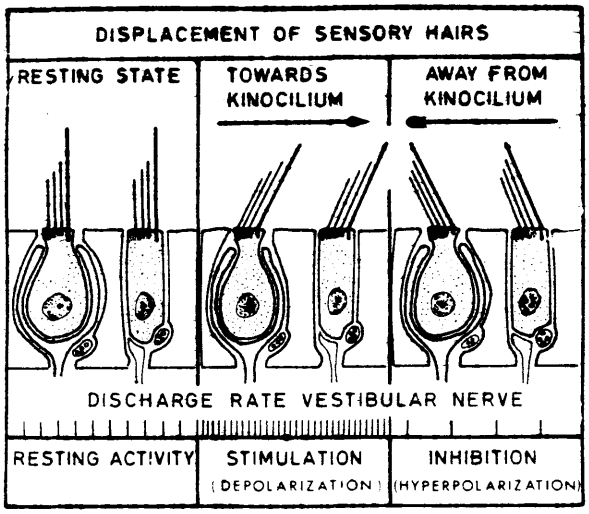


Figure 2.7

Electrical discharge rate of the hair cells as a function of displacement of the sensory hairs (ref. 158)

endolymph toward the ampulla (ampullopetal flow) produces an increase in neural discharge rate and an ampulofugal flow in the lateral canal produces a decrease in discharge rate.[115,45,95] The converse is true for the vertical canals. These experiments have also shown a remarkable linearity between the discharge rates of the canalicular neurons and the calculated and observed cupula deflections.

Since cupula deviation corresponds to the direction of endolymph flow and the sensory hairs are bent in the direction of the motion of the cupula, it has been concluded that motion of the stereocilia toward the kinocilium causes an increase in the discharge rate of the cell and motion away from the kinocilium causes a decrease in discharge rate.

In summary, the transduction characteristics of the canalicular sensory cells are well established, although the mechanism is not yet understood. The flow of endolymph brings about a cupula displacement which in turn stimulates the sensory hair cells of the crista. The nerve endings of the sensory cells then transmit electrical signals whose frequency is proportional to cupular displacement to the central nervous system.

2.4 Nystagmus as a Measure of Vestibular Stimulation

With the present state of the art, it is not possible to make direct neural recordings without radical surgery. Thus such experimentation with humans is out of the question until a non-destructive technique for recording from neurons is found. It is necessary, therefore, to use other measures of vestibular stimulation to indicate the performance of man's motion sensing system.

2.4.1

The ability of man to sense his direction of motion and give a subjective estimate of its relative magnitude is one such measure of vestibular stimulation. The mechanism for such perception is the processing of vestibularly sensed inputs, and other proprioceptive and tactile information by the central nervous system which compares them to those previously experienced, and gives the human an appropriate sensation. This technique has often been used for determination of threshold sensitivities to linear and angular accelerations and to measure the relative phase shift between the sensation of motion and sinusoidal acceleration stimulation. It suffers from the limitations that the subjective responses are influenced by the subject's experience and mental set at the time of the experiment. Further, there is no direct, continuously recordable indication of subjectively perceived responses.

2.4.2 Vestibular nystagmus - an involuntary eye movement

A more quantitative measure of vestibular stimulation can be obtained by observation of compensatory eye movements called nystagmus, in which vestibularly sensed motions produce an involuntary eye motion which drives the eyes toward their initial direction of gaze. Thus, for a clockwise angular acceleration, the compensatory mechanism drives the eyes counter clockwise with respect to the skull. The eyes move with a velocity (slow phase velocity) approximately proportional to the angular velocity of the skull until a saccadic, involuntary reflex mechanism returns them to a new position, after which they resume their slow phase velocity.

It has been shown, by direct observation of the cupula in mammals, that the slow phase velocity of vestibular nystagmus corresponds to cupula deflection from angular acceleration and caloric stimulation, and in humans, the slow phase velocity of vestibular nystagmus corresponds to the cupula displacement as calculated by the equations of van Egmond, Groen, and Jongkees.[151]

In a critical review of experimental data and supplemented by experiments, Young, et al, has shown that a nystagmus is generated by linear motion in the frontal (left-right) plane, and it is thought that this nystagmus results from stimulation of the utricular otoliths.[160]

2.4.3 The influence of habituation and alertness

A substantial decrease in nystagmus response has been observed for both man and animals when they are subjected to repeated acceleration or caloric stimuli, and it has been shown that subjects have larger nystagmus responses when kept mentally alert, by such tasks as performing mental arithmetic than when they are allowed to fall into a state of reverie. Both of these observed effects usually manifest themselves as a decrease in the slow phase velocity of the nystagmic response, and if care is exercised not to use a subject for too many repeated experiments and an attempt is made to keep the subject alert, the degeneration in nystagmic responses can be held to a minimum.

In summary, nystagmus measurements have been shown to be a quantitative measure of vestibular stimulation which is related to the position of the cupulae of the semicircular canals

and the component of linear acceleration in the frontal plane of the subject's utricular otolith. Although they are influenced by habituation and subject mental set, nystagmus recordings provide a continuous objective measure of vestibular stimulation that is relatively easy to obtain and analyze.

2.4.4 Nystagmus measurement techniques

There are several techniques available for nystagmus measurements. The four most common methods are:

a) Direct visual observation of eye movements by use of a Frensel lense is often used for the determination of the onset of nystagmus, however this technique is of little value in the determination of the velocity of slow phase nystagmus.

b) The Electro-Oculogram (EOG) measures the differential corneo-retinal potential as a function of eye movement by paste-electrodes attached at the outer corners of the eyes. This technique is very useful in that it can be used either with eyes open or closed and in a light or dark environment. Its primary drawbacks are electrode drift and the presence of "muscle noise" in the recordings.

c) Close up motion pictures of the iris and sclera are useful for measurements of both eye position and velocity, although they require a very tedious frame by frame analysis and are usually only used for measurement of rotary nystagmus where no other technique is available.

d) The most recent development in eye movement recordings is an eye movement monitor which utilizes the differential reflectivity of the iris and sclera. It uses a self-contained invisible, pulsed infrared illumination source and phase sensi-

tive detection of the reflected signal to obtain a $\pm 20^{o}$ dynamic range for horizontal eye movements. The instrument response time of one millisecond and high electronic gain make it a very stable, accurate, and easy to use instrument. One such device, a Biosystems model SGHV-1 eye movement monitor, was provided by the manufacturer for use in the experimental portions of this thesis.

CHAPTER III

THE "RIGID TUBE" DYNAMIC CHARACTERISTICS OF THE SEMICIRCULAR CANALS

3.1 Introduction

3.1.1

The classic work of Steinhausen in 1931 showed, by direct observation of the cupula (in the pike), that during angular accelerations, the interial reaction of the endolymph caused the cupula to be deflected. Subsequently, van Egmond, Groen and Jongkees (1949) put forth the theory that the dynamic properties of the semicircular canal could be modelled as a "torsion pendulum" which could be quantitatively described by the differential equation

$$\ddot{\xi} + \frac{\pi}{\theta} + \frac{\Delta}{\theta} = \alpha \qquad (3.1)$$

where

θ = moment of inertia of the endolymph

π = viscous damping torque of endolymph at unit angular velocity with respect to the skull

Δ = elastic stiffness, restoring torque per unit angular deflection of the cupula

ξ = angular deviation of the endolymph with respect to the skull

$\dot{\xi}$ = angular velocity of the endolymph with respect to the skull

$\ddot{\xi}$ = angular acceleration of the endolymph with respect to the skull

α = input angular acceleration along the sensitive axis of the canal

This differential equation description of cupula deflection can be put into the context of control theory by application of the Laplace transform, from which we obtain:

$$\frac{\xi(s)}{\alpha(s)} = \frac{1}{s^2 + 2\xi\omega_o + \omega_o^2} = \frac{1}{(s + \omega_1)(s + \omega_2)} \tag{3.2}$$

where

$$\omega_o^2 = \omega_1\omega_2 = \frac{\Delta}{\theta} \tag{3.2a}$$

and

$$\omega_{1,2} = \frac{-\frac{\pi}{\theta} \pm \sqrt{(\frac{\pi}{\theta})^2 - 4\frac{\Delta}{\theta}}}{2} \tag{3.2b}$$

where

$$\omega_1 \approx \frac{\Delta}{\pi} \qquad \omega_2 \approx \frac{\pi}{\Delta}$$

for

$$\frac{\Delta}{\pi} << \frac{\pi}{\theta} \tag{3.2c}$$

The numerical value of $\frac{\Delta}{\pi}$ can be experimentally evaluated by application of impulsive angular accelerations, and $\frac{\Delta}{\theta}$ can be evaluated from the subjective responses to sinusoidal angular accelerations.

The value of $\frac{\pi}{\Delta}$ is best determined by the measurement of the duration of the sensation of motion after an impulsive acceleration from one constant angular velocity to another. The time for the cupula to return, under the influence of its own elasticity, to its minimum perceptible deflection point is a function of the magnitude of the change in velocity.

Solution of eq. (3.1) subject to the boundary conditions $\alpha(t) = \xi(0) = 0$ and $\dot{\xi}(c) = V$ = amplitude of velocity change, gives

$$\xi(t) = V \frac{\theta}{\pi} [e^{-\frac{\Delta}{\pi}t} - e^{-\frac{\pi}{\theta}t}] \tag{3.3}$$

which under the assumption $\frac{\Delta}{\pi} < \frac{\pi}{\theta}$ reduces to

$$\xi(t) \approx V \frac{\theta}{\pi} e^{-\frac{\Delta}{\pi}t} \tag{3.4}$$

Since the time to the cessation of perception corresponds to the time for the cupula to return to its threshold value of perception ξ_{min}, then t_n can be evaluated by solving eq. (3.4) for t when $\xi = \xi_{min}$, from which we obtain

$$t_n = \frac{\pi}{\Delta} \log [\frac{\theta}{\pi} \frac{V}{\xi_{min}}] \tag{3.5}$$

Then the slope of the time of after sensation (t_n) vs. log magnitude of step change in velocity plot is $\frac{\pi}{\Delta}$. Using this technique, and naming the plot as a "subjective cupulogram," Van Egmond, Groen, and Jongkees found a value of $\frac{\pi}{\Delta} = 10$ for

the lateral canals in man.[151] In a review of the works of subsequent investigators, Young et al has reported that the observed values of $\frac{\pi}{\Delta}$ range from 8 to 10 for subjective sensation durations, and from 16 to 20 for nystagmus durations.[163] Similar measurements by Meiry on the vertical canals have yielded values of $\frac{\pi}{\Delta}$ = 7 sec for subjective sensation durations.[126]

Because of neuro-muscular delays, central nervous system computational delays and the attendant problems of measurement equipment and techniques, there has not been devised an experiment to measure $\frac{\pi}{\theta}$ directly. However, it can be calcuated from eq. (3.2a) and the measured value of ω_o.

By use of a torsion swing and the subjective sensation of perception of velocity, Van Egmond found the frequency of angular oscillation for which the cupula displacement lagged the applied sinusoidal acceleration by 90° to be ω_o = 1 rad/sec.[151] At that frequency, the perceived angular velocity corresponds to the applied angular velocity. This value has since been verified by many researchers. Thus the natural frequencies (ω_1 and ω_2) of the human lateral semicircular canal have been assumed to be those measured from the observed subjective responses:

$$\omega_1 = \frac{\Delta}{\pi} = 0.1 \text{ rad/sec}$$

$$\omega_2 = \frac{\pi}{\theta} = \frac{\pi}{\Delta} \cdot \frac{\Delta}{\theta} = 10 \text{ rad/sec}$$

or alternatively

$$\frac{\pi}{\theta} = 10 \text{ rad/sec}$$

$$\frac{\Delta}{\theta} = 1(\text{rad/sec})^2$$

3.1.2

Through various histological studies, the physical dimensions of the semicircular canals have been measured for many species, including man. There have been numerous attempts to evaluate analytically the dynamic sensory capabilities of these end organs. All such attempts to date have shown an order of magnitude difference between the calculated and measured values of $\frac{\pi}{\theta}$. For example, the damping to inertia ratio for a water filled torus with the same internal radius as the human canalicular duct, 0.14 mm, was calculated by Jones et al to be[95]

$$\frac{\pi}{\theta} = \frac{4\mu g}{\rho r^2} \approx 200$$

where

μ = viscosity of fluid

ρ = density of fluid

g = gravitational constant

r = internal radius

This large disparity between observed and calculated values of dynamic characteristics has often been attributed to the central

nervous system. However, from the results of many researchers, and in particular by a detailed analysis of the neural discharge response obtained by Crampton from Cats, Cappel has shown that the rates of change of neuron discharge from angular acceleration conform much more closely to the measured $\frac{\pi}{\theta} = 10$ than to the calculated $\frac{\pi}{\theta} = 200$. This evidence indicates that the end organ itself may display the mechanical dynamic characteristics that have been measured by objective and subjective responses. Further, the resting discharge rate of the neurons which connect to the sensory epithelium of the crista is of the order of 10 action potentials per second, and it is physiologically unrealistic that such a low frequency carrier based system would be called on to transmit information at a 200 rad/sec rate.

3.1.3

The remainder of this chapter is addressed to a detailed fluid dynamic analysis of the semicircular canal as a rigid tube structure; the purpose of this analysis is to resolve the conflict that now exists between theory and practice. The values of viscosity and density of endolymph that will be used in this analysis are those measured by the author from Appendix A. The dynamics of the cupula-endolymph system and in particular the influences of cupula drag and inertia will be considered and shown to be significant contributors to the dynamic characteristics of the end organ.

3.2 A Physical Model of the Semicircular Canals

A rigorous analytical evaluation of the dynamic sensory capabilities of the semicircular canals requires the solution of the classical Navier-Stokes equations of fluid dynamics for an incompressible fluid subject to the boundary conditions of zero flow at the inner surface of the membranous canals. These equations, in cylindrical coordinates, are:

$$\rho\left[\frac{\partial v_r}{\partial t} + v_r\frac{\partial v_r}{\partial r} + \frac{v_\phi}{r}\frac{\partial v_r}{\partial \phi} - \frac{v_\phi^2}{r} + v_z\frac{\partial v_r}{\partial z}\right] \tag{3.6a}$$

$$= F_r - \frac{\partial p}{\partial r} + \mu\left[\frac{\partial^2 v_r}{\partial r^2} + \frac{1}{r}\frac{\partial v_r}{\partial r} - \frac{v_r}{r^2} + \frac{1}{r^2}\frac{\partial^2 v_r}{\partial \phi^2}\right.$$

$$\left. - \frac{2}{r^2}\frac{\partial v_\phi}{\partial \phi} + \frac{\partial^2 v_r}{\partial z^2}\right]$$

$$\rho\left[\frac{\partial v_\phi}{\partial t} + v_r\frac{\partial v_\phi}{\partial r} + \frac{v_\phi}{r}\frac{\partial v_\phi}{\partial \phi} - \frac{v_r v_\phi}{r} + v_z\frac{\partial v_\phi}{\partial z}\right] \tag{3.6b}$$

$$= F_\phi - \frac{1}{r}\frac{\partial p}{\partial \phi} + \mu\left[\frac{\partial^2 v_\phi}{\partial r^2} + \frac{1}{r}\frac{\partial v_\phi}{\partial r} - \frac{v_\phi}{r^2} + \frac{1}{r^2}\frac{\partial^2 v_\phi}{\partial \phi^2}\right.$$

$$\left. + \frac{2}{r^2}\frac{\partial v_r}{\partial \phi} + \frac{\partial^2 v_\phi}{\partial z^2}\right]$$

$$\rho\left[\frac{\partial v_z}{\partial t} + v_r\frac{\partial v_z}{\partial r} + \frac{v_\phi}{r}\frac{\partial v_z}{\partial \phi} + v_z\frac{\partial v_z}{\partial z}\right] \tag{3.6c}$$

$$= F_z - \frac{\partial p}{\partial z} + \mu\left[\frac{\partial^2 v_z}{\partial r^2} + \frac{1}{r}\frac{\partial v_z}{\partial r} + \frac{1}{r^2}\frac{\partial^2 v_z}{\partial \phi^2} + \frac{\partial^2 v_z}{\partial z^2}\right]$$

$$\frac{\partial v_r}{\partial r} + \frac{v_r}{r} + \frac{1}{r}\frac{\partial v_\phi}{\partial \phi} + \frac{\partial v_z}{\partial z} = 0 \qquad (3.6d)$$

where

v_n = component of velocity of fluid in the n^{th} direction

F_n = component of force on fluid in the n^{th} direction

$\frac{\partial p}{\partial n}$ = pressure gradient in the n^{th} direction

r, ϕ, z = cylindrical coordinates

ρ = density of the fluid

To solve these equations it is necessary to reduce the semicircular canal to a physical model from which the equations for the boundary conditions can be derived. The simplified model shown schematically in Fig. 3.1 is obtained from the physical characteristics of the canals as shown in Figs. 2.1 and 2.6 and was used by Van Egmond, Groen, and Jongkees in their original torsion pendulum model.[151] The following analyses will utilize this closed torus model with the further assumptions of incompressible endolymph and rigid canalicular ducts to calculate the hydrodynamic drag of the endolymph in the ducts. A more detailed model of the cupula will be introduced from which the influences of cupula viscous drag and inertia will be calculated.

Examination of eq. (3.6) shows that the inertial acceleration forces and the pressure gradient forces on a particle of fluid are additive. Thus, it is possible to separate functionally the influence of the cupula and the canalicular

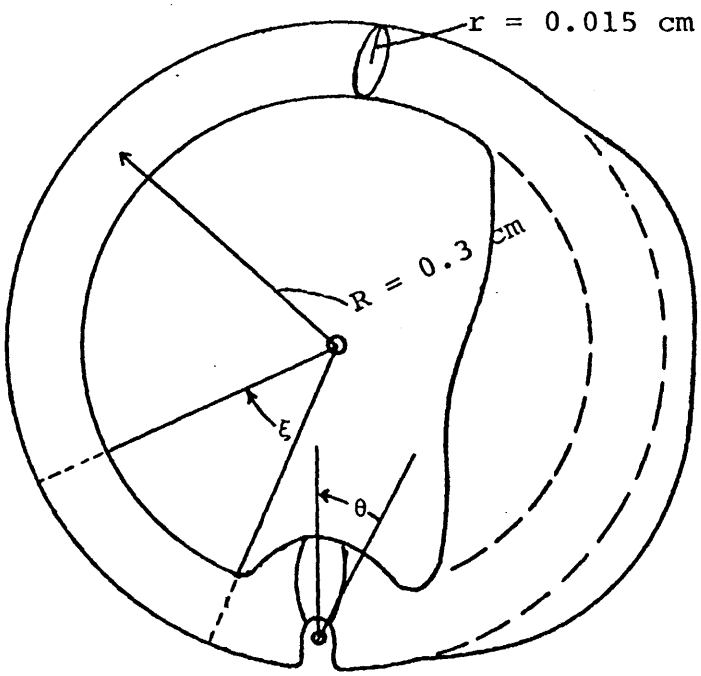


Figure 3.1

Schematic diagram of the semicircular canal
(Ref. 51)

duct on the performance of the semicircular canal. In Fig. 3.2 is presented a system block diagram which provides the necessary functional separation. The net "inertia-pressure feedback" force operates on the endolymph in the membranous duct and results in an average flow of endolymph. The inertia, drag, and elastic restraint characteristics of the cupula introduce a differential pressure feedback proportional to the average flow and flow rate of the endolymph.

The remaining sections of this chapter consider the hydrodynamic drag of the endolymph in the canalicular duct, the inertia drag and elasticity of the cupula, and finally all effects are combined to obtain the semicircular canal overall performance characteristics.

3.3 The Hydrodynamic Drag of the Endolymph in the Membranous Canalicular Duct

Histological studies have shown that the effective diameter of a crossection of the ampullary duct is nearly five times that of the canalicular duct. Therefore the endolymph contained in the ampullary region of the canal contributes far less damping to the system than the viscous drag of the endolymph in the membranous duct. To facilitate the solutions of eq. (3.6) the ampullary region is assumed not to exist and the semicircular canal is simplified to a closed rigid torus filled with a viscid incompressible fluid.

Since eqs. (3.6) are linearly dependent on time, the solution for the average flow of endolymph in the duct, for any angular acceleration input, can be calculated by application

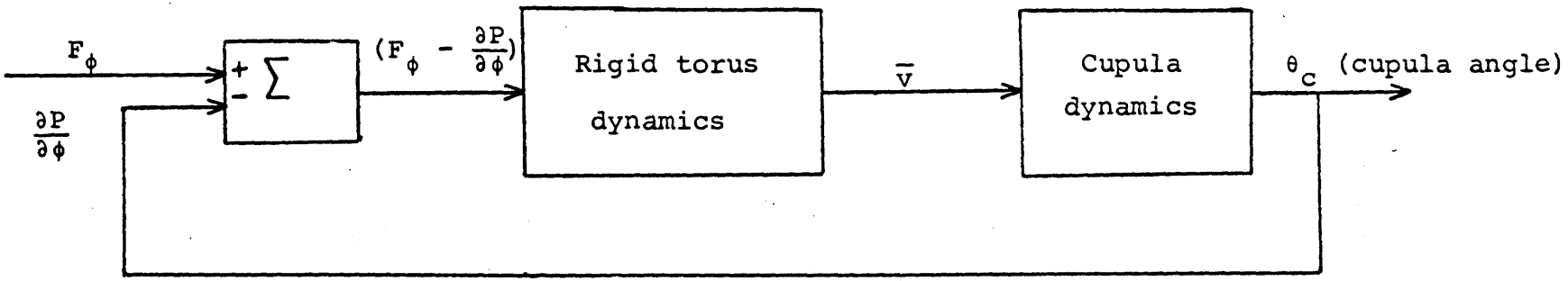


Figure 3.2
Schematic diagram for dynamics of the semicircular canal

of the convolution integral to the solution of the equations for any known transient input. Thus it is sufficient to solv eq. (3.6) for the average velocity of flow in a closed torus as the result of a step input of angular acceleration to evaluate the hydrodynamic drag of the endolymph in the canali ular duct.

With the torus at the center of the coordinate frame as shown in Fig. 3.3, the boundary condition for the flow is that

$$v(r, \phi, z, t) = 0$$

for

$$\varepsilon^2 = z^2 + (r - R)^2$$

where

$$R - a \leq r \leq R + a$$

From symmetry conditions:

$$\frac{\partial p}{\partial z} = v_r(r, \phi, z, t) = v_z(r, \phi, z, t) = 0$$

and

$$v_\phi(r, \phi, z, t) = v_\phi(r, z, t)$$

Since the only forcing functions are an angular acceleration (F_ϕ) and a pressure feedback around the torus ($\frac{\partial p}{\partial \phi}$) then

$$F_r = F_z = 0$$

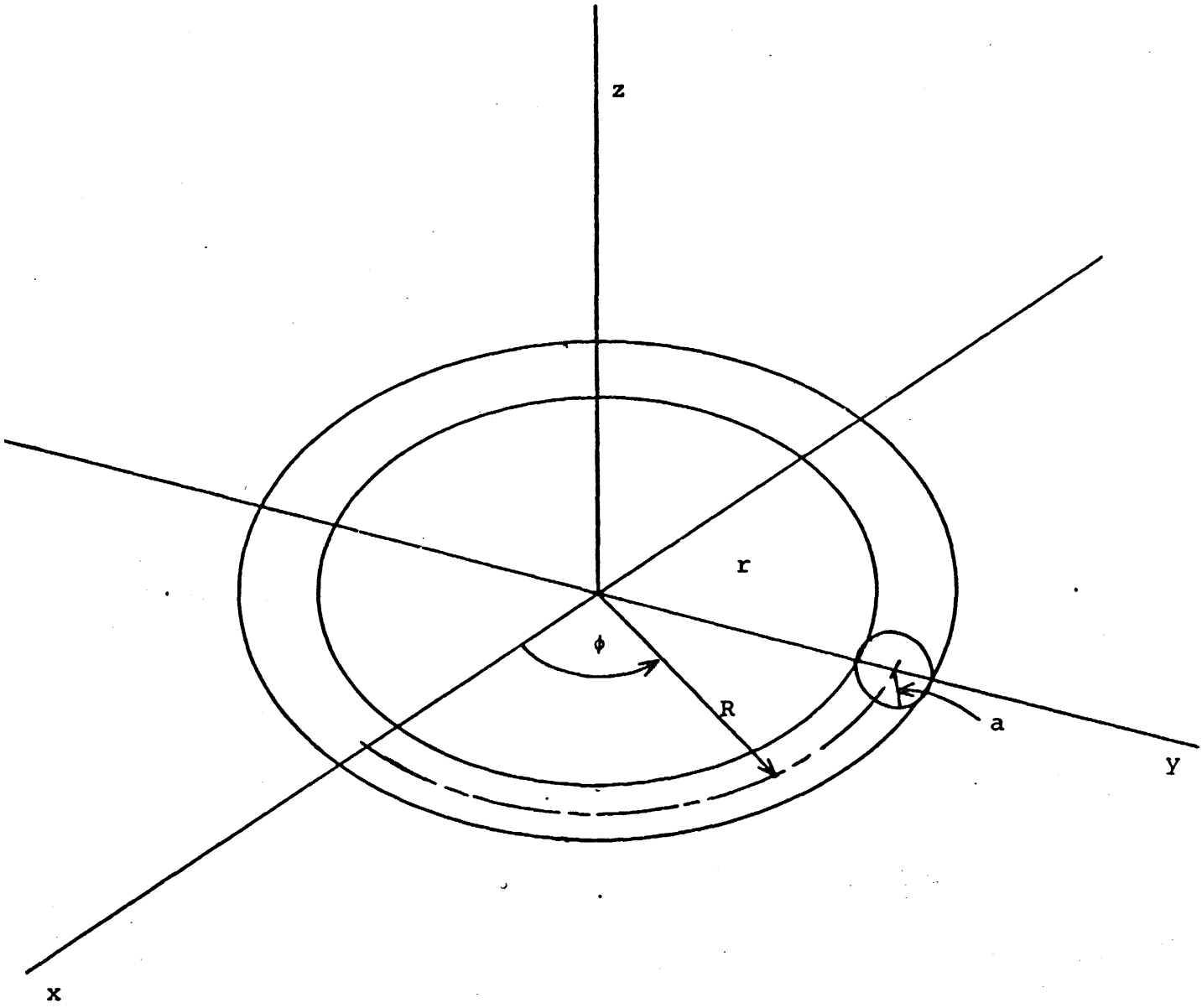


Figure 3.3
Torus placement relative to a cylindrical coordinate system for calculation of its dynamics

Under these boundary and symmetry conditions eq. (3.6) reduces to

$$-\rho \frac{v_\phi^2}{r} = \frac{\partial p}{\partial r} \tag{3.7a}$$

$$\rho \frac{\partial v_\phi}{\partial t} = F_\phi - \frac{1}{r}\frac{\partial p}{\partial \phi} + \mu\left[\frac{\partial^2 v_\phi}{\partial r^2} + \frac{1}{r}\frac{\partial v_\phi}{\partial r} - \frac{v_\phi}{r^2} + \frac{\partial^2 v_\phi}{\partial z^2}\right] \tag{3.7b}$$

Eq. (3.7a) evaluates the radial pressure gradient which results from the centrifugal force generated by the rotating fluid, but it is of no value for the determination of $v(r, z, t)$ which must be found by solution of eq. (3.7b). It is physically apparent because of the viscosity of the endolymph that for a step input of acceleration of infinite duration the velocity will reach a constant profile across the tube. Thus it is reasonable to assume that

$$v_\phi(r, z, t) = v_1(r, z) + v_2(r, z, t) \tag{3.8}$$

where

$$v_1(r,z) = -v_2(r, z, 0)$$

and

$$v_2(r, z, t) = \frac{\partial}{\partial t}\ v_2(r, z, t) \approx 0$$

for

$$t \to \infty$$

and let

$$F = F_\phi - \frac{1}{r} \frac{\partial p}{\partial \phi} \tag{3.8a}$$

Substituting eq. (3.8) into eq. (3.7b) yields

$$\rho \frac{\partial v_2}{\partial t} = F + \mu \left[\frac{\partial^2 v_1}{\partial r^2} + \frac{1}{r} \frac{\partial v_1}{\partial r} - \frac{v_1}{r^2} + \frac{\partial^2 v_1}{\partial z^2}\right] \tag{3.9}$$

$$+ \mu \left[\frac{\partial^2 v_2}{\partial r^2} + \frac{1}{r} \frac{\partial v_2}{\partial r} - \frac{v_2}{r^2} + \frac{\partial^2 v_2}{\partial z}\right]$$

Since eq. (3.9) must be valid for all time and since

$$v_2(r, z, \infty) = \frac{\partial v_2}{\partial t} (r, z, \infty) = 0$$

we obtain

$$0 = F + \mu \left[\frac{\partial^2 v_1}{\partial r^2} + \frac{1}{r} \frac{\partial v_1}{\partial r} - \frac{v_1}{r^2} + \frac{\partial^2 v_1}{\partial z^2}\right] \tag{3.10a}$$

$$\rho \frac{\partial v_2}{\partial t} = \mu \left[\frac{\partial^2 v_2}{\partial r^2} + \frac{1}{r} \frac{\partial v_2}{\partial r} - \frac{v_2}{r^2} + \frac{\partial^2 v_2}{\partial z^2}\right] \tag{3.10b}$$

Separation of eq. (3.10b) can be effected by inserting the solution $v_2(r, t, t) = R_{(r)} Z_{(z)} T_{(t)}$ from which we obtain

$$\frac{\rho}{\mu} \frac{1}{T} \frac{dT}{dt} = \frac{1}{R} \left[\frac{d^2 R}{dr^2} + \frac{1}{r} \frac{dR}{dr} - \frac{R}{r^2}\right] + \frac{1}{Z} \frac{d^2 Z}{dz^2} \tag{3.11}$$

Since eq. (3.11) must be valid for all times and values of z and r, both sides of the equality must equal the same constant. Therefore,

$$\frac{1}{\nu}\frac{1}{T}\frac{dT}{dt} = -\lambda^2 \tag{3.12a}$$

where

$$\nu = \frac{\mu}{\rho} = \text{kinematic viscosity}$$

and

$$\frac{1}{R}\left[\frac{d^2R}{dr^2} + \frac{1}{r}\frac{dR}{dr} - \frac{R}{r^2}\right] + \frac{1}{Z}\frac{d^2Z}{dz^2} = -\lambda^2 \tag{3.12b}$$

Further separation of (3.12b) yields

$$\frac{d^2R}{dr^2} + \frac{1}{r}\frac{dR}{dr} - \frac{R}{r^2} + A^2R = 0 \tag{3.13a}$$

$$\frac{d^2Z}{dz} = -BZ \tag{3.13b}$$

where

$$\lambda^2 = A^2 + B$$

Solution of eqs. (3.12a), (3.13a), and (3.13b) gives

$$v_2(r, z, t) = \sum_{i=1}^{\infty} -C_i Z_1(A_i r) \cos B_i z e^{\lambda_i^2 \nu t} \tag{3.14}$$

where $Z_1(A_i r)$ is the first order Bessel function, and

$$\lambda_i^2 = A_i^2 + B_i$$

By recalling from eq. (3.8) that

$$v_2(r, z, 0) = -v_1(r, z)$$

we obtain

$$v(r, z, t) = \sum_{i=1}^{\infty} C_i \cdot Z_1(A_i r) \cdot \cos(B_i z) \cdot [1-e^{-\lambda_i^2 \nu t}] \tag{3.15}$$

where

$$\lambda_i^2 = A_i^2 + B_i$$

The average flow over a cross-section of the canalicular duct is

$$\bar{v}(t) = \int_0^a dr \int dt \quad v(r, z, t) = D_d \sum_{i=1}^{\infty} D_i [1-e^{-\lambda_i^2 \nu t}] \tag{3.16}$$

Taking the Laplace transform of eq. (3.16) to calculate a system transfer function we obtain

$$\frac{\bar{v}(s)}{\alpha(s)} = D_d \sum_{i=1}^{\infty} \frac{D_i}{\tau_i s + 1} \tag{3.17}$$

where

$$\tau_i = \frac{1}{\lambda_i^2 \nu}$$

The dynamic characteristics of the viscous drag of endolymph can therefore be represented by a parallel sum of first order lag networks as shown in Fig. 3.4. The coefficients C_i and τ_i are found by solution of eq. (3.10a) for $v_1(r, t)$ and then equating

$$v_1(r, z) = -v_2(r, z, 0) = \sum_{i=1}^{\infty} C_i Z_1(A_i r) \cos B_i z \, e^{-\lambda_i^2 \nu t} \tag{3.18}$$

Multiplying both sides of eq. (3.18) by

$$Z_j(A_j r) \cos B_j r$$

and utilizing the orthogonality relations such as

$$Z_1'(k) = -Z_2(k)$$

and integrating both sides of the resultant expression out to the boundary conditions $v_1(a) = 0$, the coefficients can be calculated by the solution of

$$\int_0^a dr \int_0^a dz \; Z_1(A_k r)(\cos B_k Z) = \tag{3.19}$$

$$\int_0^a dr \int_0^a dz \sum_{i=1}^{\infty} C_i Z_1(A_i r) Z_1(A_k r) \cos B_i Z \cos B_k Z$$

Further calculation using "toroidal" coordinates to simplify introduction of the boundary conditions yields a simplified approximate solution from which one can evaluate the coefficients of eq. (3.17).

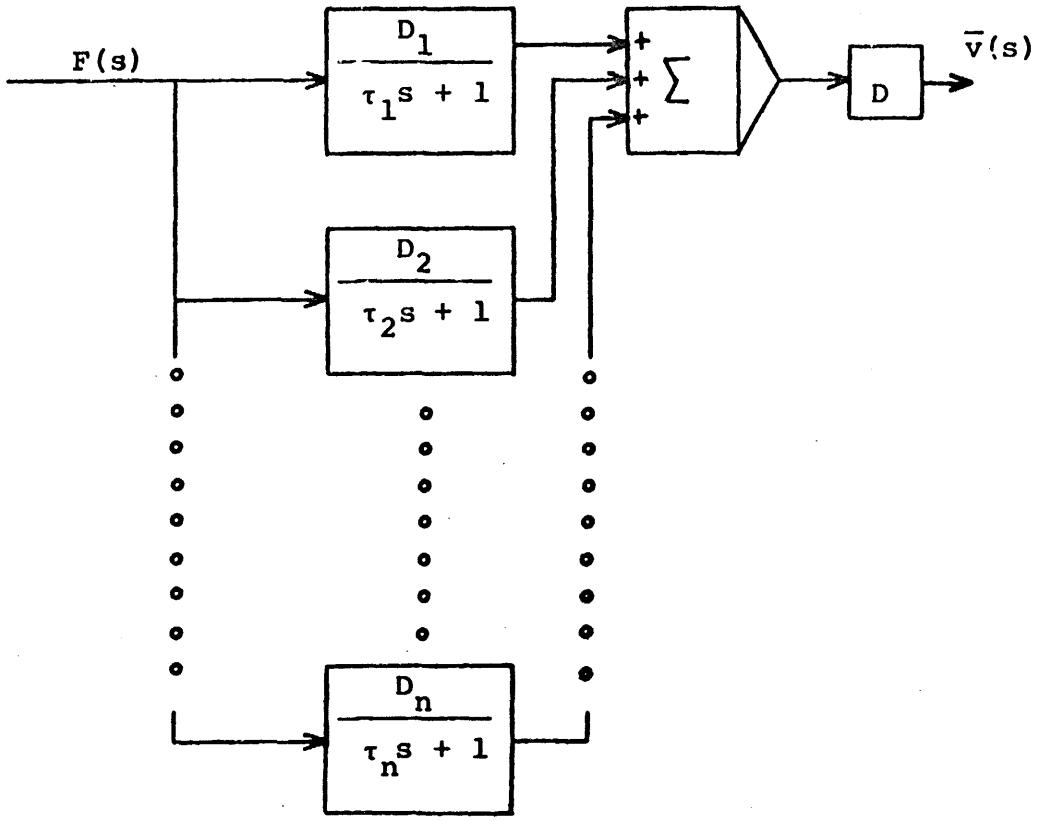


Figure 3.4
System block diagram for the average endolymph velocity ($\bar{v}$) in the canalicular duct from an input F(s)

For

$$a = 0.15 \text{ mm}$$

$$\nu = .852 \text{ cp/gm /cm}^3$$

$$\sum_{i=1}^{\infty} D_i = 1$$

$$\begin{aligned} D_1 &\approx 0.957 \\ D_2 &\approx 0.035 \\ D_3 &\approx 0.006 \\ \tau_1 &= \frac{1}{\lambda_i^2 \nu} \approx \frac{1}{220} \end{aligned} \tag{3.19a}$$

$$\tau_2 = \frac{1}{\lambda_2^2 \nu} \approx \frac{1}{1380}$$

$$\tau_3 = \frac{1}{\lambda_3^2 \nu} \approx \frac{1}{2840}$$

Since the approximation of the semicircular canal as a closed rigid torus is not strictly true and the coefficients as calculated can be in error by about 2%, the terms after $i = 2$ in the expansion of v_2 can be ignored, and since the time constant of the $\lambda_2^2 \nu$ exponential is a factor of seven faster than the first term, the hydromechanical viscous drag of the canalicular duct can for all practical purposes be considered a first order lag with a time constant of 1/220 sec.

The gain D_d of Fig. 3.4 as calculated by the evaluation of v_1 for a unit step input of F is

$$D_d = \frac{\bar{v}(\infty)}{u(t)} = \frac{a^2}{8\mu} \tag{3.20}$$

where

μ = viscosity of endolymph (in poise)

a = radius of canalicular duct (in cm)

R = large radius of torus

Which, for the human semicircular canal where a = 0.015 cm and μ = 0.852 cp, R = 0.3 cm

$$D_d = \frac{(0.015)^2}{8(0.00852)} = 3.3 \times 10^{-3} \tag{3.20a}$$

Recall from eq. (3.8a)

$$F = F_\phi - \frac{1}{r}\frac{\partial p}{\partial \phi}$$

where for the derivation of D_d were used the relations

$$F_\phi = \rho\ \alpha\ R \text{ and } \frac{1}{r}\frac{\partial p}{\partial \phi} = \frac{\Delta p}{2\pi R}$$

Thus the system transfer function for the average velocity of the endolymph in the canalicular duct (in the absence of a cupula) is given by:

$$\bar{v}(s) = \frac{3.3 \times 10^{-3}}{\frac{1}{200}s + 1}\left(\rho R\, \alpha(s) - \frac{\Delta p(s)}{2\pi R}\right) \tag{3.20b}$$

where

ρ = density of endolymph (gm/cm)

R = large radius of the torus (cm)

α = input angular acceleration (rad/sec^2)

Δp = pressure differential across the cupula

It now remains to examine in detail the influence of the cupula on the dynamic characteristics of the semicircular canals.

3.4 The Influence of Cupular Drag, Inertia, and Elasticity on the Dynamic Responses of the Semicircular Canal

Since the cupula is neutrally buoyant in the endolymph which surrounds it, many investigators have ignored the effect of its drag and inertial reaction in calculations of the performance of the semicircular canals. If, however, the cupula is considered a free body and the torques acting upon it are summed, then its own dynamic properties can be determined in terms of its physical characteristics.

The two principal external sources of torque acting on the cupula and its surrounding endolymph are that caused by the pressure differential across the ampulla and the inertial acceleration of the cupula itself. Note that an angular acceleration of the endolymph in the duct produces a pressure gradient torque on the cupula which opposes the inertial reaction torque of the cupula itself. These externally applied torques must then be exactly balanced by the torques required to overcome the drag, inertial reaction and stiffness of the cupula. From this we obtain

$$(M_p - M_I) = J_c \ddot{\theta}_c + D_c \dot{\theta}_c + K \theta \qquad (3.21)$$

where

M_p = torque on cupula due to a pressure differential across the ampulla

M_I = inertial reaction torque due to an input angular acceleration α

J_c = inertia of the cupula and its surrounding endolymph

D_c = viscous drag coefficient of the cupula

K = stiffness of the cupula

From the recent histological studies by Igarashi of the temporal bones from humans, cats, and squirrel monkeys, the dimensional characteristics of the membranous labyrinth have been accurately measured.[91] The height, width, and general shape of the cross section of the crista, the cupula, and the membranous ampulla have all been evaluated. From this information it is apparent that the cupula, crista, ampulla system can best be modelled as a rigid pie-shaped wedge with a circular cross section and hinged along its bottom edge at the crista as shown in Fig. 3.5. From this model the torque terms of eq. (3.21) can now be evaluated.

3.4.1 Cupula gain constants and torque inputs

From Fig. 3.5 the gain equivalence between cupula velocity and the flow velocity in the canalicular duct can be obtained by equating the volume of efflux from the duct to the volume displaced by deviation of the cupula, from which we obtain:

$$\dot{\theta}_c = \frac{a^2}{B^3} \bar{v}(t) \tag{3.22}$$

which for the human where a = 0.015 cm and B = 0.06 cm is

$$\dot{\theta}_c = \bar{v}(t) = R\dot{\xi} \tag{3.22a}$$

The torque M_p on the cupula due to a pressure differential across the ampulla can be computed as the force exerted on the

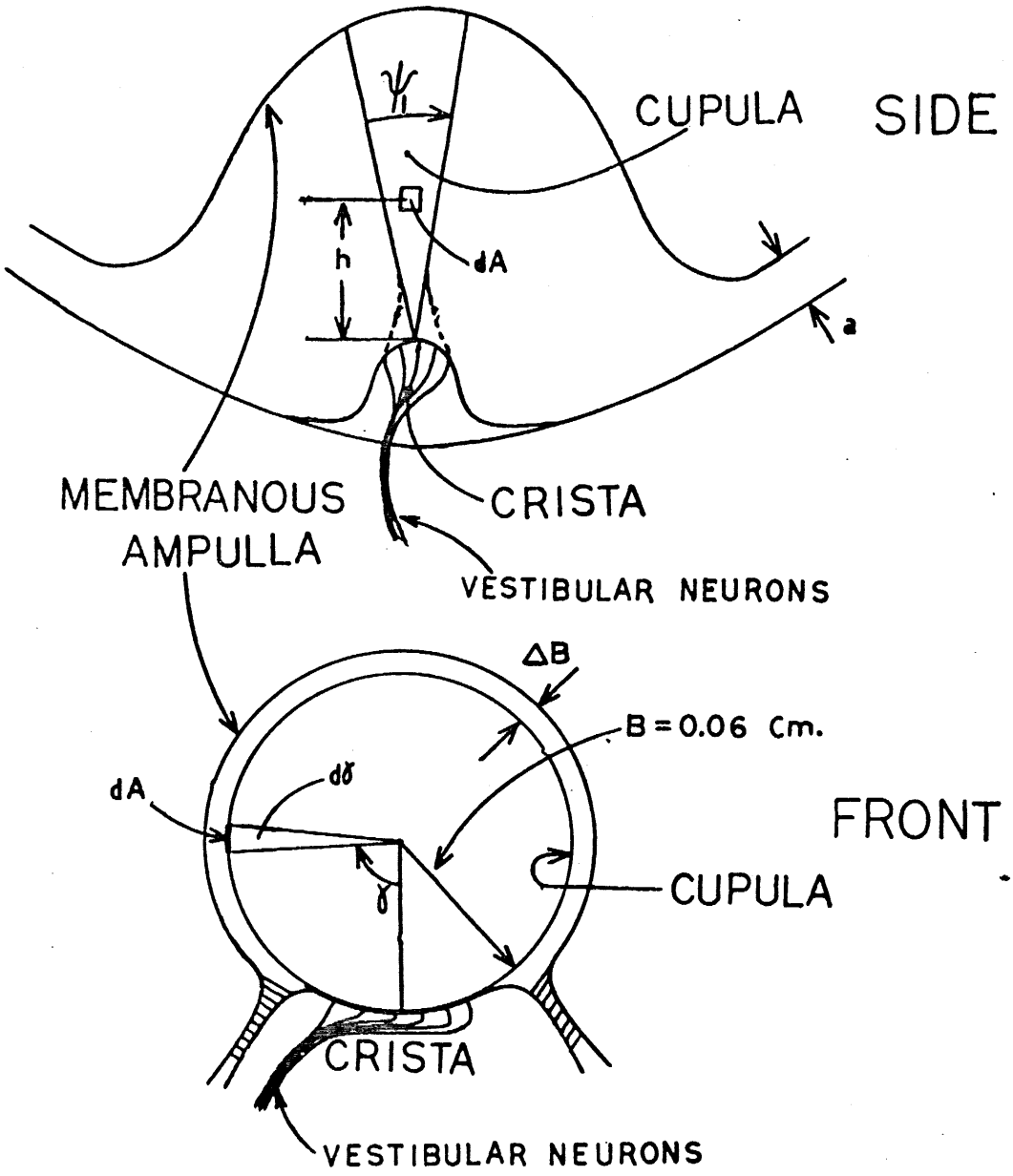


Figure 3.5
A physical model for the cupula

cross-sectional area times the moment arm from the pivot point at the crista to the centroid of the circular cross section from which obtains

$$M_c = \pi B^3 \Delta p \tag{3.23}$$

where

B = radius of the cupula's cross-sectional area

Δp = pressure differential

The inertial reaction torque M_I is given by the relation

$$M_I = J_c \alpha$$

thus

$$(\pi B^3 \Delta p - J_c \alpha) = J_c \ddot{\theta} + D_c \dot{\theta} + K\theta \tag{3.24}$$

The coefficients J_c, D_c and K will now be evaluated.

3.4.2 Viscous drag of the cupula

The torque on the cupula as a result of its viscous drag on the membranous ampulla can be calculated by integration of the torque on an elemental area at the periphery of the cupula:

$$M_d = D_c \dot{\theta}_c = \int dM_d = \int h \cdot df \tag{3.25a}$$

where

$$h = B[1 - \cos \gamma]$$

$$dF = \frac{\mu v_t dA}{\Delta B}$$

$$v_t = h\dot{\theta}_c$$

$$dA = h\, d\gamma\, B d\psi$$

thus

$$M_d = \frac{\mu B^4 \dot{\theta}_c}{\Delta B} \int_0^{\psi_1} d\psi \int_0^{2\pi} (1 - \cos \gamma)^3 \, d\gamma \qquad (3.25b)$$

$$M_d = 5\pi\mu \frac{B^4}{\Delta B} \dot{\theta}_c \psi_1 = D_c \dot{\theta}_c \qquad (3.25c)$$

where

M_d = viscous drag torque of the cupula

μ = viscosity of endolymph

B = radius of cupula's cross-sectional area

ΔB = clearance between cupula and membranous ampulla

$\dot{\theta}_c$ = angular velocity of cupula

ψ_1 = angular arc of the cupula in radians

From eq. (3.25c) we obtain

$$D_c = 5\pi\mu\psi_1 \frac{B^4}{\Delta B} \qquad (3.26)$$

3.4.3 The inertial reaction of the cupula

From the model of Fig. 3.5, the cupula and its adjacent endolymph form a section of torus. The inertia of a torus is given by

$$\left.\begin{aligned} J_T &= M(R^2 + \tfrac{3}{4}r^2) \\ M &= 2\pi^2 \rho r^2 R \end{aligned}\right\} \qquad (3.27)$$

where

J_T = moment of inertia (gm cm^2)

R = central radius of torus (cm)

r = duct radius of torus (cm)

ρ = density of material (gm/cm^3)

The torus formed by rotation of the cupula about its crista has both radii R and r equal to B, and the central angle subtended (ψ_1) is approximately 2 radians. Therefore its inertia J_c is given by

$$J_c = \frac{2}{2\pi} \rho [2\pi^2 B^3] [\frac{7}{4} B^2] = \frac{7}{2} \pi B^5 \rho \qquad (3.28)$$

3.4.4 Cupular elasticity

Whereas the influence of viscous drag of the cupula-ampulla interface can be estimated by knowledge of the dimensional characteristics, no such quantitization of cupula stiffness or elasticity can be calculated. The physical dimensional measurements that have been made on the cupula are from various histological studies; however, no researcher has yet been successful in removing a cupula either in pieces or intact from the membranous ampulla and in any way measured its physical properties. Experiments such as those of Crampton have shown that the cupula must be neutrally buoyant in the endolymph because it is not appreciably influenced by linear acceleration; those of Lowenstein have shown that it must form a near hermetic seal at the cupula-ampulla interface, and those of Van Egmond, et al, have shown that the cupula must have elasticity because it does return under its own influence to its center position.[44,72,151]

As mentioned above, the effect of cupula elasticity is to bring about a differential pressure across the canalicular duct proportional to the displacement of the cupula. By integration of eq. (3.22a) it is apparent that cupula displacement is in

turn related to the flow of endolymph into the ampulla. Therefore the cupula elasticity introduces an integration term in the pressure feedback to the canal duct. The feedback gain K represents the elasticity of the cupula and is uncalculable for lack of knowledge of the physical characteristics of the cupula.

3.5 A Dynamic Model for the Semicircular Canals

The influences of the viscous drag of the endolymph in the canalicular duct and of the inertia, drag and elasticity of the cupula can now be combined to provide a model for the dynamic performance of the semicircular canals. Expansion of the schematic diagram of Fig. 3.2 by implementation of eqs. (3.8a), (3.17), (3.20b), (3.21), and (3.22) yields a schematic representation of the cupula endolymph system as shown in Fig. 3.6.

By use of this model the cupular displacement which results from angular acceleration stimulation can be calculated to be

$$\frac{\theta_c(s)}{\alpha(s)} = \frac{D_d\left[\rho R - \frac{J_c}{2\pi^2 RB^3}\right]}{(\tau_1 + \frac{D_d + J_c}{2\pi^2 RB^3})s^2 + (\frac{D_d D_c}{2\pi^2 RB^3} + 1)s + KD_d} \qquad (3.28)$$

For the human semicircular canals

$D_d = 3.3 \times 10^{-3}$

$R = 0.3$ cm

$B = 0.06$ cm

$\tau_1 = .0045$ sec

$\rho = 1$ gm/cm^3

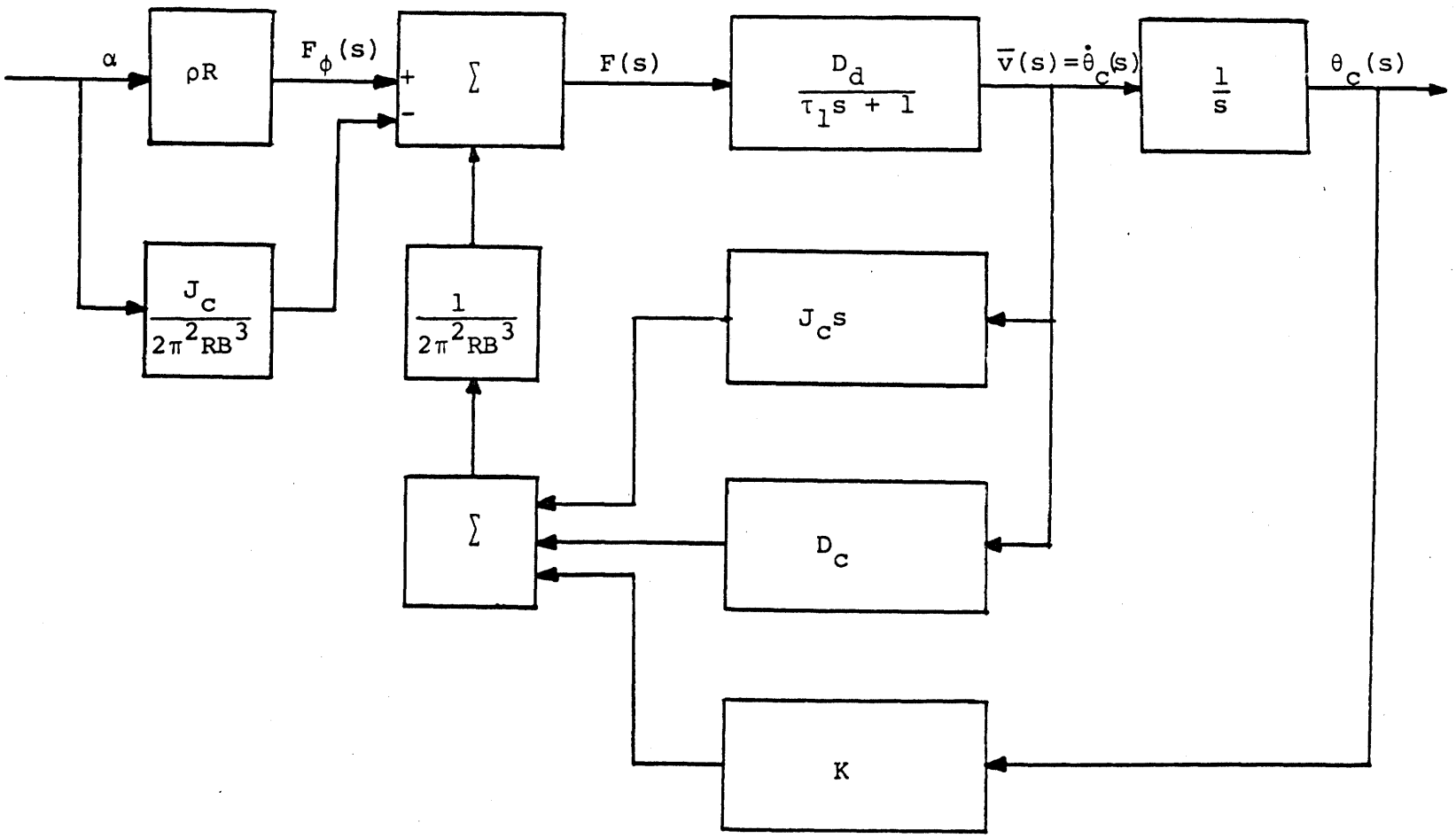


Figure 3.6
Schematic model for cupula displacement (θ_c) resulting from angular acceleration (α) inputs

$\mu = 0.0085$ poise

$\psi_1 \sim 1$ rad

From eq. (3.26)

$$D_c = 5\pi\mu\psi_1 \frac{B^4}{\Delta B} = \frac{1.74 \times 10^{-6}}{\Delta B}$$

From eq. (3.28)

$$J_c = \frac{7}{2} \pi B^5 \rho = 8.6 \times 10^{-6} \text{ gm cm}^2$$

$$\frac{1}{2\pi^2 RB^3} = 7.85 \times 10^2$$

Each of the terms in the transfer function for $\theta_c(s)/\alpha(s)$ can now be evaluated and the influence of the cupula's characteristics can be estimated.

The numerator of eq. (3.28) when evaluated for the human canals is

$$D_d[\rho R - \frac{J_c}{2\pi^2 RB^3}] = 10^{-3}$$

The reflected inertia of the cupula contributed less than 1% to this coefficient. The coefficient of the second order denominator term is

$$\tau_1 + \frac{D_d J_c}{2\pi^2 RB^3} = 4.5 \times 10^{-3} + 2.22 \times 10^{-5} \approx \frac{1}{220}$$

Here also the inertia of the cupula contributed less than 1% to the coefficient. The coefficient of the first order term in the denominator is

$$1 + \frac{D_d D_c}{2\pi^2 RB^3} = 1 + \frac{4.5 \times 10^{-6}}{\Delta B}$$

The amount of damping contributed by the viscous drag of the cupula on the ampulla is then clearly a function of the separation ΔB between the ampulla wall and the cupula. The value of ΔB can only be estimated from the photomicrograph slides from histological studies. However, even then the shrinkage which results from the fixants could have rather gross effects on the estimates.

From the histological studies of Igarashi, it appears that the separation ΔB is of the order of less than 10^{-4} cm. Further, it has been shown in animals, by injection of dye into the endolymph, that the cupula forms a near hermetic seal to the membranous ampulla. In addition, for such extremely small dimensions the irregularities of the ampulla wall might well contribute as much or more damping as the viscous drag of the endolymph.

In summary, it appears that the drag of the cupula on its ampulla wall can be a significant contributor to the dynamic properties of the semicircular canals.

Finally, the constant term in the denominator of eq. (3.28) is given by the expression

$$K D_d = 3.3 \times 10^{-3} K$$

Since none of the physical properties of the cupula have been measured, it is impossible even to estimate the value of K.

By evaluating all of the coefficients of eq. (3.28) and dividing through by the coefficient of the second order

denominator term the transfer function for cupular displacement which results from angular acceleration is

$$\frac{\theta_c(s)}{\alpha(s)} = \frac{0.22}{s^2 + 220\left(1 + \frac{4.5 \times 10^{-6}}{\Delta B}\right)s + .07K} \tag{3.29}$$

By comparing the denominator to the original equation of Van Egmond, Groen, and Jongkees

$$\ddot{\xi} + \frac{\pi}{\theta}\dot{\xi} + \frac{\Delta}{\theta}\xi = \alpha \tag{3.1}$$

we find that

$$\ddot{\theta} + 220\left(1 + \frac{4.5 \times 10^{-6}}{\Delta B}\right)\dot{\theta} + .07K\theta = .22\alpha$$

Using

$$\theta_c = R\xi = 0.3\xi \tag{3.22a}$$

$$\ddot{\xi} + 220\left(1 + \frac{4.5 \times 10^{-6}}{\Delta B}\right)\dot{\xi} + .07K\xi = .73\alpha$$

Therefore the calculated values of $\frac{\pi}{\theta}$ and $\frac{\Delta}{\theta}$ are

$$\frac{\pi}{\theta} = 220$$

$$\frac{\Delta}{\theta} = .07K$$

for

$$\Delta B \approx 10^{-4} \text{ cm}$$

From the previous sections the values of $\frac{\pi}{\theta}$ and $\frac{\Delta}{\theta}$ measured from objective and subjective responses are approximately 10 rad/sec and 1 $\frac{\text{rad}^2}{\text{sec}^2}$ respectively.

Thus the calculated damping to inertia ratio for an "ideal" rigid torus-shaped acceleration sensor with the physical

dimensions of the human semicircular canals is at least an order of magnitude higher than the subjective responses indicate. Further, although the stiffness coefficient of the cupula is not known, a value of $10 < K < 100$ dyne cm/rad is at least a realistic value for a gelatinous material such as we assume the cupula to be.

3.6 Summary and Conclusions

The analyses of this chapter have shown that the effects of the viscous drag of the endolymph in the duct of the semicircular canals can be accurately represented by a first order system with a time constant of about 0.05 sec. They further show that the drag of the cupula on the wall of the membranous ampulla contributes some additonal damping to the cupula-endolymph system. It has been shown that the fluid dynamic characteristics of the human semicircular canals have an order of magnitude higher frequency response than is observed from subjective and objective tests of the vestibular system.

It appears that the observed high frequency responses of the human semicircular canals are limited more by low carrier frequency of the vestibular neurons and that the experimentally measured values of the coefficients $\frac{\pi}{\theta}$ and $\frac{\Delta}{\theta}$ are more a measure of the response of the vestibular neurons, the "computation time" of the central nervous system, and neuro-muscular delays than of the dynamic response characteristics of the semi-circular canals.

Further consideration of the semicircular canals as flexible rather than rigid structures, which would then be influenced by the pressure variations of the perilymph in the bony labyrinth, might show the existence of additional modes of response. Such nonlinear behavior, if it exists, would have its influence at low frequencies because of the larger mass and inertia of the perilymph.

CHAPTER 4

RESPONSE OF THE SEMICIRCULAR CANALS TO CALORIC STIMULATION

4.1 Introduction

In 1860 it was found by Brown-Sequard that irrigation of the external auditory canal caused vertigo and occasional nausea. It was later shown by Breuer (1889) that caloric stimulation provoked nystagmus.

Barany, in 1906, proposed that the observed nystagmus from caloric stimulation was the result of a convection current of endolymph and a corresponding cupula displacement which were brought about by the presence of a thermal gradient across the lateral semicircular canal. This temperature gradient was effected by irrigation of the external auditory meatus. Since 1906 an overwhelming body of evidence has been uncovered by researchers in accord with Barany's convection theory.

Using an optic nystagmographic method, Dohlman (1925) showed that the slow phase velocity of caloric nystagmus was related to the difference between the temperature of the water used for irrigation and the normal body temperature at the subject's tympanic membrane. The work of Jongkees (1949), Mittermaier (1954), and Henriksson (1956) and others has further substantiated this functional relationship.

The temperature gradient across the lateral semicircular canal due to caloric irrigation was measured by Dohlman (1925) in a cadaver and by Cawthorne and Cobb (1954) in anesthetized human subjects. Although unpredictable factors such as lack of vasodilation, disruptive surgery, and effects of anesthesia were present, the results of these experiments are quite similar and again conform to Barany's proposals. Schmalz, in 1932, using a mathematical approach, provided descriptions of the physics of angular and caloric stimulation of the semicircular canal.

More recently, Bergstedt (1961), using a centrifuge, and Kellogg and Graybiel (1965), using zero-g parabolic flights, have shown a direct modulating influence of linear acceleration on the amplitude and duration of caloric nystagmus.

The remainder of this chapter is directed toward the interpretation of the results of previous investigators in the context of control systems analysis, and the presentation and experimental verification of a dynamic model for caloric stimulation.

4.2 A Dynamic Model for Caloric Stimulation

4.2.1 The thermal gradient across the lateral semicircular canals

In fig. 4.1, the proximity of the ampullar section of the lateral semicircular canal to the external auditory canal, and the proximity of the duct of the lateral canal to the brain (which is thermally regulated by blood flow) are illustrated. When the external auditory canal is irrigated at a temperature

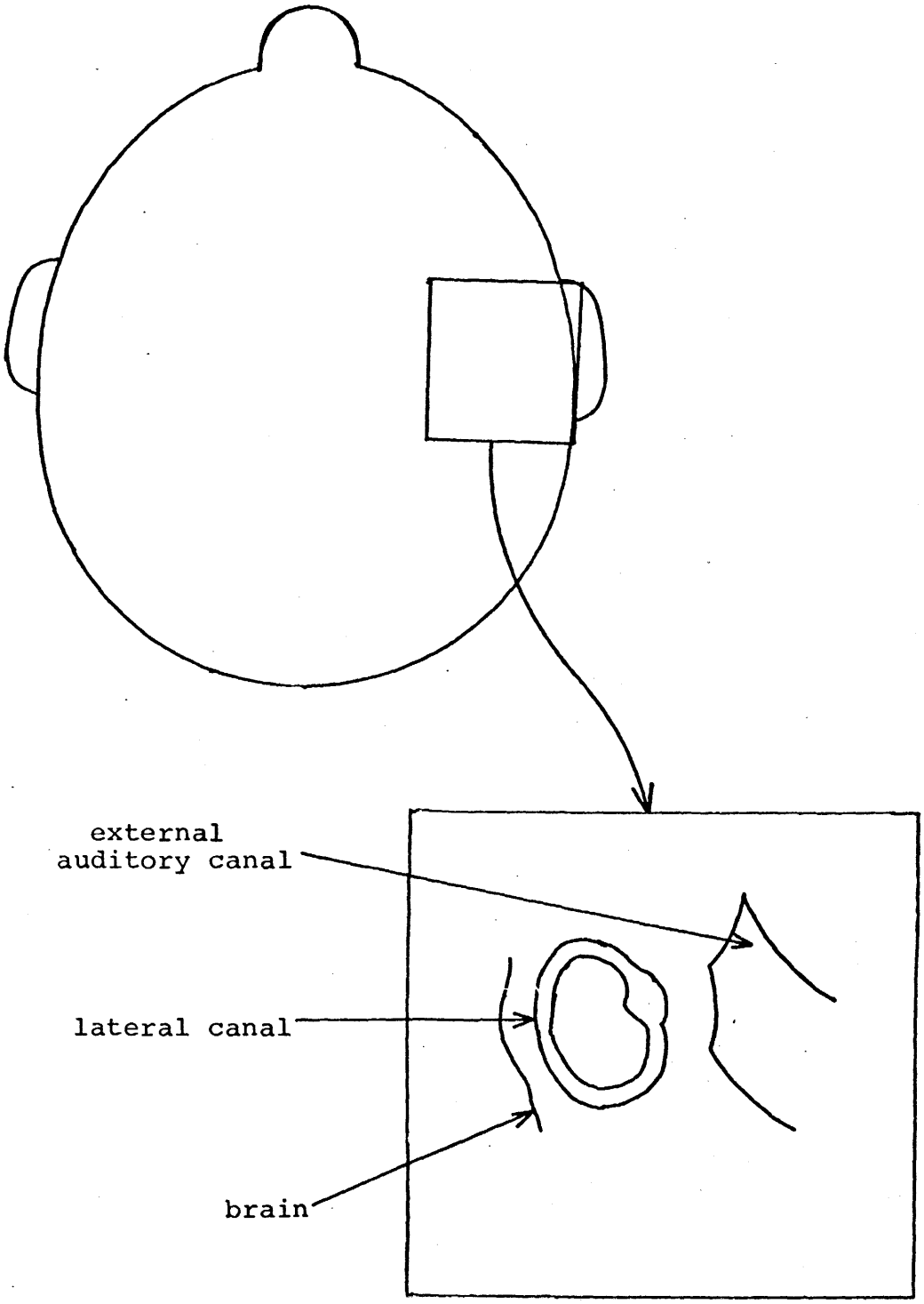


Figure 4.1
Position of lateral semicircular canal
with respect to skull

which is different from body temperature. The thermal conductivity of the bone and perilymph of the labyrinth causes a temperature gradient across the lateral canal. The aforementioned works of Dohlman and Cawthorne and Cobb measured the time history of this temperature gradient, and the work of Cawthorne and Cobb is particularly amenable to interpretation in the context of a control theory description of vestibular reaction to caloric stimulation.[47,20]

The thermal system of the vestibular apparatus is a spatially distributed system of bone, fluids, tissue, and air. The membranous labyrinth is totally enclosed in the bony labyrinth and is surrounded by the perilymph space. It is possible to describe the thermal system by a distributed parameter differential equation. However, the difficulties involved in formulating the equations of such a spatially distributed system and giving a reasonably precise representation of it are not justifiable because a sufficiently accurate description can be provided by analysis of existing measurements.

It is necessary to point out that the measurements of Cawthorne and Cobb were carried out on patients during the operation of membranous labyrinthectomy for Ménière's Disease. They were under general anesthesia, the lateral canal was surgically exposed, and miniature thermocouples were inserted into it. Thus the measurements were affected by surgical disturbance of the perilymph space and suppression of vasodilation in an unpredictable way. However, on four subjects the results were consistent, and although marked changes were noted in the amplitude of the temperature gradient, the form of its time

variation remained consistent from subject to subject. The results of their measurements are shown in fig. 4.2.

Although the assumption of system linearity is tenuous, an approximate dynamic model can be calculated by application of linear system theory. The model can then be compared to experimental data for verification of the linearity assumption.

Recall that for a linear system the weighting function w(t) can be computed from the time history of the output associated with a transient input to the system. This can be effected by implementation of the equations:

$$g(t) = \int_0^t w(t - \tau)\, f(\tau)\, d\tau \qquad (4.1)$$

where the system transfer function W(s) is given by

$$W(s) = \mathcal{L}\, w(t) = \int_0^\infty w(t)\, e^{-st}\, dt \qquad (4.2)$$

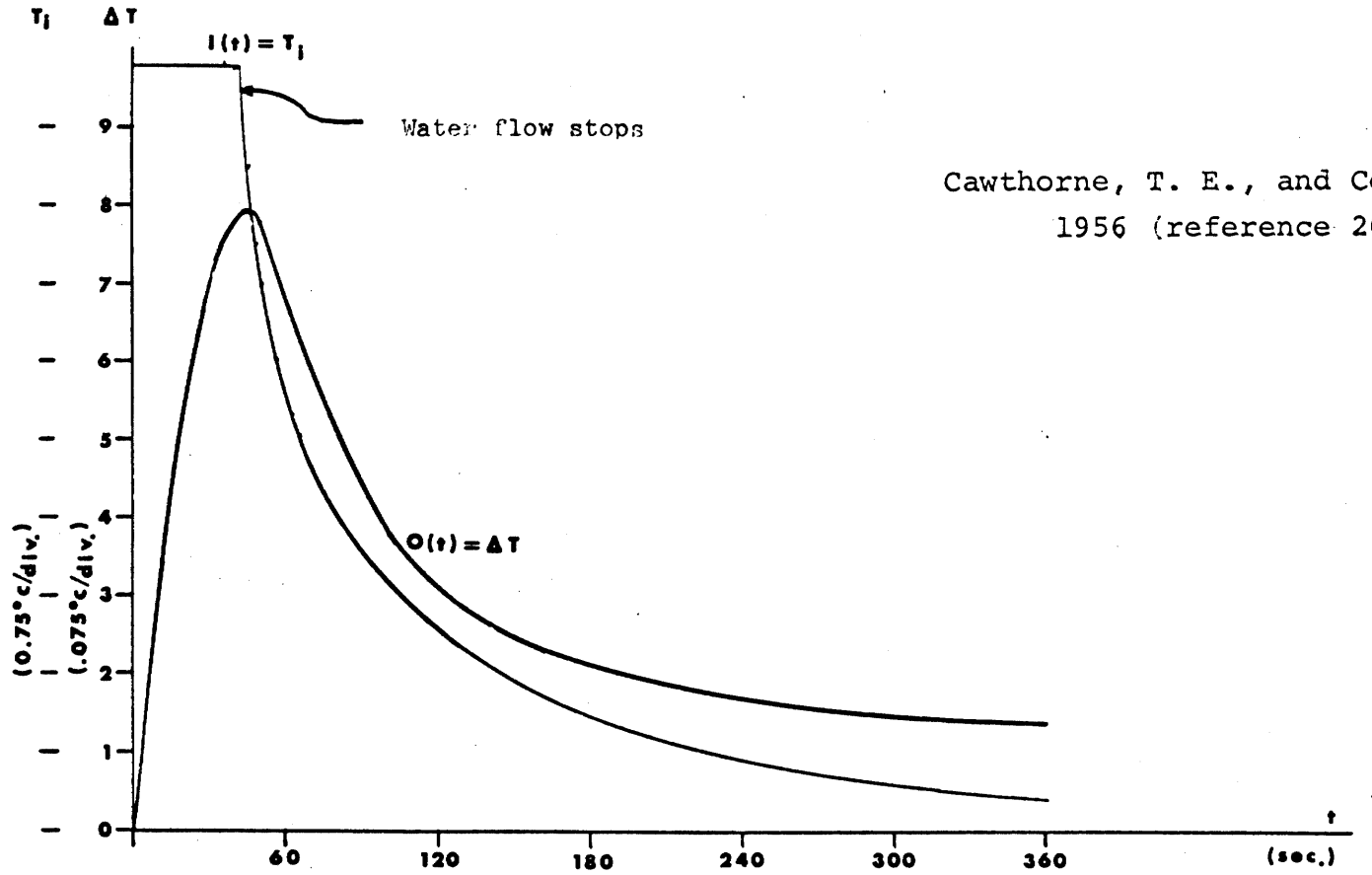
g(t) = output of system

f(t) = input to system

w(t) = weighting function (response to a unit impulse)

For a finite set of n uniformly spaced data points at intervals k, eq. (4.1) can be written in discrete form:

$$g(n) = \sum_{k=0}^{n} w(n - k)\ \ f(k) \qquad (4.3)$$



Cawthorne, T. E., and Cobb, W. A.
1956 (reference 20)

Figure 4.2

Time history of temperature across the lateral semicircular canal (ΔT) in response to caloric irrigation in the external auditory canal. The temperature at the tympanic membrane T_i is also plotted as a function of time.

from which

$$w(n) = \frac{1}{x(o)} \left[g(n) - \sum_{k=0}^{n-1} w(k)\ f(n - k) \right] \qquad (4.4)$$

Application of eq. (4.4) to the data of fig. 4.2 shows that the thermal system weighting function for the perilymph, bone, and labyrinth structure can be approximated by a first order lag. The system transfer function for the temperature gradient across the lateral semicircular canal due to an input temperature at the tympanic membrane is given by:

$$W_T(s) = \frac{\Delta T}{T_i}(s) = \frac{K}{\tau s + 1} \qquad (4.5)$$

where:

ΔT = temperature gradient across the lateral semicircular canal

T_i = temperature at the tympanic membrane (above body temperature)

τ = thermal lag time constant

K = system gain

From a minimum integral squared error fit of the data of fig. 4.2, the best values of the coefficients are

τ = 25 sec

K = 0.1

Fig. 4.3 presents both the measured temperature gradient and the gradient as computed from the analog model. The calculated response from the first order approximation of the

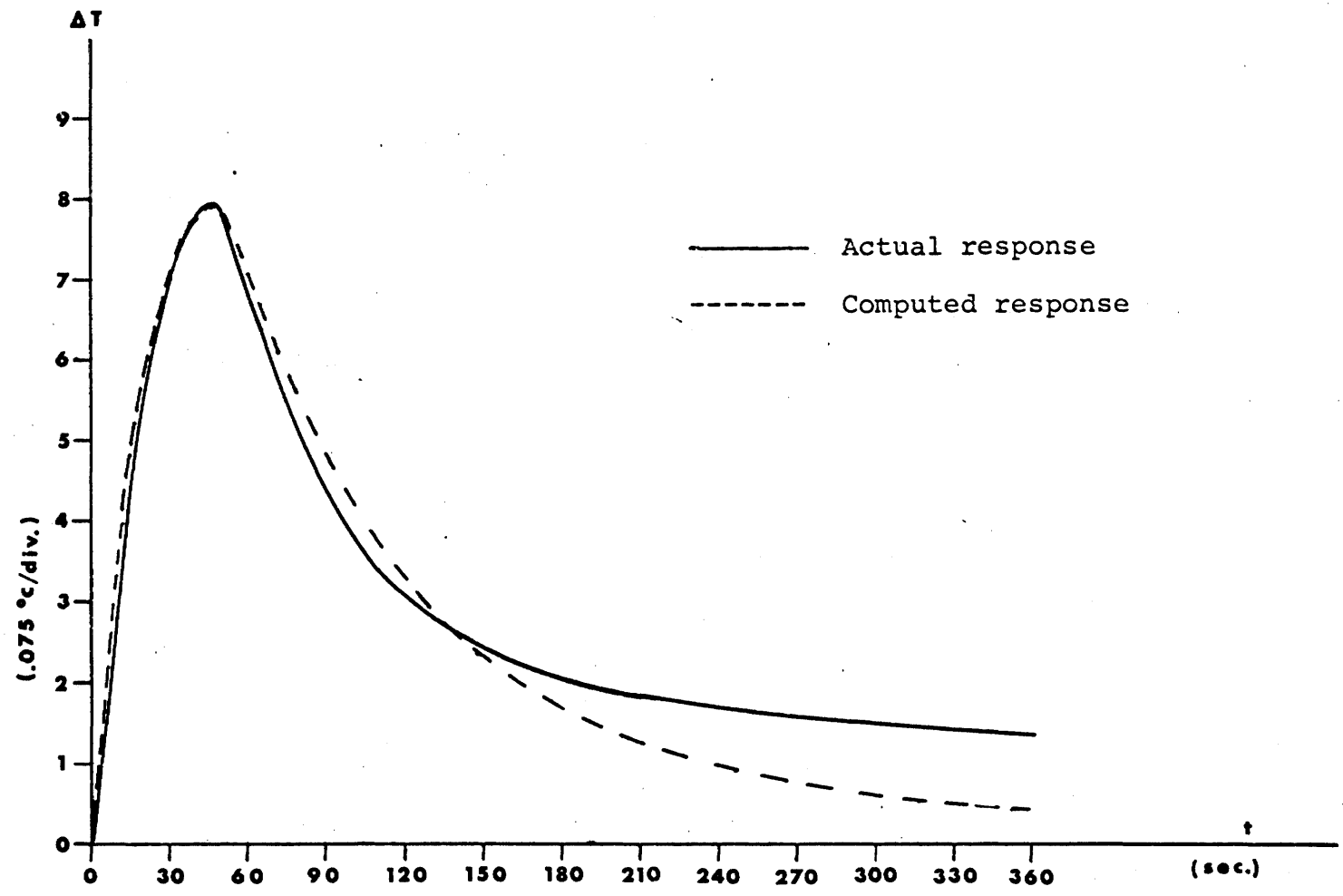


Figure 4.3
Measured and calculated temperature differences (ΔT)
across lateral semicircular canal
for stimulus applied in figure 4.2

system is better than 5% accurate for the first 120 seconds, and since there was suppression of vasodilation and thus the return to normal temperature was inhibited, there is considerable doubt about the validity of the measurements after 120 seconds. The variations in the amplitude of the gradient from subject to subject reflect only a change in the gain constant K. This variation ranges from $0.02 < K < 0.1$ for the subjects tested.

4.2.2 Torque induced on a thin torus of fluid in a uniform temperature gradient field

When a thin torus of fluid is simultaneously placed in an acceleration field and a uniform temperature gradient field, an angular torque is exerted on the fluid. This torque can be evaluated by integration of the torque about the center of the torus on an elemental volume of fluid in the closed ring of the torus. A temperature gradient, acting through the coefficient of expansion of the fluid and gravity gives rise to a force on the elemental volume, from which

$$dM = \frac{\partial \rho}{\partial T} \frac{\pi r^2 g R^2 \Delta T \cos \phi}{2} \int_0^{2\pi} (\cos \theta - \cos^2 \theta)\, d\theta \qquad (4.6)$$

$$M = - \frac{\pi^2 r^2 R^2 g}{2} \cdot \frac{\partial \rho}{\partial T} \cdot \Delta T_t \cos \phi \qquad (4.6a)$$

where

r = radius of cross-section of canal

R = radius of canal

$\frac{\partial \rho}{\partial T}$ = change in density of fluid with temperature

g = acceleration due to gravity

ΔT_t = temperature difference across canal

ϕ = angle between the plane of the thermal gradient and the perpendicular to the direction of g

M = torque exerted on fluid

Using the dimensions of the human semicircular canals and the coefficient of expansion of endolymph from Appendix A

$R = 0.3$ cm

$r = 0.015$ cm

$\frac{\partial \rho}{\partial T} = -.44 \times 10^{-3}/°C$

the steady state torque on the endolymph of the human lateral semicircular canal is

$$M = 4.0 \times 10^{-8} \, g \cos \phi \cdot \Delta T_t \text{ dyne cm.} \tag{4.7}$$

The inertia of a static "thin" torus of fluid, or a ring of invicid fluid is given by:

$$I = 2 \pi^2 r^2 R^3 \rho \tag{4.8}$$

Thus the angular acceleration (α) which will produce an equivalent torque is

$$\alpha = \frac{M}{I} = \frac{1}{4R} \left(\frac{\partial \rho}{\partial T}\right) g \, \Delta T_t \cos \phi \tag{4.9}$$

For the human lateral semicircular canal:

$$\alpha = 20 \, \Delta T_t \cos \phi \, °/sec^2 \tag{4.10}$$

Thus the physiological equivalent of an angular acceleration is generated as a result of caloric stimulation at the tympanic

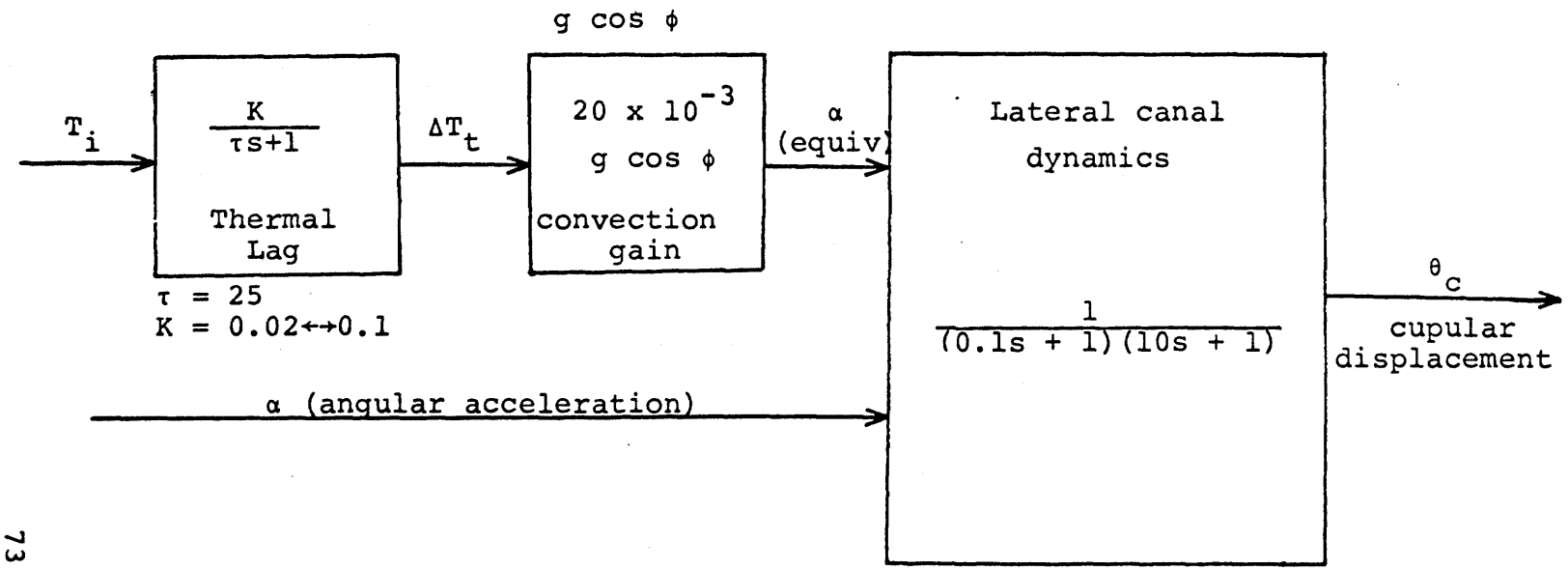


Figure 4.4
Block Diagram for Caloric Stimulation

membrane. The displacement of the cupula of the lateral semicircular canal as a result of caloric stimulation can now be evaluated. As illustrated in fig. 4.4, the temperature input to the tympanic membrane is transformed into a temperature differential across the lateral canal by the thermal inertia and conductivity of the labyrinth. This temperature differential interacts with the gravity field and produces an accelerating torque on the endolymph. The dynamic response of the semicircular canals to angular accelerations, as considered in the previous chapter, then provides the relationship between cupular displacement and the thermally induced acceleration.

4.2.3 The influence of vasodilation on caloric response

It has been well established that there is a compensatory mechanism to regulate the temperature of the vestibular apparatus.[97] This is effected by vasodilation which modifies blood flow to take heat away from or bring heat into the vestibule. The influence of this compensatory mechanism as it applies to human vestibular caloric response has been little studied and virtually no data is available from which to include its effect into an analytic vestibular model.

It has been shown by Jongkees and others that use of drugs which influence vasodilation directly affects the duration of slow phase caloric nystagmus.[105] Jongkees has also shown that caloric nystagmus disappears completely during a 6 minute irrigation even when ice water is used.[104]

From what little information is available it appears that vasodilation has the effect of destroying the temperature

gradient across the lateral canal during prolonged irrigations of several minutes, and thus it may be possible to include its effect in the model as a cascaded lead-lag with a long time constant of about 3 minutes. However, there are not sufficient data to justify such a modification, and since most clinical vestibular tests utilize irrigations of 40 seconds or less and the total durations of nystagmus are of the order of three minutes, this effect will not be included in the current model but rather offered as a suggestion for future research.

It now remains to compare the proposed model with old and new experimental results to attest to its validity.

4.3 Experimental Verification of Caloric Model

There exists in the literature several sets of experimental data which attest to the validity of the proposed model. Of these, a comparative study of thresholds of acceleration to caloric thresholds, the sensitivity of caloric nystagmus to linear acceleration, and the time history of slow phase velocity of caloric nystagmus provide the most conclusive comparisons.

Many researchers in the field have investigated the threshold level for the perception of angular acceleration in man. The value of this threshold has been measured by many techniques, some of which apply to the problem at hand. The physiological reasons for this threshold are still a subject of debate with some researchers arguing that it results from computation in the central nervous system, some arguing in favor of a mechanical "dead zone" of the cupula, and still others favoring a "neural hysteresis" explanation. However, since the thermal lag of the

caloric model of fig. 4.4 is only a function of the physical properties of the thermal system, then there should be a direct comparison between the thresholds of caloric and angular acceleration perception.

From the measurements of Clark and Stewart, and Meiry, both of which utilize the forced-choice method of subjective response and a 75% correct identification of direction of rotation, the thresholds of angular acceleration for the lateral semicircular canal is of the order of $0.15°/sec^2$.[28,126] Therefore, from the dynamic model of fig. 4.4, the tnreshold for a constant input of T_i at the tympanic membrane is given by

$$T_{i(min)} = \frac{\alpha_{min}}{20\ K\ \cos\ \phi}$$

Since the range of thermal gain K ccmputed from the data of Cawthorne and Cobb is $0.02 < K < 0.1$, then for subjects whose $K = 0.1$

$$T_{i(min)} = 0.1°C$$

For subjects whose $K = 0.02$

$$T_{i(min)} = 0.5°C$$

These results compare favorably with the caloric threshold measurements of McLeod and Meek who found that 50% of their tested subjects exhibited a nystagmus response to a forty second irrigation with a 0.2°C increment above or below normal body temperature and 75% responded to ±0.5°C irrigations.[123] It appears that because of the long thermal lag, longer irrigation times would have shown the thresholds to be lower.

Kellogg and Graybiel have shown the acceleration dependence of caloric nystagmus by stimulating subjects during a sequence of parabolic zero-g flights.[106] Their results show that caloric nystagmus is suppressed during the zero-g portion and returns with increased duration and amplitude during the 1.5 to 2.0 g pullup. Lack of adequate instrumentation did not permit evaluation of the direct multiplicative effect on nystagmus that the model predicts. Bergstedt, utilizing caloric tests with subjects on a centrifuge, has shown a clear, nearly linear, relationship between the speed of slow phase nystagmus and linear acceleration for acceleration fields up to 2 g.[9]

The most conclusive verification of the caloric model results from comparison of the slow phase velocity of vestibular nystagmus, which is, as described in Chapter 2, a reasonable measure of cupular deflection, to the calculated values of cupular displacement.

Assuming, as in fig. 4.4, that the dynamic properties of the semicircular canal are those of the torsion pendulum, and that therefore the inertia of the fluid ring is considered constant, then the overall system transfer function from temperature input to cupular displacement can be written

$$\frac{\theta_c(s)}{T(s)} = \frac{20\ K/\tau_1\tau_2\tau_3\ \cos\phi}{(s + 1/\tau_1)(s + 1/\tau_2)(s + 1/\tau_3)} \qquad (4.11)$$

The time history of the motion of the cupula for a step input of caloric stimulation of amplitude T_i can be obtained from the solution of the equation:

$$\theta_c(t) = A\, T_i \left[\mathcal{L}^{-1} \frac{1}{s\left(s + \frac{1}{\tau_1}\right)\left(s + \frac{1}{\tau_2}\right)\left(s + \frac{1}{\tau_3}\right)} \right] \qquad (4.12)$$

where

$\theta_c(t)$ = time history of cupular displacement due to a step input of caloric irrigation

τ_1 = 25 sec = thermal lag coefficient

τ_2 = 10 sec = long time constant of lateral canal

τ_3 = 0.1 sec = short time constant of lateral canal

A = system gain constant

T_i = temperature at tympanic membrane (above normal body temperature)

In fig. 4.5 is presented the normalized calculated cupular displacement for a 40 second step input of caloric stimulus and for a step input which decays exponentially after 40 sec with a 60 sec time constant. The latter input is a good approximation to the actual stimulation during caloric irrigation because after the initial 40 sec irrigation the water flow is stopped and the temperature at the tympanic membrane returns to normal with a slow exponential decay rather than a step return.

Of the many published records of the time history of caloric nystagmus from Jongkees, Henriksson, Collins and others, the most striking fit of experimental data comes from the publication of Dohlman in 1925.[105,87,30,47] This data is plotted to a normalized scale in fig. 4.5 along with the calculated cupular response. The fit of this experimental data to the calculations from the model attests to the validity of the principles and assumptions upon which the model is based.

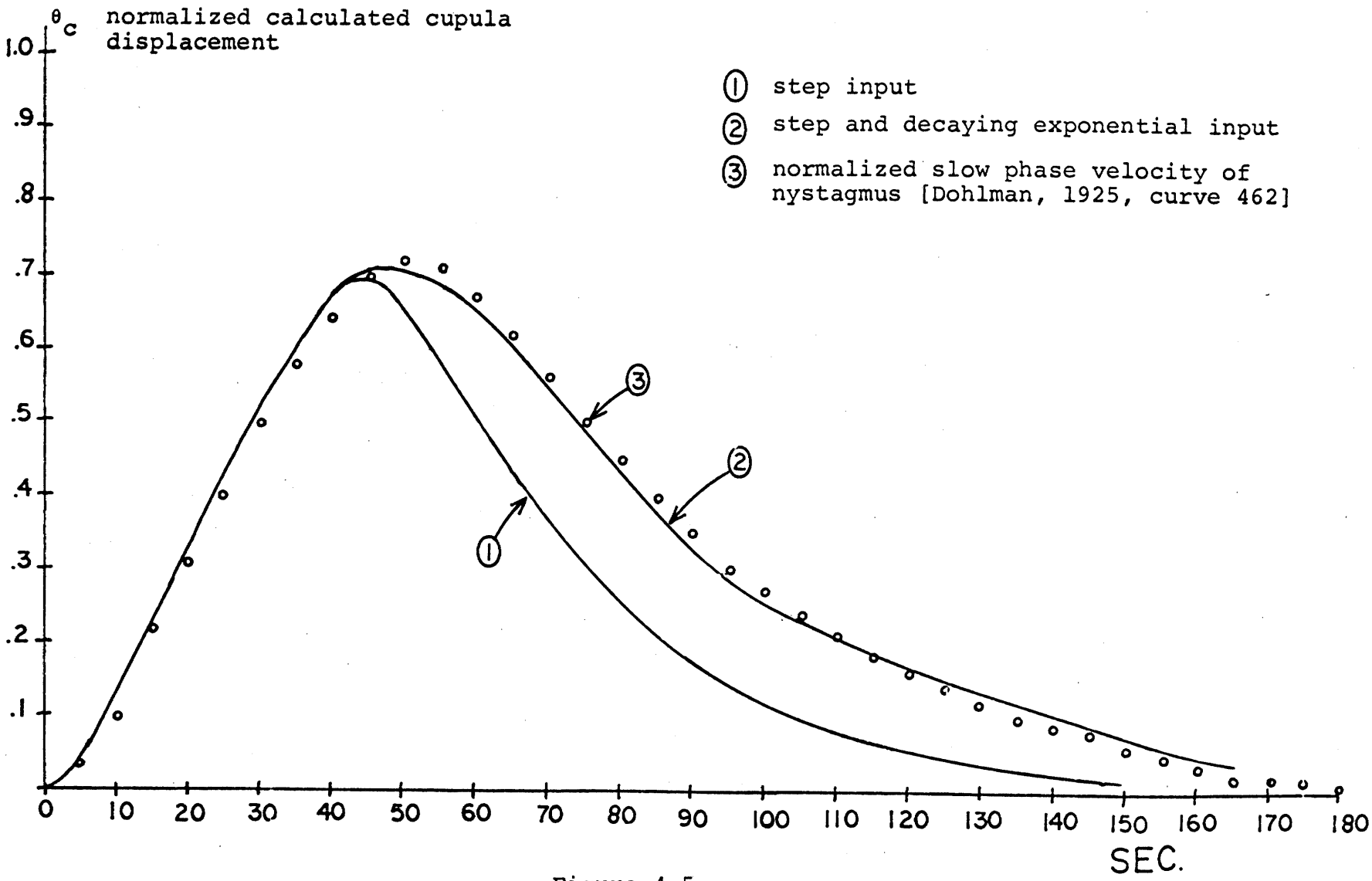


Figure 4.5

Calculated cupula displacements
for step and step-exponential caloric stimuli
and slow phase nystagmus velocity from caloric irrigation

4.4 The "Caloric Latency Product"

4.4.1 Definition and analytic evaluation of "caloric latency product"

A measure that is often used in evaluation of vestibular performance is the latency time to the onset of sensation of motion for a step input of angular acceleration. The relationship between the amplitude of the stimulus and the latency time, referred to as the "Muelder Product," results from the time necessary for the threshold cupular displacement to be reached and a vestibular reaction sensed by the subject.

By solving eq. (4.12) for the cupular displacement resulting from a step input of temperature T_i we obtain

$$\theta_c(t) = A\, T_i\, [1 - B_1\, e^{-t/\tau_1} - B_2\, e^{-t/\tau_2} - B_3\, e^{-t/\tau_3}] \qquad (4.13)$$

$$\theta_c(t) = A\, T_i\, f(t) \qquad (4.14)$$

It should now be possible to show experimentally, analogous to the "Muelder Product," that the latency time to the onset of caloric nystagmus follows the relationship

$$f(t_\ell)\, T_i = C = \text{constant} = \theta_{min} \qquad (4.15)$$

4.4.2 Experimental verification of "Caloric Latency Product" (experiment by author)

In an effort to establish the functional relationship between the latency of caloric nystagmus and the magnitude of the caloric stimulus, twelve male subjects between the ages of 20 and 28 were each subjected to a sequence of caloric

irrigations at 1°C, 3°C, 5°C, and 7°C above and below normal body temperature (37°C) to obtain a total of eight data points per subject. A random sequence of alternate hot and cold temperatures was selected for one half of the subjects and the reverse order was used for the remaining half. Three subjects were discontinued after the first irrigation because spontaneous nystagmus made their records impossible to read.

Irrigations were performed using the conventional circulating water system to reduce the temperature drop in the delivery tubes. The water is delivered through a nozzle built into an aural speculum which is introduced into the meatus under direct visual observations. The duration of the irrigation was continued until nystagmus was clearly established and ranged from 20 to 60 seconds.

Nystagmus measurements were performed with an electro-oculogram (EOG) with subjects' eyes open but blindfolded to simulate darkness. A 20 minute rest period was allowed between irrigations to minimize correlation of the responses by allowing the thermal transients to settle down.

The data was analyzed in an attempt to find the beginning of the first slow phase nystagmus beat. However, the velocity of the first slow phase nystagmus stroke is generally smaller than the noise level from muscle noise on the EOG recordings and therefore it was found to be necessary to use the first fast or return phase beat to measure the latency times. Since the return phase of nystagmus presupposes the existence of a slow phase, the measure latency times will always be somewhat longer than the actual ones, but they are the only clearly defined parameter than can be measured.

Of the nine sets of records that were obtained, the majority gave results that could easily be read, and a few of the records were corrupted with high amplitude muscle noise, occasional saccades, and spontaneous nystagmus beats and were therefore very difficult to interpret. In fig. 4.6 is presented the latency time vs. magnitude of stimulus for both hot and cold irrigation for the four subjects whose records were the most readable. Fig. 4.7 shows the mean latency times and their standard deviations vs. amplitude of stimulus for the nine subjects tested. The large deviations for lower temperatures are to be expected, because small deviations in either body temperature or irrigation temperature represent a significant percentage change in stimulus.

For purposes of comparison, in fig. 4.8 are presented a composite of the subjective latency times of Clark and Stewart, and Meiry, and the latency times for the onset of nystagmus from the results of Fluur and Mendel for constant angular acceleration stimulation. As would be expected, the caloric latencies are longer, as a result of the additional thermal lag.

The data presented in fig. 4.7 shows, as predicted by the model, an approximately hyperbolic relationship between latency times and strength of stimulus. From previous threshold and thermal lag considerations, the proposed analytic model predicts a latency of about 20 sec for a ±3°C stimulus. From fig. 4.7 the observed latencies for +3°C and -3°C stimuli are 24 sec and 18 sec respectively. Thus the average of the hot and cold latencies for a 3°C stimulus is in reasonable agreement with the estimated latency.

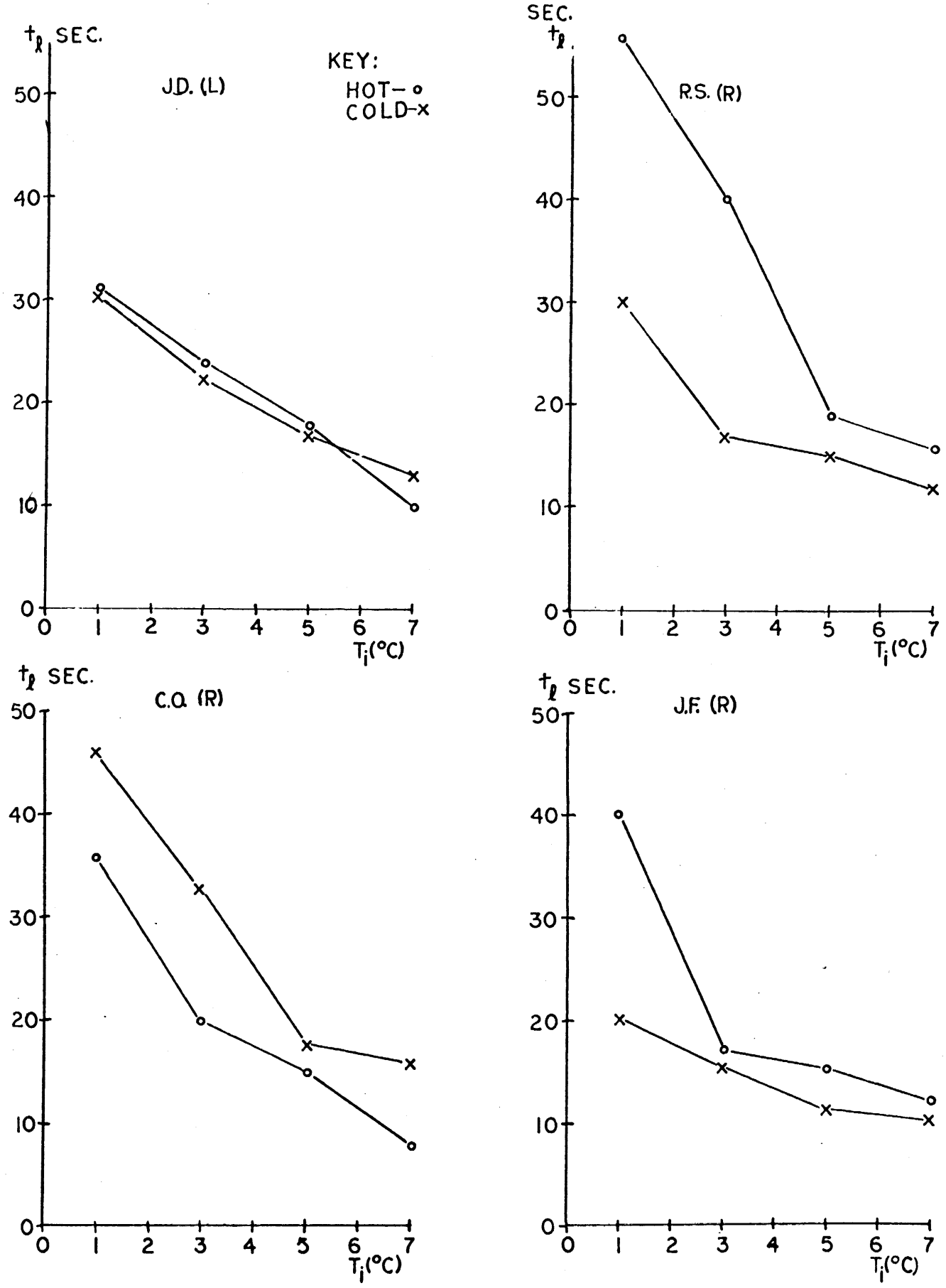


Figure 4.6

Latency time (t_L) vs. temperature T_i for four experimental subjects

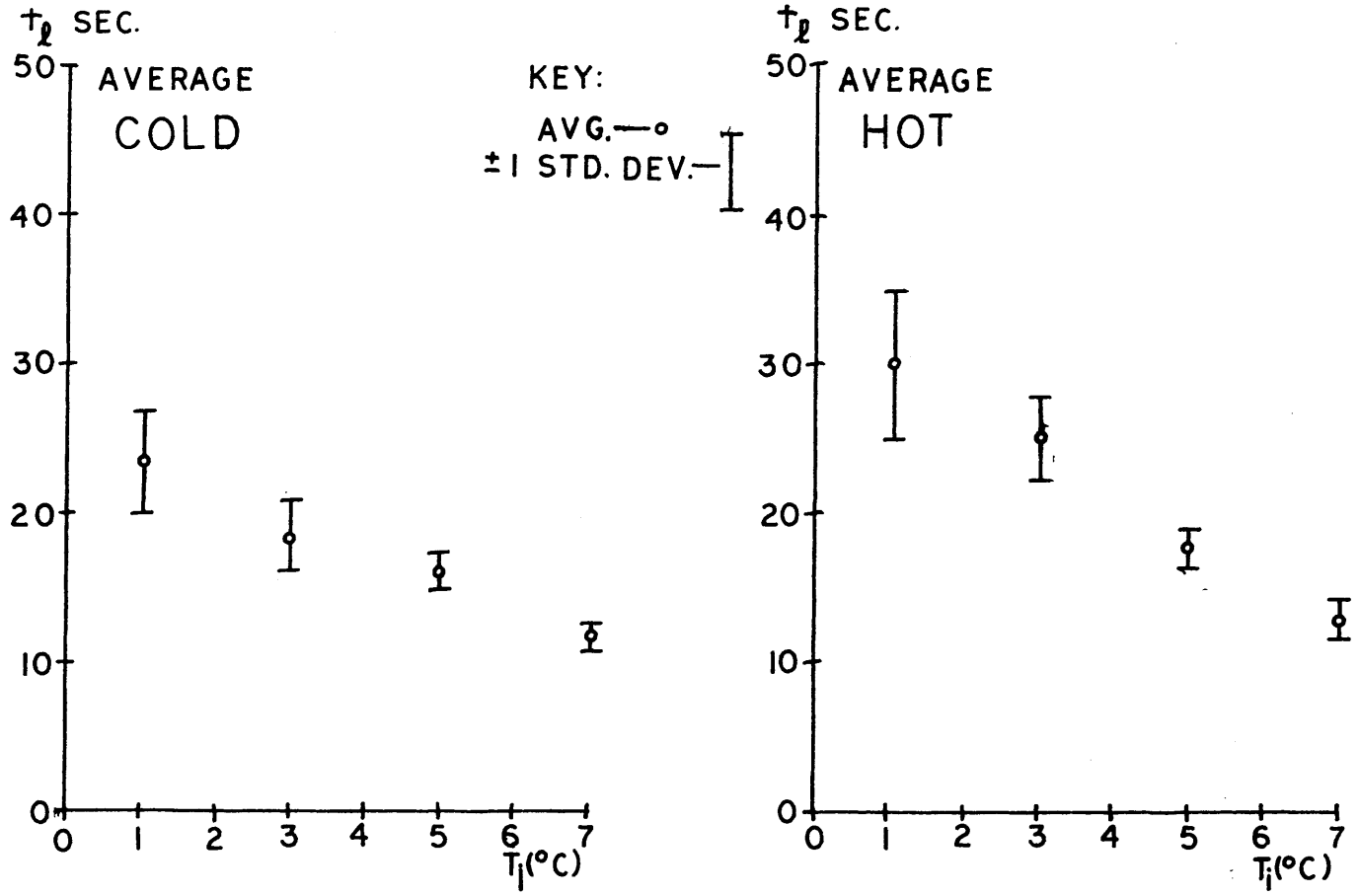


Figure 4.7

Average latency times vs. temperature for hot and cold caloric stimuli

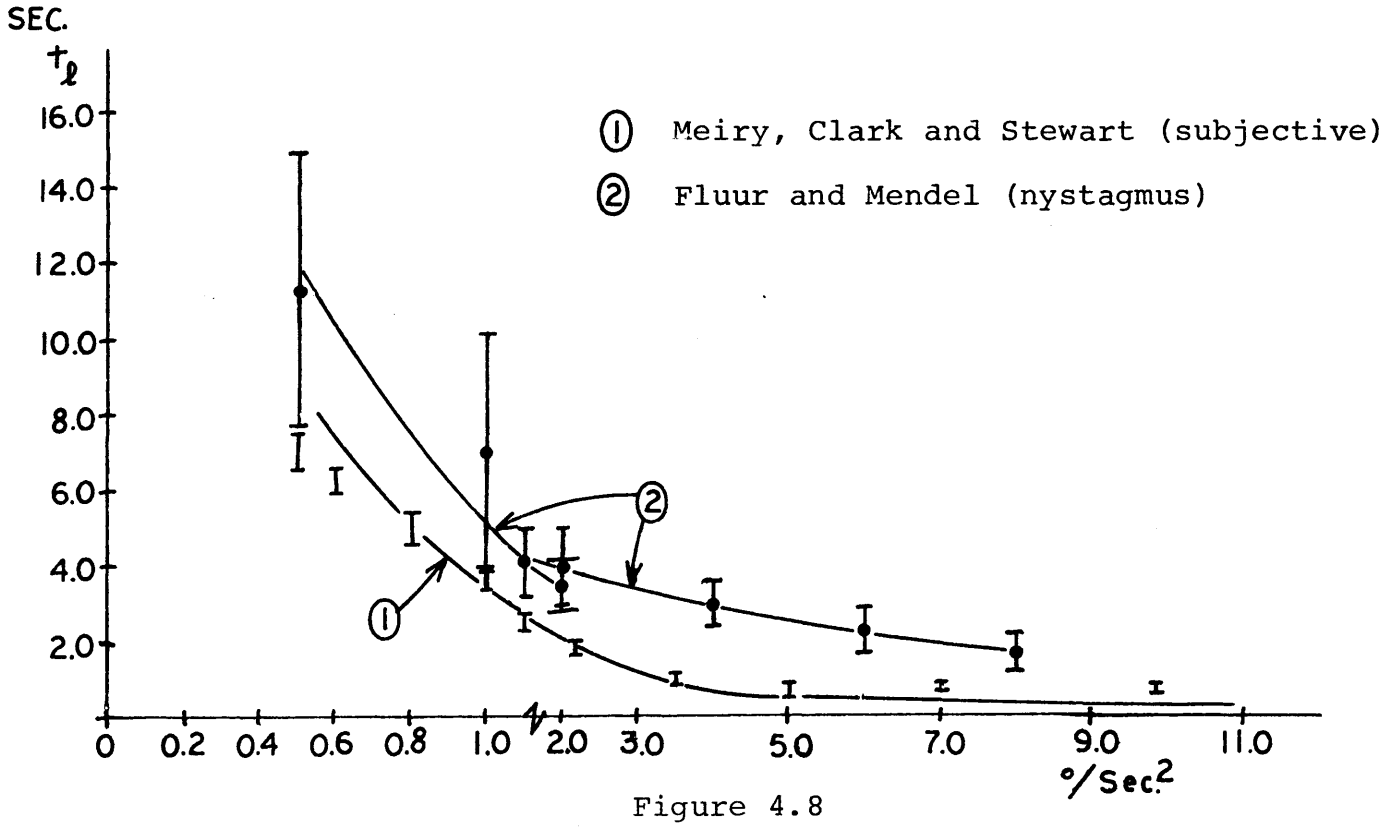


Figure 4.8

Latency times to onset of subjective sensation and nystagmus for angular acceleration stimulation

The differences in the responses to hot and cold stimuli have also been observed by other researchers and merit further investigation. Fitzgerald and Hallpike observed that 80% of their tests showed cold caloric responses were of longer duration than those from hot irrigations, and Weiss has noted a stronger reaction to cold caloric irrigations for younger subjects (less than 40 years old), whereas for subjects over 40 there is a tendency for stronger caloric reactions to hot stimuli.[52,155] There are several plausible explanations for this difference in response, two of the most significant of which will be considered in the following paragraphs.

There exists some experimental evidence which points to a direct modulating influence of temperature on the spontaneous activity of the sensory cells. Since the entire bony labyrinth is elevated (or lowered) in temperature by caloric irrigation, it is possible that a shift in the spontaneous discharge rate during irrigation can account for the observed differential response to hot and cold irrigations. The short term zero-g tests of Kellogg and Graybiel seem to discount this notion; however, long duration zero-g space flight experiments are necessary either to prove or to lay to rest this theory.

Vasodilation could equally well account for the observed differential response. It may be somewhat easier for the vascular system to add or remove heat by expanding vesicles and allowing a higher blood flow rate than it is to contract them and restrict blood flow. Thus it is possible that vasodilation has a larger effect on one of the two modes of caloric irrigation than on the other. This hypothesis could

be further investigated by consideration of the influence of several vasodilators and vasoconstrictors on the strength and duration of hot and cold caloric responses.

In summary, the data presented further substantiate the previously observed differential response between hot and cold caloric irrigations. The mean latency times for hot and cold irrigations and the observed hyperbolic functional relationship between latency times and the magnitude of the caloric stimulus are in good agreement with the latencies predicted by the analytic model.

The subjective responses reported by the participants ranged from giddyness to no sensation to discomfort and various degrees of sensation of rotation. It was apparent that subjective sensation of rotation was not a good measure of caloric vestibular stimulation, for although most subjects did report some sensation of rotation, they found that the onrush of water in the ear distracted them to the point where they could not determine when the sensation began. Further, all subjects reported that the sensation of rotation showed either its onset or a marked increase in velocity at the instant the irrigation was terminated. Thus, whereas the subjective sensation has sometimes been considered to be a more sensitive measure of vestibular stimulation to angular acceleration than is nystagmus, the nature of the stimulus and the unpleasantness of its application make subjective sensations an unreliable performance index for caloric response.

In conclusion, the proposed system model for caloric stimulation, which is based on the simple principles of physics is substantiated by the experimental data from past

and present researchers and by the author's own experiments, and as such it represents a useful model for estimation of vestibular responses for different amplitudes, durations, and profiles of caloric stimulation, so long as they remain within the physiological bounds from which the model was derived.

CHAPTER 5

THE RESPONSE OF THE SEMICIRCULAR CANALS TO ROTATION IN A LINEAR ACCELERATION FIELD

Several of the experiments which have been devised to study man's vestibular reactions to unusual motion environments have elicited modes of response that cannot be accounted for by existing physical descriptions or analytic models of the vestibular system. Of particular importance are the results of recent experiments which show that rotation of subjects at a constant angular velocity about a horizontal longitudinal axis provokes continuous vestibular nystagmus and subjective sensation of rotation. Classical concepts of the vestibular sensors predict only a transient nystagmus response which decays to zero for this stimulus and for constant velocity rotation about any axis. Thus it has become necessary to re-examine these classical concepts to determine which receptors are responsible for this mode of stimulation.

In this chapter the experiments which illustrate this mode of vestibular response are reviewed. It is shown that the semicircular canals, through "roller pump" action of the flexible membranous duct, can be stimulated by constant rotation in a linear acceleration field. An analytic model, based on roller pump action, is proposed and experiments are performed to evaluate its undetermined coefficients.

5.1 Vestibular Responses to Constant Rotation in a Linear Acceleration Field

It has been found by Benson, Bodin, and Guedry that a continuous nystagmus results from constant velocity rotation of human experimental subjects about a horizontal longitudinal axis.[8,75] As illustrated in fig. 5.1, the slow phase velocity of the observed nystagmus has a steady state bias component and a sinusoidal component with its frequency at the rate of rotation. Hixon has observed that head over heels rotation provokes a prolonged vertical nystagmus and the dynamic counterrolling data of Kellogg shows both bias and sinusoidal components of rotary nystagmus.[8,107] Further, Guedry has shown that such a response is either not elicited or substantially reduced for labyrinthine defective subjects.[80]

Money, using a counter-rotating platform, has recorded similar nystagmus from humans, normal cats, and cats without utricular function, and he has shown that the phenomenon is not observed in cats with plugged canals.[136]

Crampton has shown by recordings from the vestibular nucleus in cats that linear acceleration does not modify cupular deflection and has suggested that the bias and the sinusoidal components of nystagmus recorded by the aforementioned researchers are functionally separate.[44]

More recently, Jones, and Jones, Guedry, and Benson have recorded from cells of the vestibular projection in cats.[102] By using angular and linear acceleration tests they have identified neurons which respond only to angular accelerations and are thus assumed to be from the semicircular canals.

When these canalicular neurons are stimulated by a counter-rotating motion, which in effect is stimulation by a rotating linear acceleration vector, they exhibit a steady state increase in discharge rate for one direction of counter-rotation and a decreased rate for counter-rotation in the opposite direction. There is very little cyclicity in the discharge rates of these neurons which further substantiates Crampton's findings that the cupula is not displaced by linear accelerations.

The influence of linear acceleration on nystagmus has been studied by Guedry, Niven, Hixon, Graybiel, Lansberg, Mayne, and Meiry and Young.[80,90,63,110,126,160,161] Their works show that acceleration in the saggital (fore-aft) plane produces no horizontal or vertical nystagmus, but that frontal (left-right) oscillation provokes horizontal nystagmus (L-nystagmus). The horizontal axis rotation experiments of Benson and Bodin, and Guedry both confirm that the peak velocities of the observed sinusoidal component of slow phase nystagmus occur at the right and left ear down positions.[8,75] Further, Kellogg's counterrolling data also shows that the peaks of the slow phase velocity of rotary nystagmus occur at the left and right ear down positions where the subject has the full one g acceleration acting along his frontal (left-right) axis.[107]

In summary, the evidence is strong that the observed sinusoidal component of nystagmus results from utricular reception of the sinusoidal component of acceleration that is present in the subject's frontal plane as a result of rotation

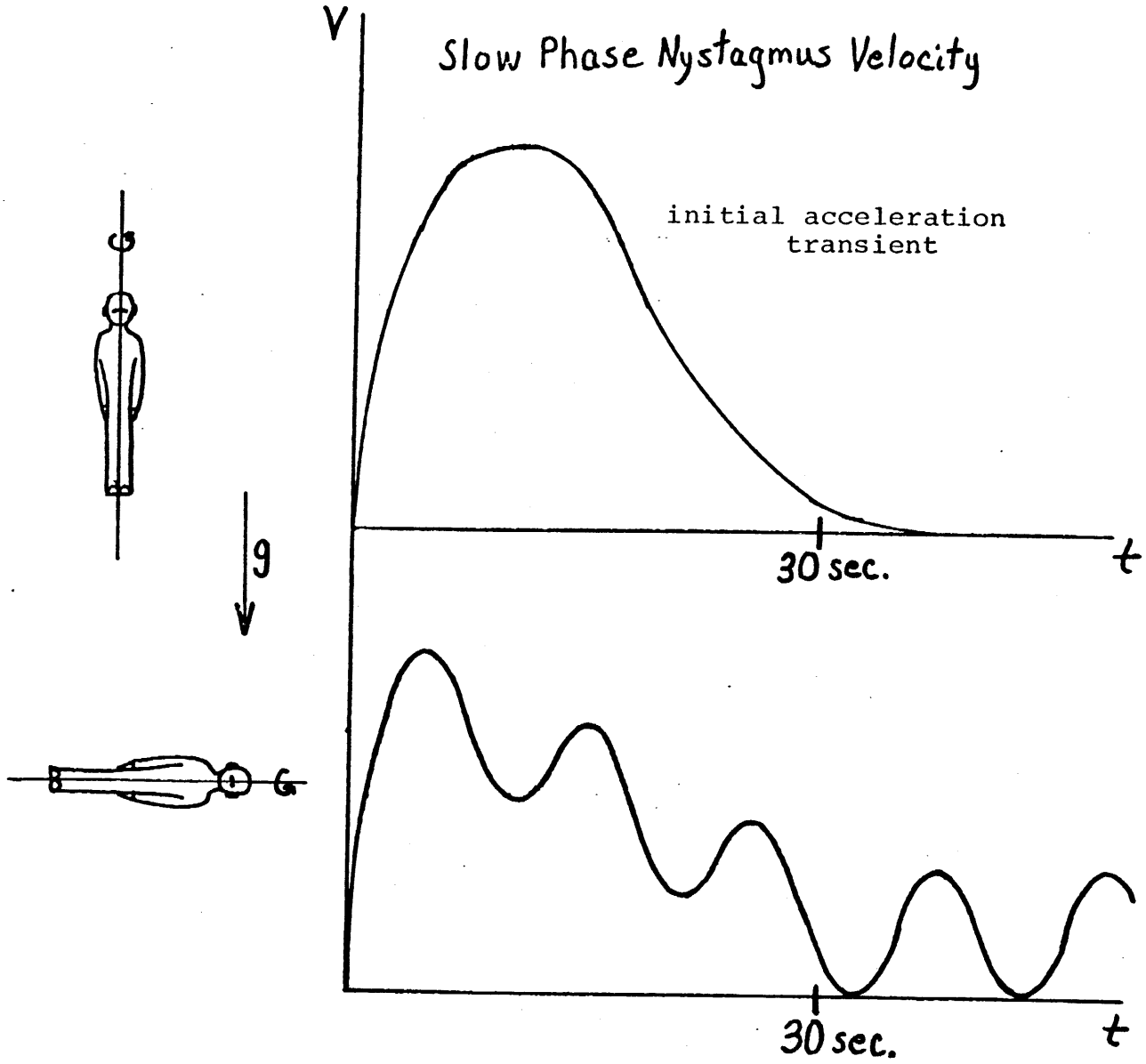


Figure 5.1
Slow phase velocity of vestibular nystagmus from constant velocity rotation about vertical and horizontal axes.

in a linear acceleration field. It corresponds to the "L nystagmus"identified by Young et al. However, the bias component of nystagmus that is evident at rotation rates below 10 rpm appears to be canalicular in origin.[160] It is now necessary to reconsider the classical concept that the semicircular canals are exclusively angular accelerometers which, after the initial acceleration transient has subsided, would give no output for constant angular velocity about any axis.

5.2 The Flexible Nature of the Semicircular Canals

From histological studies by Igarashi and the observations of Engstrom and others, it is apparent that the duct of the membranous canal is attached by fibrous connections along its outer periphery to the bony canal.[91,49] However, the inner periphery is relatively unattached and flexible, and Money has shown for pigeons that the duct is denser than either the endolymph or perilymph that surrounds it.[133] Under the influence of pure angular acceleration about an axis in the direction of the gravity field, the duct flexibility and density will have no significant consequences. However, if the gravity field is not colinear with the axis of rotation, a component of it will act upon the mass unbalance and can produce a movement of endolymph within the duct.

5.3 The Flexible Torus as a "Roller Pump"

A flexible duct immersed in an containing an incompressible fluid will be distended by the influence of a linear acceleration if its density is different from the fluid, and a density difference between the interior and exterior fluids will further

accentuate this distension. As shown in fig. 5.2, a flexible circular duct which is attached along its outer periphery to a rigid structure and is denser than the fluid surrounding it will have a constricted cross sectional area where the acceleration field pushes it against its support, and it will be expanded where the acceleration pushes it away from its support.

Further, as also illustrated in fig. 5.2, if the linear acceleration vector $\bar{a}$ is slowly rotated at a constant angular velocity ω, the constriction will move along the outer periphery of the duct in phase with the rotation of the acceleration vector. The effect of the moving constriction is then to move or pump the fluid in the duct in the direction of the rotation. This pumping action works against the viscosity and inertia of the fluid, and at high angular rotation rates the fluid that is being pushed by the moving constriction cannot be displaced fast enough and thereby builds up a pressure gradient which expands the duct toward a uniform circular cross section. Thus, for high angular rotation rates of the linear acceleration vector, the mass of the fluid acts as a hydromechanical filter which reduces the duct constriction and along with it the pumping action of the flexible tube.

For a flexible tube with an elastic flow restraint such as the cupula of the semicircular canals, the fluid is initially pumped against and displaces the elastic restraint which then produces a pressure differential across the tube. A static equilibrium state is then reached where the displaced elastic restraint provides sufficient pressure feedback to

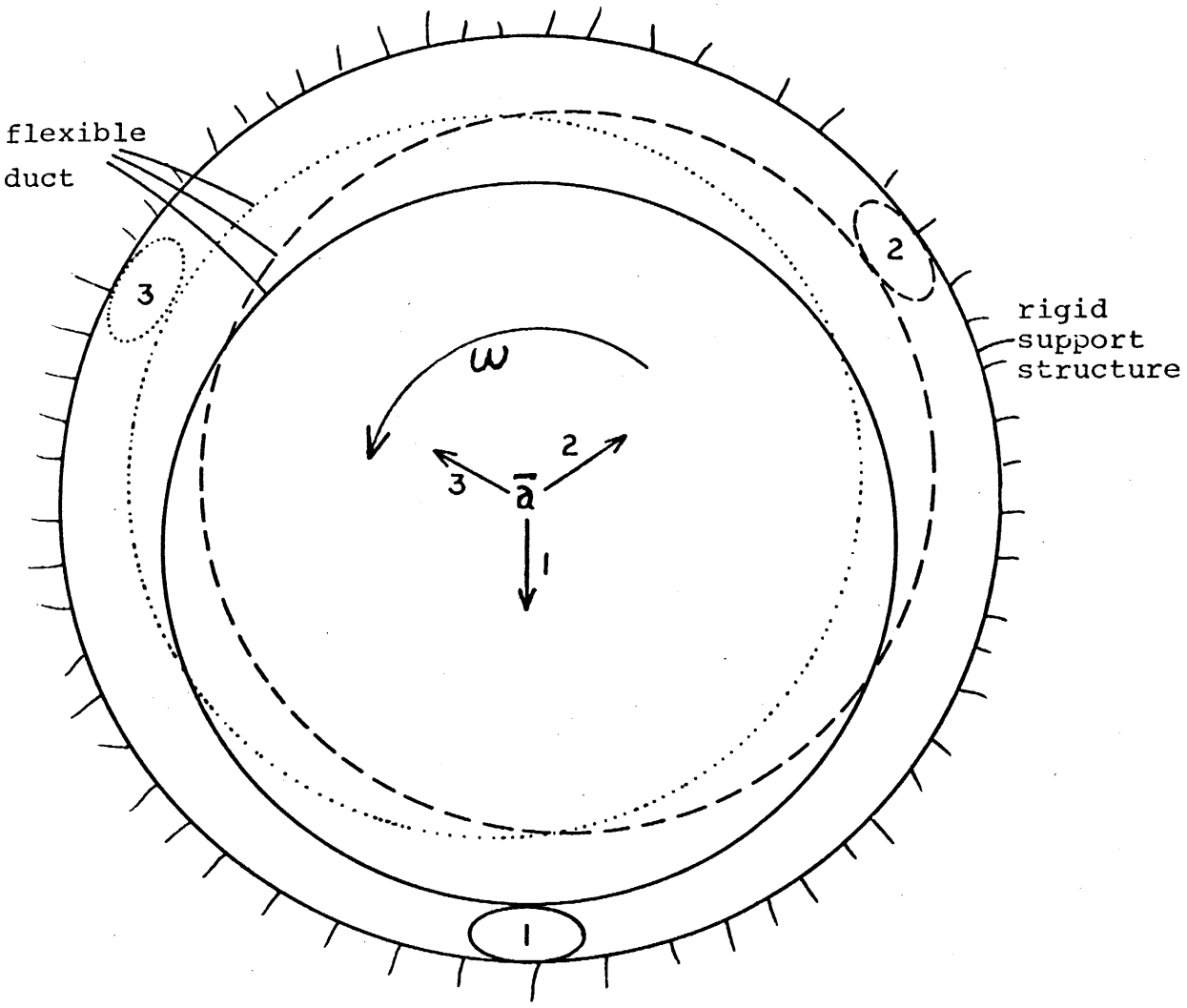


Figure 5.2

Illustration of the pumping action of the distended duct when the linear acceleration field is rotated at a uniform angular velocity

inhibit further flow. Thus, for a constant velocity of rotation in a linear acceleration field, a constant cupula displacement can be maintained by this flexible roller pump action.

5.4 A Model for Canalicular Response to Rotating Linear Acceleration Stimulation

For constant rotation of the semicircular canals the steady state displacement of the elastic cupula provides a pressure differential across the cupula which inhibits further flow. All of the fluid displaced by the moving constriction must therefore flow back through the constriction, and the pressure drop of this "back flow" must exactly balance that caused by the displaced cupula.

The average velocity $\bar{v}(\frac{A_c}{A})$ of the backflow is given by the equation

$$\bar{v}(\frac{A_c}{A}) = \frac{(A - A_c)\ \omega\ R}{A} \tag{5.1}$$

where

A = cross sectional area of the unrestricted portion of the duct

A_c = cross sectional area of the constricted portion of the duct

ω = rotation rate of the linear acceleration vector

R = radius of the torus

The static pressure differential Δp which can maintain an average flow of endolymph can be calculated from the fluid dynamic analysis of Chapter 3 to be:

$$\Delta p = \frac{2\pi R}{D_d} \bar{v}\left(\frac{A_c}{A}\right) \tag{5.2}$$

where

$$D_d = \frac{a^2}{8\mu} \tag{3.20}$$

From equations (5.1) and (5.2) the cupular pressure differential Δp that a rotating constriction can maintain is

$$\Delta p = \frac{16\ \pi\ \mu}{a^2} \left(1 - \frac{A_c}{A}\right)\ \omega\ R^2 \tag{5.3}$$

Further, it was also found from the derivations of Chapter 3 that a pressure differential Δp across the membranous duct produces a cupular response which is related to angular acceleration stimulation, α, by the equation

$$\Delta p = 2\ \pi\ R^2\ \rho\ \alpha \tag{5.4}$$

From equations (5.3) and (5.4) we obtain the relationship between the rate of angular rotation, the magnitude of the duct restriction and the equivalent constant angular acceleration that would produce the same steady state cupular displacement in a one-g acceleration field

$$\alpha_{equiv} = \frac{8\ \mu\ \omega}{a^2\ \rho\ G} \left(1 - \frac{A_c}{A}\right) \tag{5.5}$$

For the human semicircular canals where

$a = 0.015$ cm

$R = 0.3$ cm

$\rho = 1$ gm/cm^3

$\mu = 0.0085$ poise

$$G = 980 \text{ cm/sec}^2$$

we can evaluate:

$$\alpha_{equiv} \simeq 0.3 \left(1 - \frac{A_c}{A}\right) \omega \text{ rad/sec} \qquad (5.5a)$$

To establish the applicability of the roller pump principle to the semicircular canal the relative magnitudes of the bias component of slow phase nystagmus from rotation in a linear acceleration field and the steady state nystagmus stimulated by constant angular acceleration can now be compared to determine how large a distension of the duct is necessary to produce a significant physiological response.

From the data of Guedry, a 6°/sec bias component of vestibular nystagmus is noted for a 1 rad/sec rotation about a horizontal longitudinal axis. Several experiments have shown that such a 6°/sec slow phase velocity would also result from a $0.6°/\text{sec}^2$ or 0.01 rad/sec^2 constant angular acceleration.[80] Solution of equation (5.5a) for the value of $\frac{A_c}{A}$ when

$$\omega = 1 \text{ rad/sec}$$

$$\alpha_{equiv} = 0.01 \text{ rad/sec}^2$$

gives

$$\frac{A_c}{A} = .97 \qquad (5.6)$$

Which is to say that a mere 3% constriction in duct area, or correspondingly, a 1.5% contraction of the radius of the membranous canalicular duct can produce sufficent roller pump

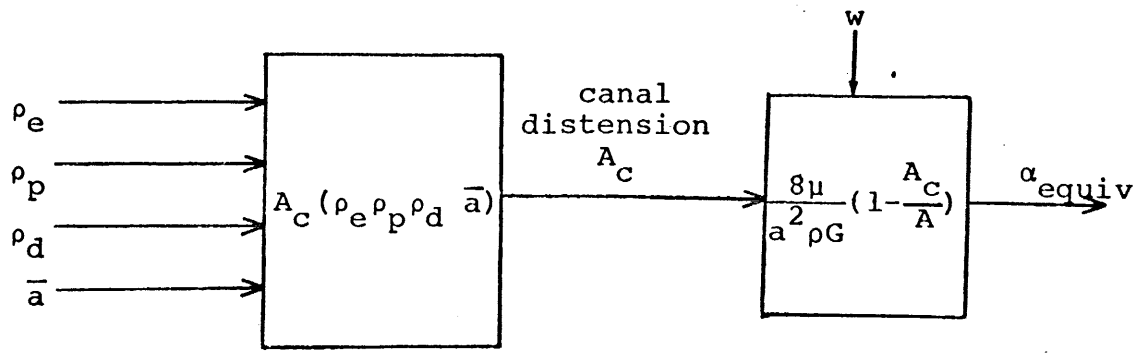
action to account for the observed bias component of nystagmus which results from constant rotation at 1 rad/sec in a one-g acceleration field.

The question of whether or not a 3% constriction in duct area is a realistic value remains a matter of conjecture. However, since it has been shown by Money that there is a density difference of the order of 0.1% between endolymph and perilymph (in pigeons) and that the duct is more dense than either fluid, by at least 1%, and since the duct tissue is only a few cell layers thick and thus quite flexible, it is at least plausible that the duct is sufficiently elastic to permit a 3% constriction in area in the presence of the one-g linear acceleration field.[133]

The rotation rates ω_1 and ω_2 at which the roller pump action diminishes is determined by the elasticity and strength of the fibrous attachments of the duct and is not readily calculable. However, this cut off frequency can be accounted for by adjoining to equation (5.5) a second order lag term to provide for a diminished response at higher rates of rotation. From which we obtain:

$$\alpha_{equiv} = \frac{8\mu}{a^2 \rho G} \left(1 - \frac{A_c}{A}\right) \frac{\omega}{\left(1 + \frac{\omega}{\omega_1}\right)\left(1 + \frac{\omega}{\omega_2}\right)} \qquad (5.7)$$

The functional dependence of the equivalent angular acceleration on the densities of the labyrinthine fluids, the membranous duct, and the strength and rotation rate of the acceleration field is illustrated in fig. 5.3. In the remaining section of this chapter are described a sequence of



ρ_e = density of endolymph

ρ_p = density of perilymph

ρ_d = density of membranous canal

$\bar{a}$ = linear acceleration

$A_c(\rho_e\rho_p\rho_d\ \bar{a})$ = functional dependence of the duct constriction on the variables ρ_e, ρ_p, ρ_d, and $\bar{a}$

w = rotation rate of canal in acceleration field

α_{equiv} = constant angular acceleration which will produce the same steady state nystagmus response

Figure 5.3
The functional dependence of the flow of endolymph on the physical properties of the labyrinthine fluids and membranous ducts and the rotation rate in a linear acceleration field.

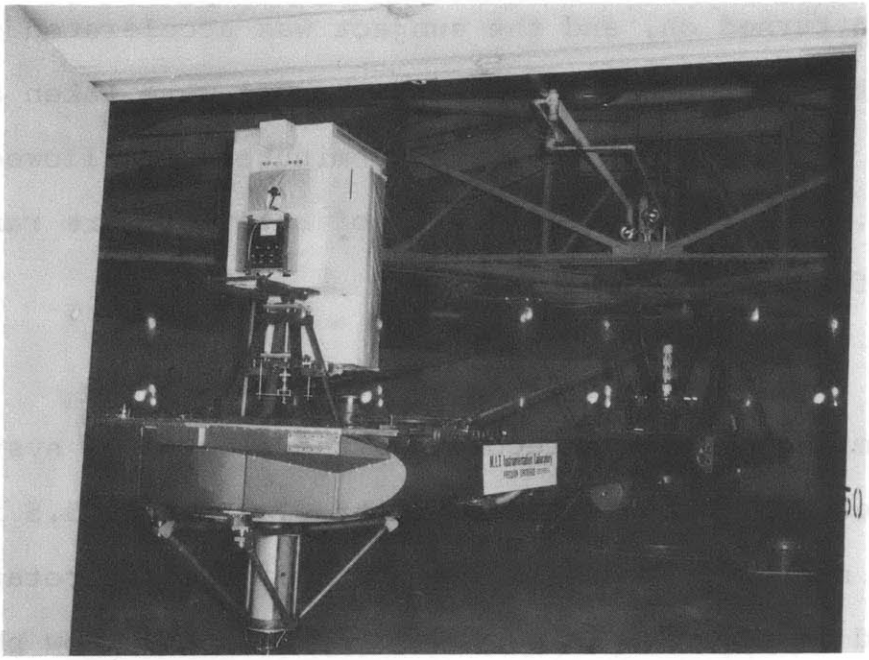
experiments performed by the author to evaluate experimentally the cut off frequencies, ω_1 and ω_2.

5.5 Experimental Verification of the Model

5.5.1 Experiments by the author

To investigate the variation of the bias and the amplitude of the sinusoidal component of vestibular nystagmus as a function of rotation rate, the M.I.T. Instrumentation Laboratory Precision Centrifuge with a rotating platform at a 32 ft. radius was fitted with the Man-Vehicle Control Laboratory rotating chair simulator and six experimental subjects were rotated at 5, 7.5, 10, 20, 30, and 40 rpm in a 0.3 g horizontal acceleration field. Nystagmus was measured with eyes open in the dark by use of a Biosystems, Inc., pulsed-infrared eye movement monitor. The experimental setup is shown in fig. 5.4.

To minimize the influence of habituation and physical discomfort, the total rotation times were kept to a minimum. The subjects were brought up to the desired rotation rate relative to the boom while the boom was stopped. Nystagmus recordings were monitored until the acceleration transient subsided; then the centrifuge room lights were shut off to eliminate all possible light leaks in the rotating chair. The eye movement monitors were calibrated, and the subjects were instructed to look straight ahead. The boom of the centrifuge was then brought up to speed (5.5 rpm) in about five seconds, held there for 2 minutes, then returned to zero. After the nystagmus from deceleration subsided, the eye movement monitors were again calibrated to insure that no movement of the glasses had occurred during the run. Lights



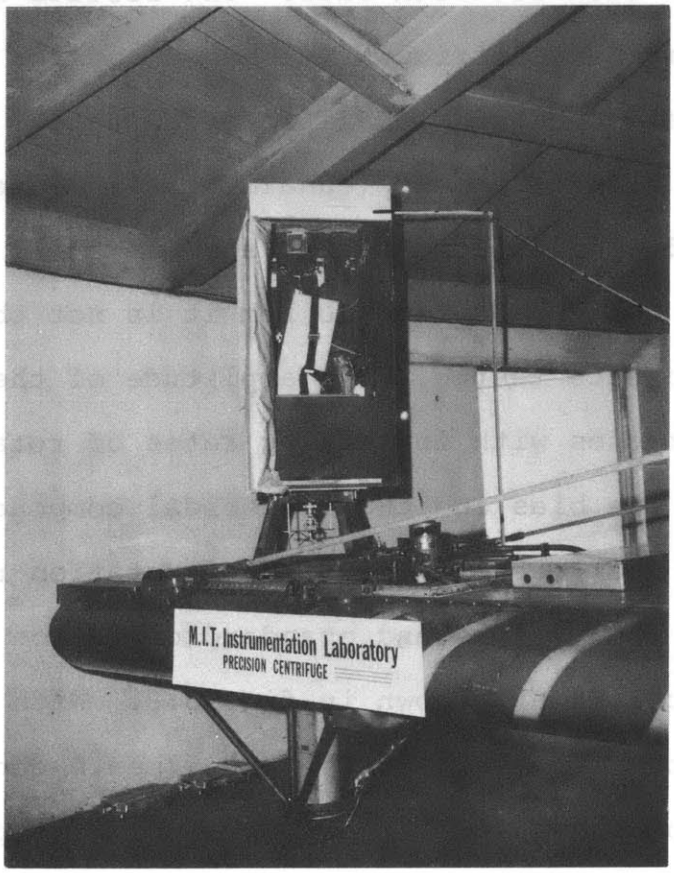


Figure 5.4
Experimental set-up for rotation
in a lateral acceleration field

were then turned on, and the subject was accelerated to a different rotation rate. Three data runs were taken at each sitting, and a rest of at least 20 minutes was allowed between sittings. The rate and direction of rotation were randomly ordered for each subject.

5.5.2 Interpretation of experimental results

From the nystagmus recordings the slow phase nystagmus velocities were calculated and plotted. In fig. 5.5 is shown a sample nystagmus recording for each of the six rotation rates used, and in fig. 5.6 is shown a sample of the slow phase velocities for each rotation rate. The results show a persistent sinusoidal component (utricularly sensed) at the period of rotation for all subjects at all rotation rates. For most subjects a clear bias component (canalicularly sensed) is observed for 5 and 7.5 rpm and for some it still exists at 10 rpm; however, for 20, 30, and 40 rpm it is not observable in any of the subjects tested. The amplitude of the sinusoidal component increases with increasing rates of rotation. The amplitudes of the bias and the sinusoidal components of nystagmus are plotted as a function of rotation rate in fig. 5.7, and their mean values and standard deviation range for the six subjects tested are shown in fig. 5.8. With a sample as small as six the results of these experiments can hardly be considered conclusive, and it now remains to compare these results with those of the aforementioned researchers.

5.5.3 Relationship of the model to experimental results

To compare these results with those of the horizontal rotation experiments, it is necessary, even though the assumption

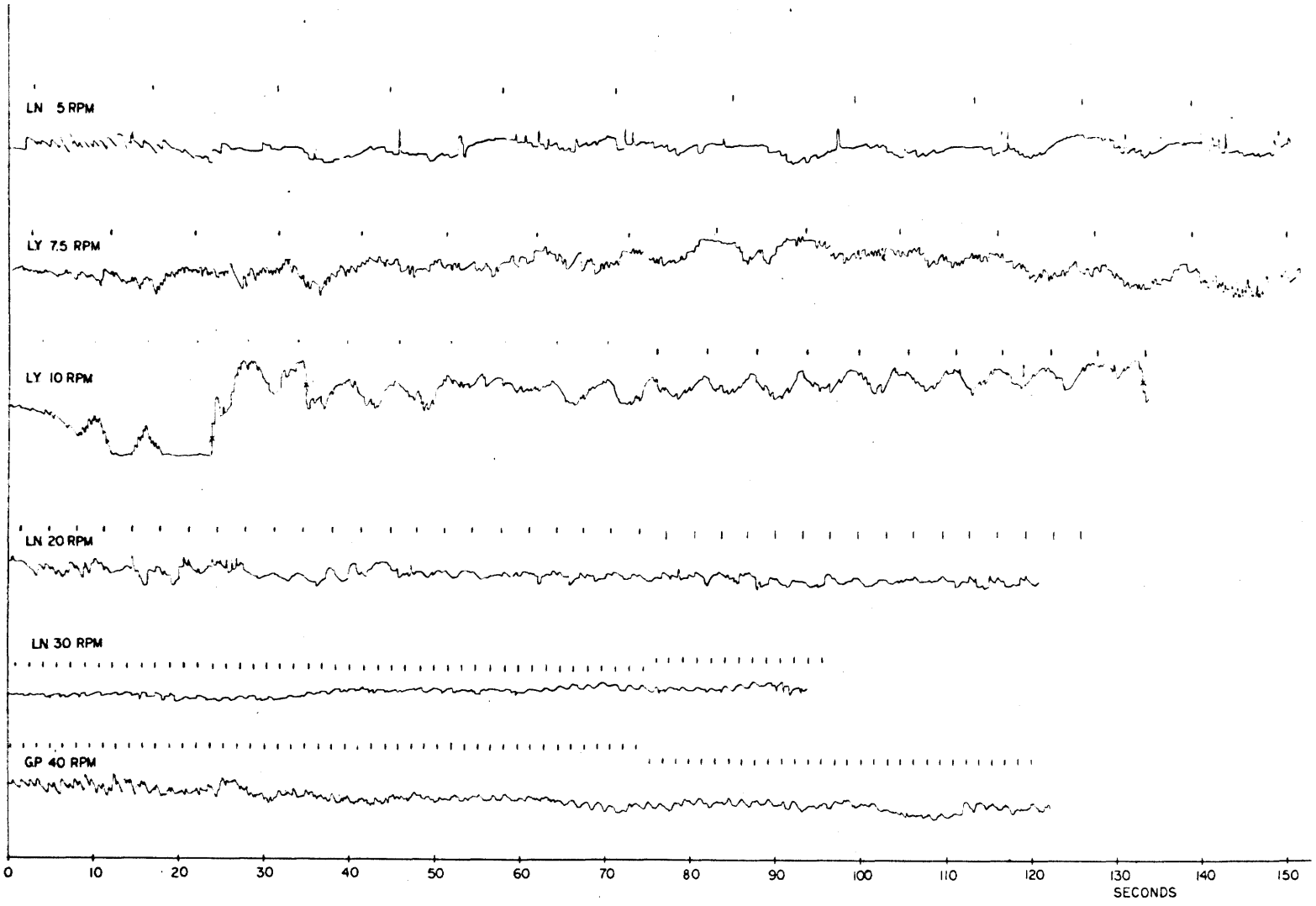


Figure 5.5

Sample eye movement records for rotations in 0.3 g lateral field

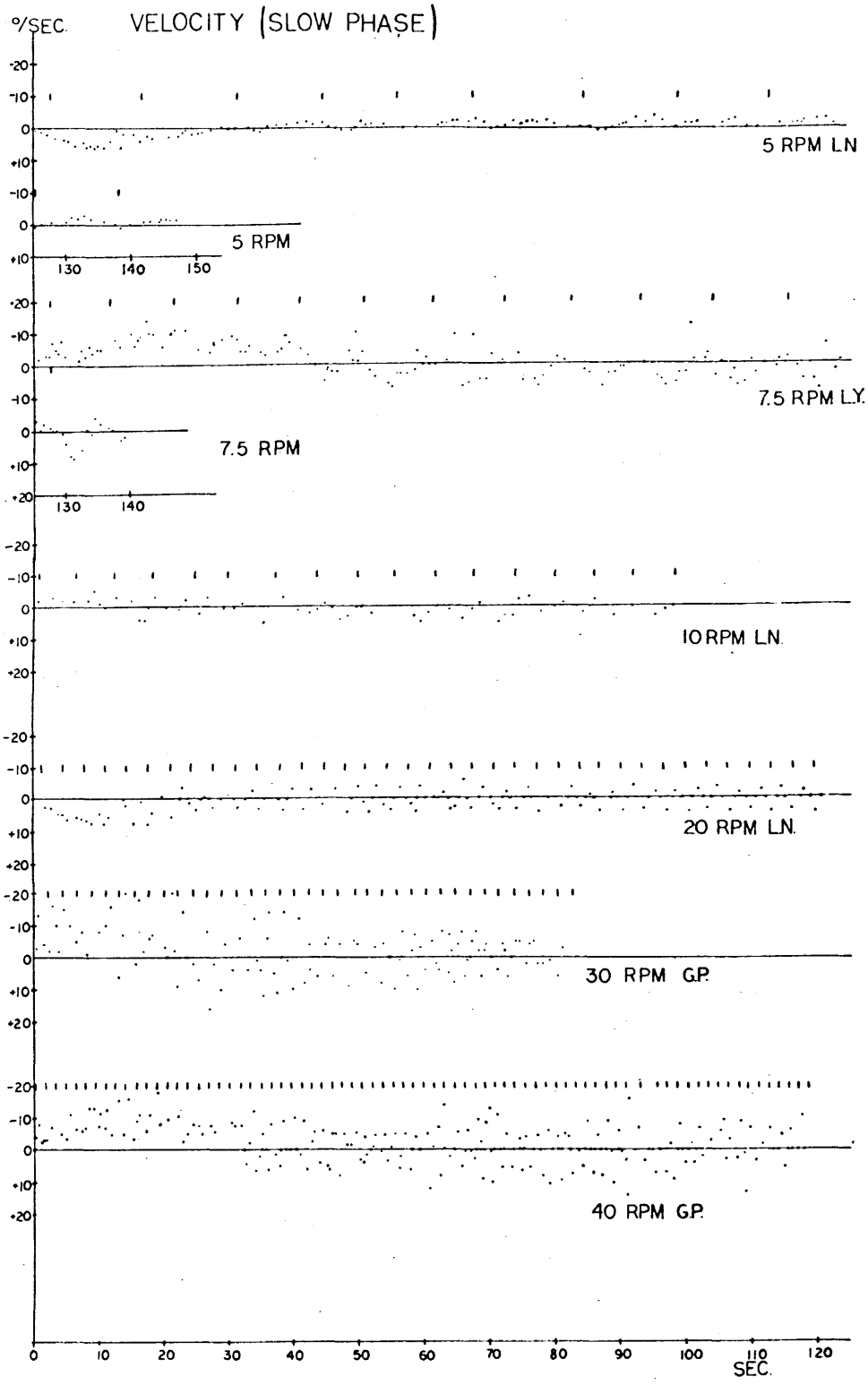


Figure 5.6

Slow phase nystagmus velocities from rotation in 0.3 g field

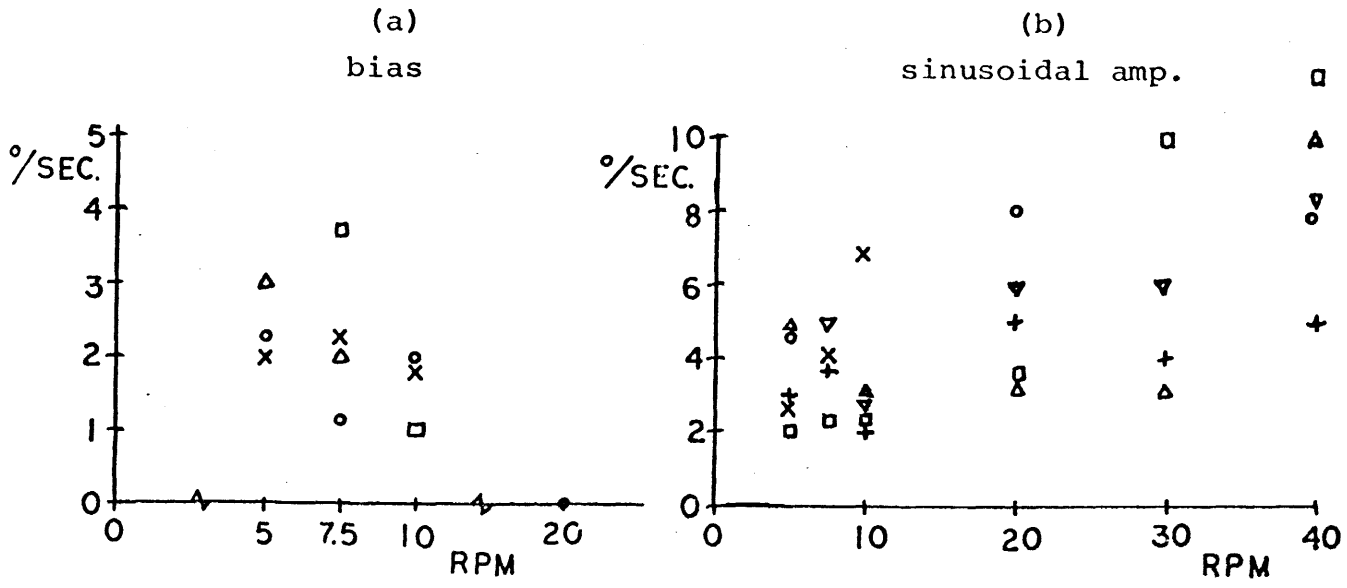


Fig. 5.7
Bias (a) and sinusoidal amplitude (b) of slow phase nystagmus from rotation in 0.3 g field

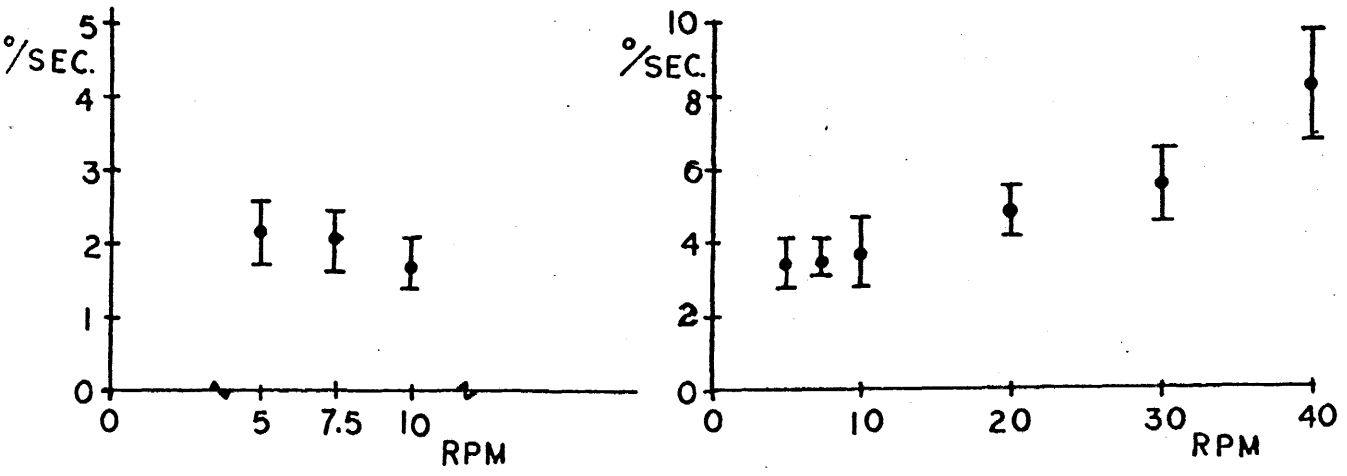


Fig. 5.8
Average values of bias and sinusoidal amplitude ($\pm 1\sigma$) for rotation in 0.3 g field (6 subjects)

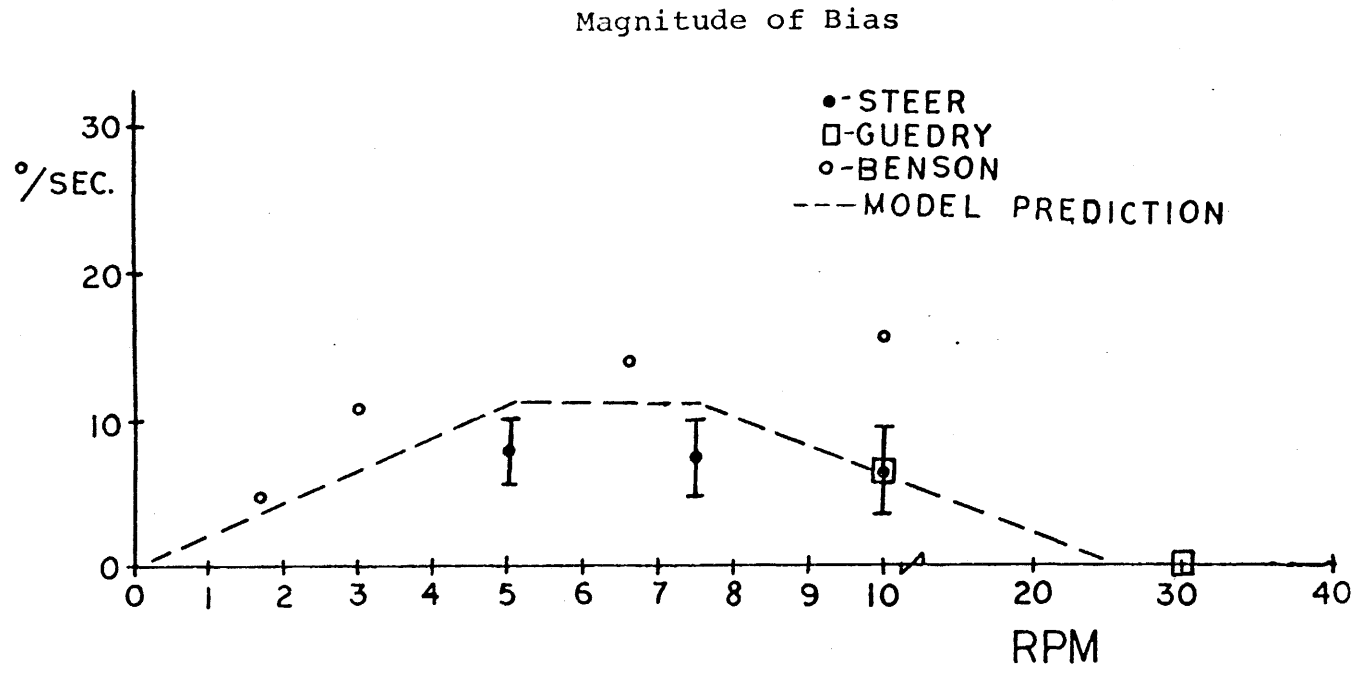


Figure 5.9

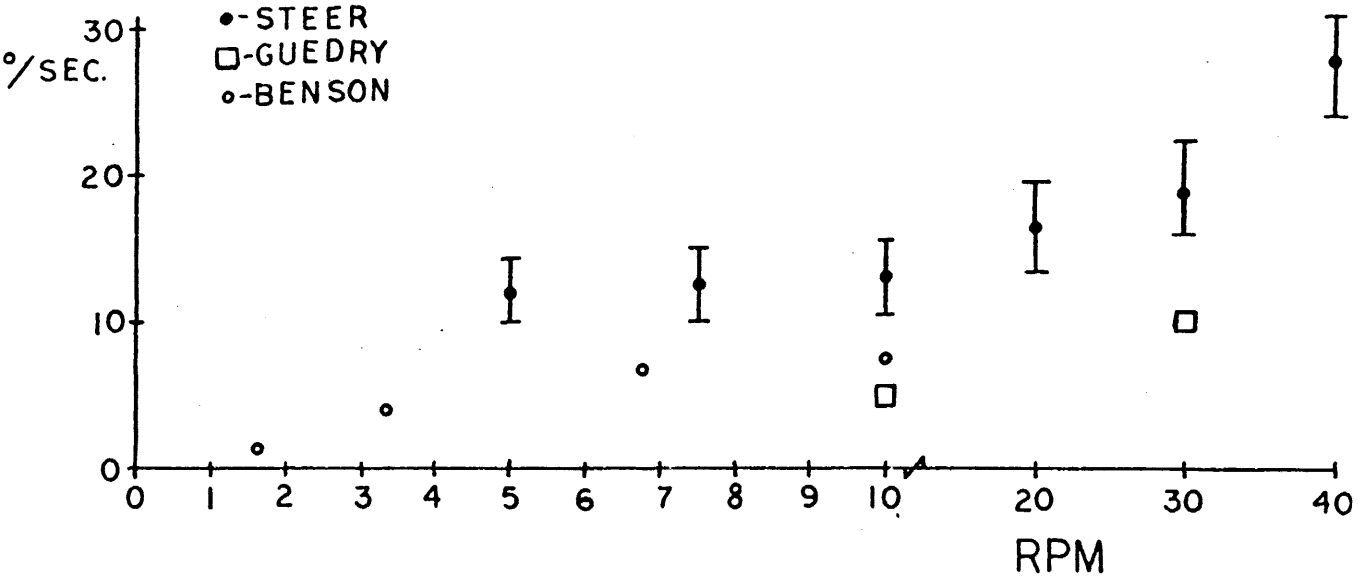


Figure 5.10

Summary of available data of normalized bias and sinusoidal amplitude of vestibular nystagmus from rotation in a 1 g field

of linearity is tenuous, to normalize the results of the author's experiments with respect to a one-g gravity field. In fig. 5.9 and 5.10 the author's normalized results are plotted along with those of Benson and Guedry.[8,80] The model predicted bias component is also plotted in fig. 5.9 for assumed upper break frequencies of $\omega_1 = \omega_2 = 7.5$ rpm.

There are many physiological factors which can account for the observed disparities in results. The larger amplitudes of the sinusoidal components observed by the author are very likely to result from the presence of the one-g vertical bias acceleration that the centrifuges subjects had, but those rotated about a horizontal axis did not have. There is a considerable body of experimental evidence which supports the theory that the otoliths require a "bias field" to keep calcium carbonate grains near the macula so that their motions can excite the sensory epithelia of the macula. Under such a theory, the presence of the one-g field orthogonal to the macula would greatly increase the sensitivity of the receptor in comparison to the horizontal rotation case, where there is no acceleration field orthogonal to the macula. The results of this experiment seem to give further support to this theory.

The average bias components as measured by Guedry for 12 subjects at 10 rpm agree precisely with those found by the author; however, those found by Benson for 8 subjects differ by about a factor or two.[80,8] Since the experimental set ups of Guedry and Benson were quite similar, there is no obvious reason for the discrepancies in their results.

It does appear that the predicted responses from the "roller pump" model are born out by the data in that at low

and high rotation rates, the bias component is not observable, and there is a general shape of measured response that does conform to the predicted second order system. Further, the experimental data show that the upper break frequencies, which we were unable to calculate because of insufficient data, are in the range from 5 to 10 rpm.

In summary, these experiments, which provide a slightly different vestibular stimulation than the "barbecue spit" experiments of Guedry and Benson or the "revolution without rotation" experiments of Money, further verify the hypothesis that rotation at a constant velocity in a linear acceleration field does provoke vestibular nystagmus.[80,8,136] The results of the analysis of this chapter show that a duct area constriction of only 3% provides sufficient roller pump action to generate the observed bias component of nystagmus. And the upper cut off frequencies ω_1 and ω_2 were found experimentally to be in the range between 7.5 and 10 rpm.

CHAPTER 6

RESULTS, CONCLUSIONS, AND RECOMMENDATIONS

6.1 Results and Conclusions

The objective of this research was to evaluate the dynamic characteristics of the human semicircular canals by a detailed examination of their physical properties and to correlate them with physiological and behavioral data. The degree to which this objective was realized is outlined as follows.

6.1.1 Physical properties of labyrinthine fluids

The properties of viscosity, thermal coefficient of viscosity, density, and thermal coefficient of expansion were measured for endolymph and perilymph and were used to evaluate the coefficients of the equations of the dynamic response of the semicircular canals. These measured properties and the measurement accuracies are presented in Appendix A.

A microviscometer was designed, built, and calibrated for use on 1-2 microlitre fluid samples. The design and operational procedures of the microviscometer and sample handling techniques are presented in Appendix B.

6.1.2 Canalicular response to angular acceleration and rotation in a linear acceleration field

Hydromechanical analysis of the semicircular canals as a rigid torus filled with fluid and subjected to a constant angular acceleration showed that the damping to inertia ratio of the canalicular duct was an order of magnitude higher than is calculated from the observed objective and subjective resonses of man to angular accelerations. Investigation of the influence of viscous drag of the cupula on the membranous ampulla showed that for the dimensions of the cupula and the clearance between the cupula and the ampulla that is observed from histological studies, the cupula drag contributes some additional damping to the semicircular canals, but that the hydrodynamic drag of endolymph in the canalicular duct is the predominant drag term. The effective moment of inertia of the cupula and the endolymph that surrounds it in the ampulla is shown to contribute an insignificant increase to the inertia of the fluid in the duct. The semicircular canals are found in fact to have an order of magnitude higher frequency response than is observed from objective and subjective measurements and this difference is attributed to a combination of low neural carrier frequency and central nervous system and neuromuscular lags.

Further examination of the structure of the membranous canal duct showed it to be flexible, denser than the surrounding endolymph and perilymph, and attached by fibrous connections along its outer periphery to the bony canal. The distension of the duct under the influence of linear acceleration, which

acts on the density differences between the duct and the fluids, was shown to be responsible for a "roller pump" action when the canal is rotated about an axis orthogonal to the linear acceleration field. This roller pump action produces a steady state cupula deviation in response to a constant rotation in an acceleration field, and offers a realistic physical explanation for the observed bias component of neural discharge from cat canalicular neurons when the animals are subjected to counter-rotating motion. It is shown that less than a 3%/g constriction in duct cross-sectional area can produce the bias component of vestibular nystagmus that has been observed in experiments where the subjects were constantly rotated about a horizontal longitudinal axis, in the author's experiments where subjects were rotated about a vertical axis in a lateral acceleration field by use of a rotating chair mounted on the boom of a centrifuge, and in the analysis of experiments showing the bias component of rotary nystagmus observed from dynamic counterrolling.

This canalicular response to rotation in a linear acceleration field is of some consequence in that it gives the human a significant vestibular input of the same physiological character as an angular acceleration. If rotating environments are to be used for gravity simulation or space station stabilization, then man's ability to interpret correctly and adapt to this new vestibular information must be carefully considered.

6.1.3 Canalicular response to thermal stimulation

Caloric stimulation was shown to produce the physiological equivalent of an angular acceleration. A torque is induced on the endolymph as the result of a temperature gradient across the lateral semicircular canal when the external auditory meatus is irrigated with water at a temperature different from normal body temperature. Analysis of the published results of previous researchers, who measured the time history of the temperature gradient across the lateral canal due to caloric irrigation, produced a system transfer function description relating the temperature of irrigation to an equivalent angular acceleration. It is of the form of a first order lag with a 25 second thermal lag and a gain constant that is consistent with the ratio of the threshold levels of caloric and angular acceleration stimulations. The time history of cupula displacement calculated by cascading the thermal lag transfer function with the hydrodynamic transfer function of the canal was shown to be in close agreement with the time history of the slow phase velocity of caloric vestibular nystagmus. Experiments by the author to evaluate the latency time to the onset of caloric vestibular nystagmus confirm the computed functional relationship and show it to be analogous to the Muelder product which relates the latency time to the onset of subjective sensation of rotation and the strength of angular acceleration stimulation.

6.1.4 Summary

In summary, the results of this investigation have yielded new information on the physical properties of the labyrinthine

fluids. The influences of the inertia and viscous drag of the cupula, and of the flexible membranous canalicular duct, have resulted in a new dynamic model for the response of the semicircular canals to angular and linear acceleration. Further, the demonstrated physiological equivalence between caloric stimulation and angular acceleration now permits inclusion of caloric stimulation in this description of the sensory capabilities of the semicircular canals. The new model, as shown in fig. 6.1, is compatible with available data and shows the sensitivity of the semicircular canals to angular and linear accelerations and caloric stimulation.

6.2 Recommendations for Further Research

From the viewpoint of aerospace medicine and aerospace engineering there are several areas of vestibular research which warrant further investigation.

One area of particular importance is the necessity for a dynamic analysis of the sensing capabilities of the otolith organs. The characteristics of these sensors which have been classically considered to be man's linear motion sensors are not clearly understood, and there is a great deal of speculation and concern over the effects of long term weightlessness on their performance. Histological and physiological studies are now in progress to determine their properties and the time is now appropriate for a detailed analysis of their physical and dynamic properties.

Several topics for further investigation emerged during this investigation. These topics lie in the realm of verifying or supplementing the various topics which were

considered in this work.

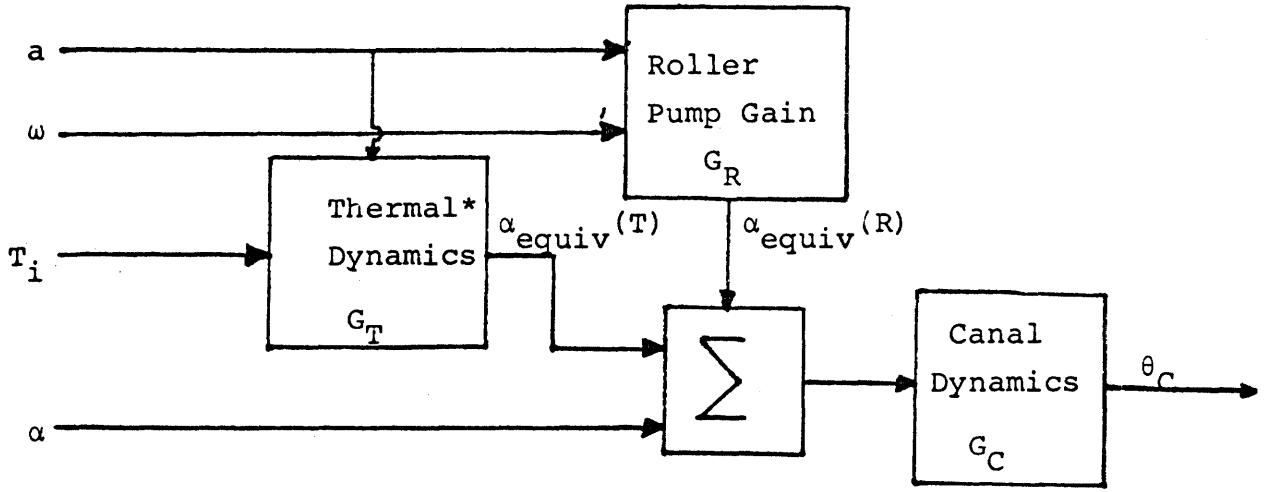
The large disparity between measured and calculated dynamic characteristics could be further investigated by detailed examination of the neural recordings and nystagmus responses from various species of animals. Direct neural recordings during impulsive stimuli could show occasional high speed response of the cupula if neurons with a higher discharge rate can be found and recorded from.

The thermal transfer function from which one can evaluate the time history of cupular response from caloric stimulation can be further investigated by a comparative study of neuron recordings and nystagmus records from animals. The thermal impedance of the tympanic membrane and the surrounding bone and tissue structure must be evaluated to extend the application of the caloric model to the "minimum caloric" tests and small volume (30 cc) ice water injections that are currently being used by some investigators. Also, long term zero-g caloric experiments can point out the influence of direct thermal stimulation of the canalicular neurons.

A critical experiment to test the validity of the roller pump theory of canalicular stimulation by rotation in a linear acceleration field is necessary. Since the roller pump action requires canalicular duct flexibility, rendering the ducts rigid would be a means to test the principle. This could possibly be effected by filling the perilymph space in the bony canal with a fluid which solidifies. Great care

will have to be taken to insure that the canals are still functional and that the solidification process is confined to the perilymph space.

$$G_r = .3\left(1 - \frac{A_c}{A}\right)\omega\,\frac{a}{G}$$



$$G_T = \frac{10^{-3}a}{25s + 1} \qquad G_C = \frac{C}{\alpha(s)} = \frac{.22}{s^2 + 220\left(1 + \frac{4.5 \times 10^{-6}}{\Delta B}\right)s + .07K}$$

* For lateral canal only

Figure 6.1
Block diagram for cupula response to linear and angular acceleration and caloric stimuli

APPENDIX A

PHYSICAL PROPERTIES OF LABYRINTHINE FLUIDS

A.1. Introduction

The properties of density, coefficient of thermal expansion, viscosity, and thermal coefficient of viscosity have been measured for human endolymph and perilymph and cat perilymph, and are presented in table 1. Descriptions of the instruments used for these measurements are given in Appendix B.

The human and cat endolymph and perilymph samples were obtained through the cooperation of the staff at the Massachsetts Eye and Ear Infirmary, and in particular with the assistance of Dr. Herbert Silverstein.

A.2. Newtonian Behavior of Human Endolymph

By operation of the microviscometer at two different angles of inclination (20^{o} and 35^{o}) it was found that the viscosities did not vary appreciably, even though the terminal velocities of the rolling sphere was nearly doubled. The viscosity was also measured after setting for one day, and again after one week, and within the 2% accuracy limitation of the instrument, no measurable change in viscosity was noted. Thus it appears that endolymph is not a shear thinning fluid nor does its

Physical Properties of Labyrinthine Fluids at 35°C

	Human Endolymph	Human Perilymph	Cat Perilymph	Measurement Accuracies	H_2O
Specific Gravity	1.00	1.00	1.00	$\pm$2%	1.00
Coefficient of Expansion	$-4.4 \times 10^{-4}/^{o}C$	$-4.4 \times 10^{-4}/^{o}C$	$-4.4 \times 10^{-4}/^{o}C$	$\pm$5%	$4.0 \times 10^{-4}/^{o}C$
Viscosity (centipoise)	.852	.802	.780	$\pm$2%	.7225
Specific Viscosity	1.18	1.11	1.08		
Temperature Coefficient of Viscosity	$-2.4\%/^{o}C$	$-2.3\%/^{o}C$	$-2.5\%/^{o}C$	$\pm$10%	$-2.0\%/^{o}C$

Table 1

viscosity change with "setting time." Further, its chemical analysis shows a low protein content that is typical of Newtonian fluids.

APPENDIX B

INSTRUMENTS USED TO MEASURE THE PHYSICAL PROPERTIES OF THE LABYRINTHINE FLUIDS

B.1. Viscosity Measurements

A microviscometer was designed, tested, calibrated, and used to measure the viscosities of 1 μl samples of endolymph and perilymph at several temperatures near 35°C.

The instrument was designed around the principle of Flowers' rolling sphere viscometer. Flowers used a sphere in a closed tube of fluid lying on an inclined plane, and showed that the viscosity of a fluid measured by this technique to a first order approximation is given by the equation

$$\mu = \frac{K}{v} (\rho B - \rho F) = A\ t\ (\rho B - \rho F) \qquad (B.1)$$

where

ρB = density of sphere

ρF = density of fluid

v = terminal velocity of sphere in fluid

t = time for ball to travel a fixed distance

K, A = gain constants of the instrument

Using the analysis of Hershey, it can be shown that the relative error obtained by ignoring initial acceleration to terminal velocity, for fluids with a viscosity near that of water, is of the order of 0.2% for the dimensions of this instrument. To further improve the accuracy of the measurement of the terminal velocity of the rolling ball, in our viscometer the velocity is measured over a 1 cm. distance at the end of the tube, long after terminal velocity has been reached. One further source of error arises from the variation of the gain "constant" of the instrument, A, with temperature. This variation is taken into account by careful calibration of the instrument with fluids of known viscosities at several temperatures.

Description of the Microviscometer

The basic velocity (or time) measurement unit is an epoxy block with two prefocused miniature lamps which form two 0.020 in. diameter light beams, and two high speed photo diodes to measure the time of travel of a 0.010 in. diameter tungsten carbide sphere in a miniature pipette. A modified five microliter lambda pipette (0.016 in. inside diameter) containing the sample is mounted in such a manner that each light beam is broken by the rolling sphere and the time interval between the interruptions as registered by the amplified outputs of the photo diodes is recorded by an external electronic counter. As shown in figure B.1 an electrically grounded aluminum shield is sandwiched between the sections of the epoxy block and serves both as an electrostatic shield for the rolling sphere and as a temperature

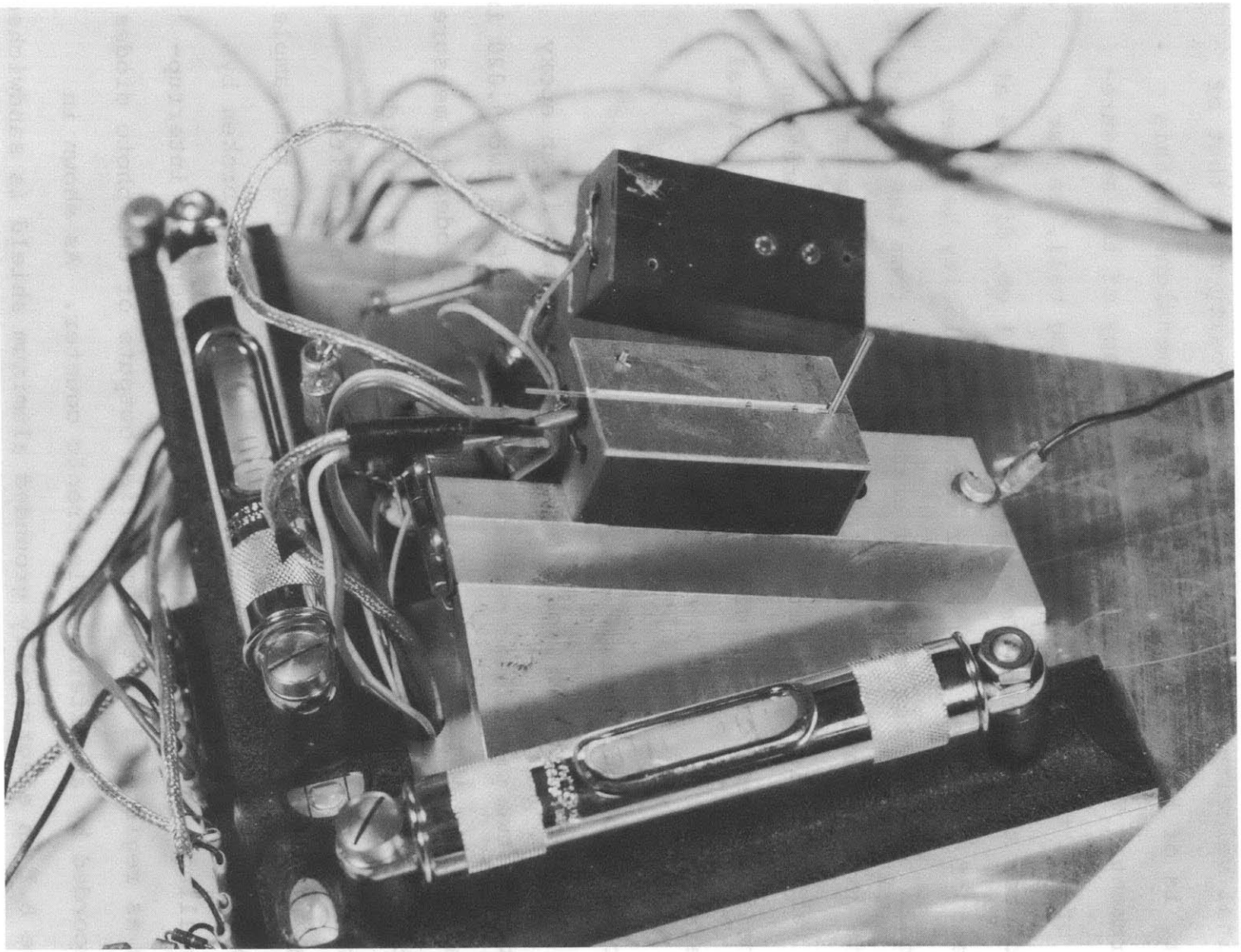


Figure B.1
Close up view of microviscometer

regulator for the sample. The temperature of the aluminum shield, and thus of the sample, is regulated to an accuracy of $\pm .1^{o}C$ through power resistors mounted in both halves of the block and a sensitive calibrated thermistor attached to the underside of the shield plate.

The velocity measurement unit is mounted on a hinged inclined plane at an angle of twenty degrees from its base and is provided with an external cable to tilt the platform to return the ball to the beginning of the tube. The inclined plane is mounted on a ten inch triangular plate which is provided with two levels and two micrometer adjustable legs for leveling. The entire apparatus is confined by an aluminum covered plexiglass case which improves temperature stability, and provides a Faraday cage for the elimination of electromagnetic pick up. The measurement set up is shown in figure B.2. In figure B.3 is shown the electronic schematic for the photo diode amplifier and the temperature control system.

B.2. Sample Handling Technique

Because of the small quantity and volatility of endolymph and perilymph, extreme care must be exercised in transferring the samples into the calibrated pipettes. The most successful technique to date uses mineral oil as a seal for the open end of the capillary tube, and a ten microliter hypodermic syringe custom equipped with an 0.008 in. o.d. needle is used to transfer the samples. A four step (alcohol, acetone, ether, air) cleaning process is used on the tubes and syringe before reloading a new sample. After loading a sample it is necessary

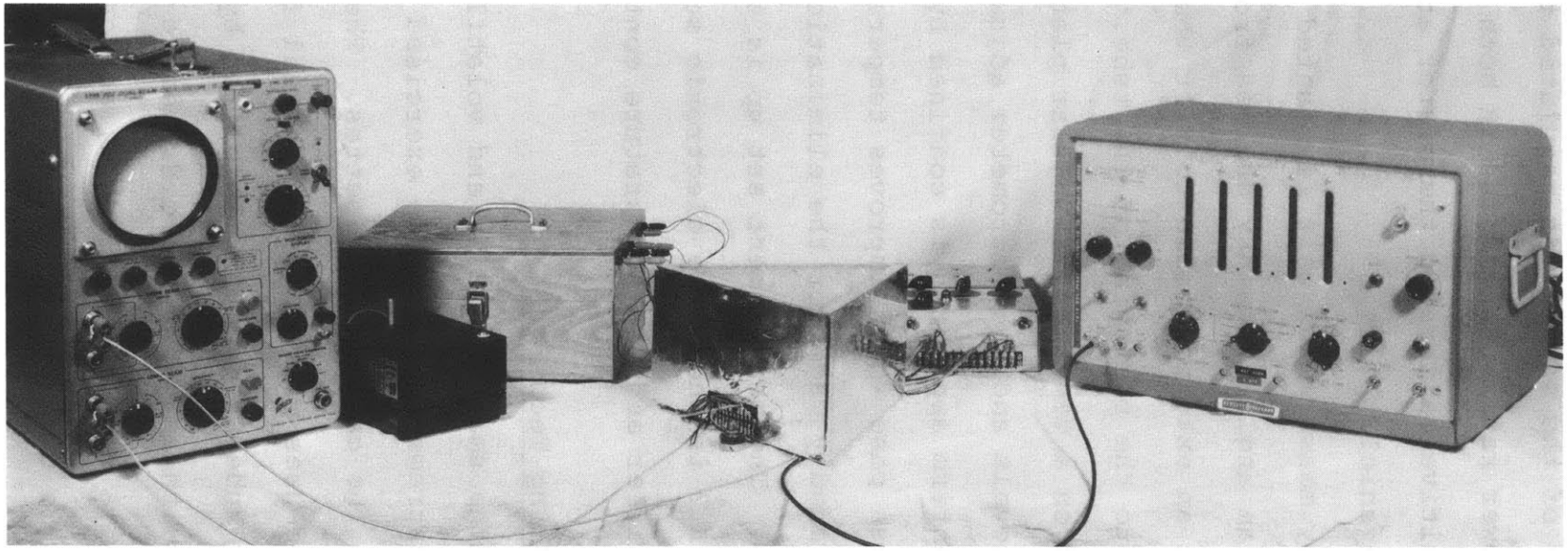


Figure B.2
Viscosity test set up

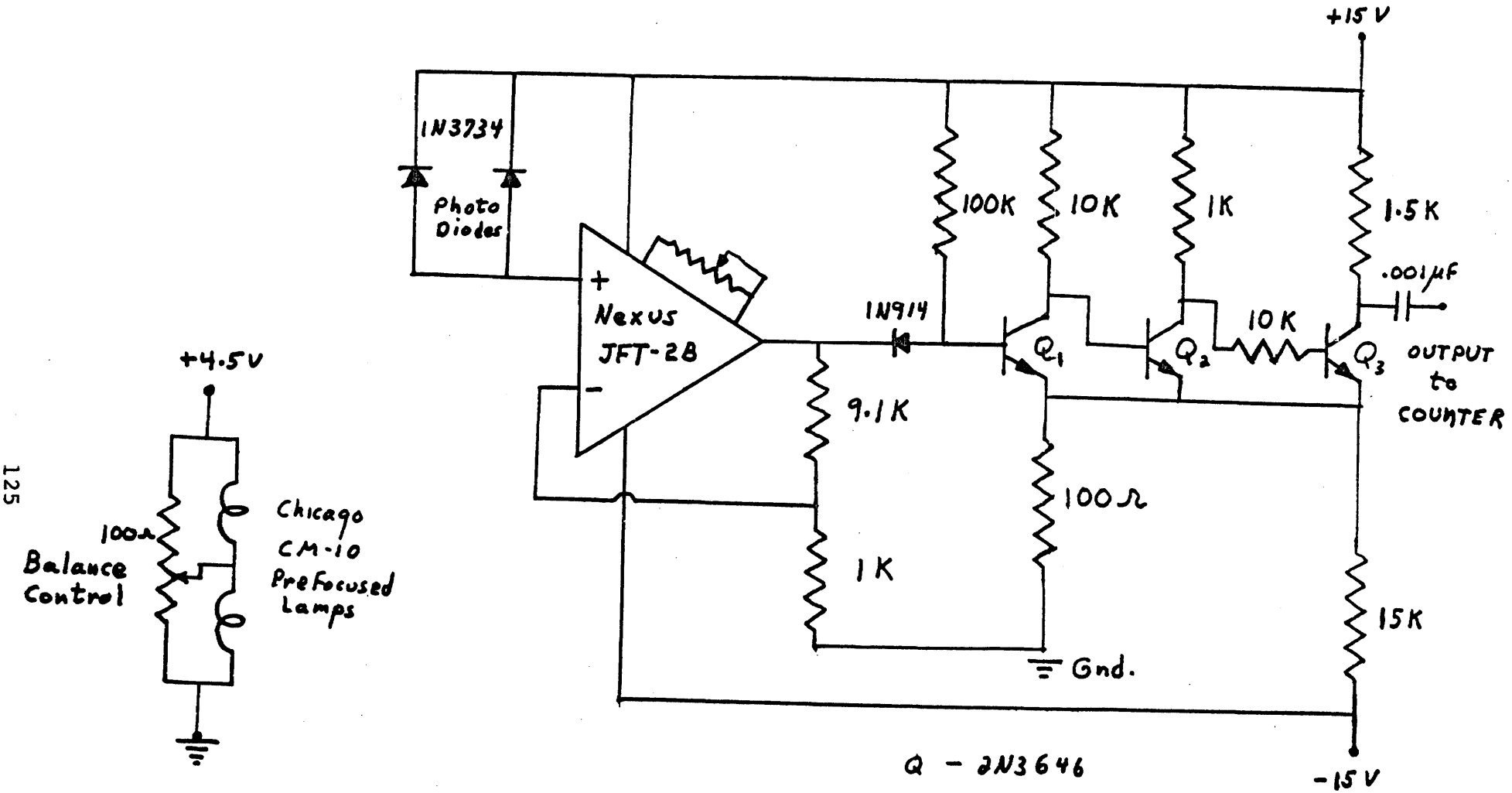


Figure B.3
Electrical schematic for microviscometer

to centrifuge it to separate the oil droplets from the sample. The oil in the open end of the tube provides a barrier which the sphere cannot penetrate because of its high surface tension forces.

The sample with its ball and cap is demagnetized to eliminate any magnetic forces acting on the ball (which was inserted into the tube with magnitized tweezers). The sample is then inserted in the "V" groove in the microviscometer and allowed fifteen minutes to reach the proper temperature. The syringe and a section of a calibrated tube with a sphere enclosed are shown in figure B.4.

B.3. Calibration of Microviscometer

The capillary tubes to be calibrated are cleaned, sealed at one end with an alcohol burner, then fitted with a clean sphere. They are then filled with distilled water and a drop of mineral oil and are centrifuged to eliminate bubbles, and to separate the oil from the water. A "standard" tube is sealed at both ends and used as a "calibration reference." The tubes are then run in the viscometer at the desired temperature and at least thirty measurements are made to determine the "gain constant" of the tube-ball assembly. It was found that for a clean tube the standard deviation of the thirty measurements was approximately 0.2%.

In calibrating the tube in this manner we are actually evaluating

$$A = \frac{\mu(H_2O)}{t_o(\rho_B - \rho H_2 0)} \tag{B.2}$$

Rewriting eq. (B.1) using the above value of A

$$\frac{\mu}{\mu_{(H_2O)}} = \frac{t}{t_o(\rho_B - \rho_{H_2O})} (\rho_B - \rho_{H_2O} + \rho_{H_2O} - \rho_F)$$

$$= \frac{t}{t_o} \left(1 + \frac{\rho_{H_2O} - \rho_F}{\rho_B - \rho_{H_2O}}\right)$$

Since the specific gravity of tungston carbide is (13 ± .1) then a difference in densities, between water and the fluid measured, of 2% contributes less than .2% to the measured value of μ.

For each of the samples measured, the transit times for thirty repeated measurements showed a standard deviation of from .2% to .4%. Also, to an accuracy of ±2% the densities of the fluids were indistinguishable from that of water at 35°C. Thus after combining the randomness in the measurement of t and t_o, and the possible density error of ±2%, the overall accuracy (3σ) of the instrument is ±2%.

B.4. Density Measurement of Labyrinthine Fluids

By weighing a calibrated micropipette when empty, filled with water, and filled with cat or human endolymph or perilymph,

it was found, as stated in the last paragraph, that to an accuracy of ±2%, their densities were the same as water. Since this accuracy was sufficient for accurate computation of their viscosities, the more accurate "density gradient column" technique was not used. These results, although not as precise, are consistent with the findings of Money who has reported the specific gravity of pigeon endolymph and perilymph to be 1.0033 and 1.0022 respectively.[133]

Thermal Coefficient of Expansion

For calculation of the torque on the endolymph due to caloric stimulation, it is necessary to know the change in density of endolymph due to variations in temperature. For this purpose it is convenient to recall that

$$\frac{\partial v}{v \partial T} = - \frac{\partial \rho}{\rho \partial T} \qquad (B.3)$$

where

v = volume

ρ = density

T = temperature

The coefficient of expansion $(\frac{\partial v}{v \partial T})$ was obtained by measuring the change in length of a 0.500 inch column of fluid in a glass capillary by a microscope equipped with a micrometer adjustable with a resolution of 0.05×10^{-3} in. By measuring the change in length for a 10^{o}C change in temperature and accounting for the expansion of the glass pipette, the coefficient

of expansion of cat and human endolymph and perilymph was found to be $4.4 \times 10^{-4}/^{o}C$ ±5%.

REFERENCES

1. Abramowitz, M., and Stegun, I. A., Handbook of Mathematical Functions, AMS 55, National Bureau of Standards, 1965

2. Aschan, G., "Response to Rotary Stimuli in Fighter Pilots," Acta Oto-Laryngologica, Supp. 115, 1954

3. Aschan, G., 1955, cited by Henriksson, N., Acta Oto-Laryngologica, Supp. 125, 1956

4. Barany, R., Mschr. Ohrenheilk, 50, 229, 1956

5. Barany, R., Mschr. Ohrenheilk, 50, 191, 1906

6. Barlow, John S., "Inertial Navigation as a Basis for Animal Navigation," Neurophysiology Lab. of Neurology Service, Massachusetts General Hospital

7. Barnhill, J. H., Surgical Anatomy of the Head and Neck, The Williams and Watkins Co., Baltimore, 1940

8 Benson, A. J., "Modification of Pre- and Post-Rotational Responses by the Concomitant Linear Acceleration," Second Symposium on the Role of the Vestibular Organs in Space Exploration, NASA SP-115, January 25, 1966

9. Bergstedt, M., "The Effect of Gravitational Force on the Vestibular Caloric Test," Acta Oto-Laryng., 53, 1961, pp. 551-562

10. Billingham, J., "Russian Experience of Problems in Vestibular Physiology Related to Space Environment," Second Symposium on the Role of the Vestibular Organs in Space Exploration, NASA SP-115, January 1966

11. Biosystems, Inc., "Biological Control Systems: A Critical Review and Evaluation," Second Quarterly Progress Report

12. Breuer, J., Pflugers Arch. ges. Physiol., 44:135, 1889

13. Brodal, A., "Fiber Connections of the Vestibular Nuclei," Neural Mechanisms of the Auditory and Vestibular Systems, Charles C. Thomas, Springfield, Illinois, 1962

14. Brown, J. L., Lechner, M., "Acceleration and Human Performance," J. of Aviation Med., 27:32-49, 1956

15. Brown, S. C., Course Lectures on the Physiology and Pathology of the Central Nervous System, Philadelphia, p. 187, 1860

16. Buys, E., Rev. d'Oto-Neuro-Ocul., 2:641, 1924

17. Cappel, K. L., "Determination of Physical Constants of the Semicircular Canals from Measurement of Single Neural Unit Activity Under Constant Angular Acceleration," Second Symposium on the Role of the Vestibular Organs in Space Exploration, NASA SP-115, January 1966

18. Capps, M., and Collins, W. E., "Effects of Bilateral Caloric Habituation on Vestibular Nystagmus in the Cat," Acta Oto-Laryng., 59, 1965

19. Cawthorne, T., Dix, A R., Hallpike, C. S., and Hood, J. D., "Vestibular Function," British Medical Bulletin, 12:2, 1956 (Neuro-Otology), 131-142

20. Cawthorne, T., and Cobb, W. A., "Temperature Changes in the Perilymph Space in Response to Caloric Stimulation in Man," Acta Oto-Laryng., 44:580, 1956

21. Cawthorne, T., Fitzgerald, G., and Hallpike, S. C., "Studies in Human Vestibular Function,II: Observations on the Directional Preponderance of Caloric Nystagmus ("Nystagmusbereitschaft") Resulting from Unilateral Labyrinthectomy," Brain, 65:138-160, 1942

22. Clark, W. B., and Graybiel, A., "The Lag Effect Associated with Stimulation of the Semicircular Canals as Indicated by the Oculogyral Illusion," Proj. Rept. NM 001 059.01.25, Nov. 1950

23. Clark, W. B., and Graybiel, A., "Human Performance During Adaptation to Stress in the Pensacola Slow Rotation Room," Aerospace Med., No. 32, pp. 93-106, February 1961

24. Clark, W. B., and Graybiel, A., "Vertigo as a Cause of Pilot Error in Jet Aircraft," J. Aviation Med., 28:469-78

25. Clark, W. B., Nicholson, M. A., "Aviator's Vertigo: A Cause of Pilot Error in Naval Aviation Students," J. Aviation Med., 25:171-179, 1954

26. Clark, W. B., and Graybiel, A., "Perception of the Postural Vertical as a Function of Practice in Normal Persons and Subjects with Labyrinthine Defects," NASA Rept. No. 63, Bureau of Medicine and Surgery, Project MR 005.13-6001

27. Clark, W. B., Graybiel, A., and MacCorquodale, "The Illusory Perception of Movement Caused by Angular Acceleration and by Centrifugal Force during Flight, II: Visually Perceived Motion and Displacement of a Fixed Target During Turns," J. Exp. Psychol., 38:298-309, 1948

28. Clark, W. B., and Stewart, J. D., "Perception of Angular Acceleration About the Yaw Axis of a Flight Simulator," Aerospace Med., 33, December 1962

29. Collins, W. E., "Effects of 'Double Irrigations' on the Caloric Nystagmus of the Cat," Acta Oto-Laryng., 59, July 1, 1964

30. Collins, W. E., "Subjective Responses and Nystagmus Following Repeated Unilateral Caloric Stimulation," Annals of Otology, Rhinology, and Laryngology, December 1965, Vol. 74, No. 4, p. 1034

31. Collins, W. E., "Methodology in Caloric Test of Vestibular Function," Third Symposium on the Role of the Vestibular Organs in Space Exploration, January 1967

32. Collins, W. E., "Further Studies of the Effects of Mental Set Upon Vestibular Nystagmus," U.S. Medical Research Lab., Fort Knox, Ky., Report No. 443, December 1960

33. Collins, W. E., and Guedry, F. E., "Arousal Effects and Nystagmus During Prolonged Constant Angular Acceleration," U.S. Army Medical Research Lab., Fort Knox, Ky., Rept. No. 500, August 1961

34. Collins, W. E., Crampton, G. H., and Posner, J. B., "The Effects of Mental Set Upon Vestibular Nystagmus and the Electroencephalogram," U.S. Army Medical Research Lab., Fort Knox, Ky., Report No. 439, September 1960

35. Collins, W. E., Guedry, F. E., Posner, J. B., "Control of Caloric Nystagmus by Manipulating Arousal and Visual Fixation Distance," U.S. Army Medical Research Lab., Fort Knox, Ky., Rept. No. 485, August 1961

36. Collins, W. E., "Inverse Caloric Nystagmus Obtained by Unilateral Stimulation of the Cat," Nature, 195:4843, August 25, 1962

37. Collins, W. E., "Primary, Secondary, and Caloric Nystagmus of the Cat Following Habituation to Rotation," J. of Comparative and Physiological Psychology, 57:3, pp. 417-421, 1964

38. Collins, W. E., "Repeated Caloric Stimulation of the Human Labyrinth and the Question of Vestibular Habituation," NASA Symposium on the Role of the Vestibular Organs in Space Exploration, NASA SP-77, January 1965

39. Collins, W. E., "Problems in Spatial Orientation: Vestibular Studies of Figure Skaters," Abstract from 17th Annual Session of the American Academy of Ophthalmology and Otolaryngology, Chicago, Nov. 14-19, 1965

40. Collins, W. E., "Nystagmus Responses of the Cat to Rotation and to Directionally Equivalent and Non-Equivalent Stimuli after Unilateral Caloric Habituation," Acta Oto-Laryng., 58, December 6, 1963

41. Collins, W. E., "Task-Control of Arousal and the Effects of Repeated Unidirectional Angular Acceleration of Human Vestibular Responses," Acta Oto-Laryng., Supp. 190, 1964

42. Correia, M. J., Guedry, F. E., "Influence of Labyrinth Orientation Relative to Gravity on Responses Elicited by Stimulation of the Horizontal Semicircular Canals," Bureau of Medicine and Surgery, Project MR005.13-6001, NASA Rept. No. 100, NASA Order No. R-93

43. Cramer, R. L., Dowd, P. J., and Helms, D. B., "Vestibular Responses to Oscillation about the Yaw Axis," Aerospace Med., 34:1031-1034, 1963

44. Crampton, G. H., "Does Linear Acceleration Modify Cupular Deflection?" Second Symposium on the Role of the Vestibular Organs in Space Exploration, NASA SP-115, January 1966

45. Crampton, G. H., "Response of Single Cells in Cat Brain Stem to Angular Acceleration in the Horizontal Plane, NASA Symposium on the Role of the Vestibular Organs in Space Exploration, NASA SP-77, January 1965

46. Dodge, R., "Thresholds of Rotation," J. of Exp. Psych., pp. 107-137, June 1923

47. Dohlman, G., "Physikalische und Physiologische Studien zur Theorie des Kalorischen Nystagmus," Acta Oto-Laryng., Supp. 5, 1925

48. Dohlman, G., Acta Oto-Laryng., 26:425, 1938

49. Engstrom, H., Lindeman, H., and Ades, H., "Anatomical Features of the Auricular Sensory Organs," Second Symposium on the Role of the Vestibular Organs in Space Exploration, NASA SP-115, January 1966

50. Engstrom, H., "On the Double Innervation of the Sensory Epithelia of the Inner Ear," Acta Oto-Laryng., 49:109-118, 1958

51. Egmond, A. A. J van, Groen, J. J., and Jongkees, L. B. W., "Rotational Test," J. Physiol., 110:1, 1949

52. Fitzgerald, G., and Hallpike. C. S., Brain, 65:115, 1942

53. Fleishman, E. A., "The Influence of Fixed Versus Free Head Position on the Perception of Body Position," Perceptual and Motor Skills Research Lab., Lackland AFB, Texas, Research Bulletin 53-37, October 1953

54. Fluur, E., "The Mechanism of Nystagmus," Acta Oto-Laryng., 54:181-188, 1962

55. Fluur, E., and Mendel, L., "Habituation, Efference, and Vestibular Interplay," Acta Oto-Laryng., 56

56. Fluur, E., and Mendel, L., "Relation Between Strength of Stimulus and Duration of Latency Time in Vestibular Rotary Nystagmus," Acta Oto-Laryng., 61, February 1966

57. Gazenko, O. G., Chekhonadskiy, N. A., Razumeyev, A. N., and Yegorov, B. B., "An Elementary Model of the Vestibular Apparatus," NASA TT-F-368, Problems in Space Biology, USSR, 1965

58. Gerathewohl, S. J., and Stallings, H. D., "The Labyrinthine Posture Reflex (Righting Reflex) in the Cat During Weightlessness," J. Aviation Med., Vol 28, No. 4, pp. 345-55, August 1957

59. Gernandt, B. E., Igarashi, M., Ades, H. W., "Effects of Prolonged Caloric Stimulation Upon Oculomotor, Vestibulospinal, and Segmental Spinal Activity," Naval School of Aviation Medicine, Pensacola, Florida, NSAM-934, NASA No. R-93, June 1965

60. Goody, W., and Reinhold, M., "Some Aspects of Human Orientation in Space," 2 parts, Brain, Vol 76, Part 3, pp. 337-363

61. Grahe, K., Hirn und Ohr, Leipzig, p. 32, 1932

62. Gray's Anatomy, 33rd Edition, Longmaus, Green & Co., 1962

63. Graybiel, A., Clark, B., "Perception of the Horizontal or Vertical with the Head Upright, on the Side, and Inverted under Static Conditions, and During Exposure to Centripetal Force," Bureau of Medicine and Surgery, NASA Rept. No. 60, August 1961

64. Graybiel, A., and Deane, F. R., "Transfer of Habituation on Change in Body Position Between Upright and Horizontal in a Rotating Environment," Third Symposium on the Role of the Vestibular Organs in Space Exploration, January 1967

65. Graybiel, A., Kerr, W. A., and Bartley, H., "Stimulus Thresholds of the Semicircular Canals as a Function of Angular Acceleration," The Am. J. of Psych., 61:21-36, January 1948

66. Graybiel, A., Clark, B., and Zarriello, J. J., "Observations on Human Subjects Living in a 'Slow Rotation Room' for Periods of Two Days," AMA Archives of Neurology, 3:55-77, July 1960

67. Graybiel, A., Clark, B., "Visual Perception of the Horizontal Following Exposure to Radial Acceleration on a Centrifuge," J. Comparative and Physiological Psych., 44:6, December 1951

68. Graybiel, A., Guedry, F. E., Johnson, W., and Kennedy, R., "Adaptation to Bizarre Stimulation of the Semicircular Canals as Indicated by the Oculogyral Illusion," Aerospace Med., Vol 32, pp. 321-327, April 1961

69. Graybiel, A., Niven, J. I., and Walsh, T. E., "The Differentiation Between Symptoms Referable to the Otolith Organs and Semicircular Canals in Patients with Nonseparative Labyrinthitis," The Laryngoscope, 62:9, pp. 924-933, September 1952

70. Graybiel, A., and Johnson, W. H., "A Comparison of the Symptomatology Experienced by Healthy Persons and Subjects with Loss of Labyrinthine Function when Exposed to Unusual Patterns of Centripetal Force in a Counter-Rotating Room," Annals of Otology, Rhinology, and Laryngology, 72:2, p. 357, June 1963

71. Graybiel, A., Kennedy, R., Guedry, F. E., McLeod, M. E., Colehour, Miller, Knoblock, Mertz, "The Effect of Exposure to a Rotating Environment (10 rpm) on Four Aviators for a Period of 12 Days," Symposium on the Role of the Vestibular System in Space Exploration, NASA SP-77, January 1965

72. Groen, J. J., Lowenstein, O., and Vendrik, A. J., J. Physiol., 117:329, 1952

73. Groen, J. J., "The Semicircular Canal Systems of the Organs of Equilibrium, I and II," Physics in Medicine and Biology, 1, 1956-57

74. Gualtierotti, T., Gerathewohl, S. J., "Spontaneous Firing and Responses to Acceleration of Single Otolith Units of the Frog During Short Periods of Weightlessness During Parabolic Flight," NASA Symposium on the Role of the Vestibular Organs in Space Exploration, NASA SP-77, January 1965

75. Guedry, F. E., "Comparison of Vestibular Effects in Several Rotating Environments," NASA Symposium on the Role of the Vestibular Organs in Space Exploration, NASA SP-77, January 1965

76. Guedry, F. E., Collins, W. E., and Sheffey, L., "Perceptual and Oculomotor Reactions to Interacting Visual and Vestibular Stimulation," U.S. Army Med. Research Lab., Fort Knox, Ky., Rept. No. 463, March 1961

77. Guedry, F. E., and Graybiel, A., "The Appearance of Compensatory Nystagmus in Human Subjects as a Conditioned Response During Adaptation to a Continuously Rotating Environment," U.S. Army Med. Research Lab., Fort Knox, Ky., Rept. No. 531, March 1962

78. Guedry, F. E., and Montague, E. K., "Relationship Between Magnitudes of Vestibular Reactions and Effective Coriolis Couples in the Semicircular Canal System," U.S. Army Med. Research Lab., Fort Knox, Ky., Rept. No. 456, December 1960

79. Guedry, F. E., "Orientation of the Rotation Axis Relative to Gravity: Its Influence on Nystagmus and the Sensation of Rotation," Bureau of Medicine and Surgery, Rept. No. 96, June 1964

80. Guedry, F. E., "Influence of Linear and Angular Accelerations on Nystagmus," Second Symposium on the Role of the Vestibular Organs in Space Exploration, NASA SP 115, January 1966

81. Guedry, F. E., and Kalter, H., "Description of Human Rotation Device," U.S. Army Med. Research Lab., Ft. Knox, Ky., Rept. No. 242, May 1956

82. Guedry, F. E., and Graybiel, A., "Compensatory Nystagmus Conditioned During Adaptation to Living in a Rotating Room," J. of Applied Physiology, 17:3, May 1962

83. Guedry, F. E., Peacock, L. J., and Cramer, R. L., "Nystagmic Eye Movements During Interacting Vestibular Stimuli," U.S. Army Medical Research Lab., Ft. Knox, Ky., Rept. No. 275, March 1957

84. Guedry, F. E., and Lauver, L. S., "The Oculomotor and Subjective Aspect of the Vestibular Reaction During Prolonged Constant Angular Acceleration," U.S. Army Med. Research Lab., Ft. Knox, Ky., Rept. 438, September 1960

85. Hallpike, C. S., and Hood, J. D., Proc. Roy. Soc, London, B:141, 216, 1953

86. Hammer, L. R., "Perception of the Visual Vertical Under Reduced Gravity," Aerospace Medical Div., Wright-Patterson AFB, Ohio, Rept. MRL-TDR-62-55, May 1962

87. Henriksson, H. G., "Speed of Slow Component and Duration in Caloric Nystagmus," Acta Oto-Laryng., Supp. 125, 1956

88. Henriksson, N. G., "Tests of Canal Functions with Special Reference to Central Vestibular Pathways," Third Symposium on the Role of the Vestibular Organs in Space Exploration, January 1967

89. Hildebrand, F. B., Advanced Calculus for Applications, Prentice Hall

90. Hixson, W. C., and Niven, J. I., "Application of the System Transfer Function Concept to a Mathematical Description of the Labyrinth: I, Steady-State Nystagmus Response to Semicircular Canal Stimulation by Angular Acceleration," Bureau of Med. and Surg., Rept. No. 57, 1961

91. Igarashi, M., "Dimensional Study of the Vestibular End Organ Apparatus," Second Symposium on the Role of the Vestibular Organs in Space Exploration, NASA SP-115, January 1966

92. Johnson, W. H., and Smith, B., "Functions of the Utricular Macula: A Preliminary Report," Canad. J. of Bioch. Phys., 37:605-6, 1959

93. Johnson, W. H., "Head MOvement Measurements in Relation to Spatial Disorientation and Vestibular Stimulation," J. of Aviation Med., 27:148-52, March 1955

94. Johnson, W. H., Money, K. E., and Graybiel, A., "Some Vestibular Responses Pertaining to Space Travel," NASA Symposium on the Role of the Vestibular Organs in Space Exploration, NASA SP-77, January 1965

95. Jones, G. M., Barry, W., and Kowalsky, N., "Dynamics of the Semicircular Canals Compared in Yaw, Pitch, and Roll," Aerospace Med., 35:984-989, 1964

96. Jones, G. M., "On the Dependence of Oculo-Motor Response Upon the Neural Response of the Vestibular System," Third Symposium on the Role of the Vestibular Organs in Space Exploration, January 1967

97. Jones, G. M., Personal Communication, 1967

98. Jones, G. M., "Predominance of Anti-Compensatory Oculomotor Response During Rapid Head Rotation," Aerospace Med., 35:10, 1964

99. Jones, G. M., and Milsum, J. H., "Spatial and Dynamic Aspects of Visual Fixation," IEEE Trans. on Bio-Medical Engineering, Vol. BME-12, No. 2, pp. 54-62, April 1965

100. Jones, G. M., and Spells, K. E., "A Theoretical and Comparative Study of the Functional Dependence of the Semicircular Canal Upon its Physical Dimensions," Proc. Roy. Soc., B, 1957

101. Jones, G. M., "Vestibulo-Ocular Disorganization in the Aerodynamic Spin," Aerospace Med., 36:10, October 1965

102. Jones, G. M., Guedry, F. E., and Benson, A. J., unpublished data, January 1967

103. Jongkees, L. B. W., "Methods Used in Determining Otolith Function," Third Symposium on the Role of the Vestibular Organs in Space Exploration, January 1967

104. Jongkees, L. B. W., Arch. Otolaryng., 48:402, 1948 and 49:594, 1949

105. Jongkees, L. B. W., "Uber die Untersuchungsmethoden des Gleichgewichtsorgans," Fortschr Hals-, Nas,- Ohrenheilk, I, I. S. Karger, Basel/New York, 1953

106. Kellogg, R. S., and Graybiel, A., "Lack of Response to Thermal Stimulation of the Semicircular Canals in the Weightless Phase of Parabolic Flight," Second Symposium on the Role of the Vestibular Organs in Space Exploration, NASA SP-115, January 1966

107. Kellogg, R. S., "Dynamic Counterrolling," Third Symposium on the Role of the Vestibular Organs in Space Exploration, January 1967

108. Knoblock, E. C., "Biochemical Responses to Vestibular Stimulation," NASA Symposium on the Role of the Vestibular Organs in Space Exploration, NASA SP-77, January 1965

109. Krauss, R. N., "Disorientation in Flight," Aerospace Medicine, 30:664-673, April 1959

110. Lansberg, M. P., "The Modulating Influence of the Otolith Organs on Semicircular Canal Functions," NASA Symposium on the Role of the Vestibular Organs in Space Exploration, NASA SP-77, January 1965

111. Lansberg, M. P., Guedry, F. E., and Graybiel, A., "The Effect of Changing the Resultant Linear Acceleration Relative to the Subject on Nystagmus Generated by Angular Acceleration," Bureau of Medicine and Surgery, Rept. No. 99, September 1964

112. Lorente d No', R., 1936, cited by Fitzgerald, E., and Hallpike, C. S., Brain, 65:115, 1942

113. Lowenstein, O., Osborne, M. P., and Wersal, J., "Structure and Innervation of the Sensory Epithelia of the Labyrinth in the Thornback Ray (Raja Clavata)," Proc. Roy. Soc., B, 160:1-12, April 14, 1964

114. Lowenstein, O., Sand, A., "The Activity of the Horizontal Semicircular Canal of the Dogfish, Scyllium Canicula," J. Exptl. Biology, 13:416-28, 1936

115. Lowenstein, O., "The Functional Significance of the Ultra Structure of the Vestibular End Organs," Second Symposium on the Role of the Vestibular Organs in Space Exploration, NASA SP-115, January 1966

116. Lowenstein, O., and Sand, A., Proc. Roy. Soc., London, B. 129:256, 1940

117. MacCorquodale, K., "Effects of Angular Acceleration and Centrifugal Force on Nonvisual Space Orientation During Flight," J. Aviation Med., 19:146-157

118. Mann, C. W., "Visual Factors in the Perception of Verticality," J. Exp. Psych., Vol. 44, 1952

119. Mansurov, A. R., and Markaryan, S. S., "Effect of Rotation of the Human Organism with the Trunk Inclined at Various Angles," NASA TT F-368, Problems in Space Biology, USSR, 1965

120. Martin, J. F., and Jones, G. M., "Theoretical Man-Machine Interaction which Might Lead to Loss of Aircraft Control," Aerospace Med., 36:8, August 1965

121. Mayne, R., "The 'Match' of the Semicircular Canals to the Dynamic Requirements of Various Species," NASA Symposium on the Role of the Vestibular Organs in Space Exploration, NASA SP-77, January 1965

122. Mayne, R., Appendix, Farnsworth, N. B., "Three Dimensional Aspects of the Semicircular Canals," Goodyear Aerospace Co., Arizona Div. Litchfield Park, Arizona, Gera-1057, September 1965

123. McLeod, M. E., and Meek, J. C., "A Threshold Caloric Test: Results in Normal Subjects," U.S. Naval School of Aviation Medicine, NASA NO. R-47, July 1962

124. McLeod, M. E., and Correia, M. J., "Use of Caloric Test in Evaluating the Effects of Gravity on Cupula Displacement," U.S. Naval School of Aviation Medicine, Pensacola, Florid . NASA NO. R-93, April 1964

125. Meiry, J. L., and Young L. R., "Biophysical Evaluation of the Human Vestibular System," First Annual Status Rept. on NASA Grant NGR 22-009-156, June 1966

126. Meiry, J. L., "The Vestibular System and Human Dynamic Space Orientation," Sc.D. Thesis, M.I.T., 1965

127. Merrington, Viscometry, Edward Arnold & Co., London, 1951

128. Miller, E. F., and Graybiel, A., "A Comparison of Ocular Counterrolling Movements Between Normal Persons and Deaf Subjects with Bilateral Labyrinthine Defects, NASA Rept. No. 68, Bureau of Medicine and Surgery, February 1962

129. Miller, E. F., and Graybiel, A., "Otolith Function as Measured by Ocular Counterrolling," NASA Symposium on the Role of the Vestibular Organs in Space Exploration, NASA SP-77, January 1965

130. Milojevic, B., "Influence of the Otoliths on the Duration of Post-Caloric Nystagmus," NASA Symposium on the Role of the Vestibular Organs in Space Exploration, NASA SP-77, January 1965

131. Mishkin, S., and Jones, G. M., "Predominant Direction of Gaze During Slow Head Rotation," Aerospace Med., 17:1, 1966

132. Mittermaier, R., Acta Oto-Laryng. 44:574, 1954

133. Money, K. E., Sokoloff, M., and Weaver, R. S., "Specific Gravity and Viscosity of Endolymph and Perilymph," Defense Research Medical Lab. Research Paper No. 629, 1965, and Second Symposium on the Role of the Vestibular Organs in Space Exploration, NASA SP-115, January 1966

134. Money, K. E., "Vestibular Problems in Rotating Spacecraft," NASA Symposium on the Role of the Vestibular System in Space Exploration, NASA SP-77, 1965

135. Money, K. E., "Tests of Semicircular Canals and Otoliths in Cats," Third Symposium on the Role of the Vestibular Organs in Space Exploration, January 1967

136. Money, K. E., Personal communication, January 1967

137. Muller, W., "Zum Problem der Anlaufstromung einer Flussigkeit inn geraden Rohr mit Kreisring - und Kreisquerschnitt," ZAMM, p. 227, 1936

138. Newton, G. C., Gould, L. A., and Kaiser, J. F., Analytical Design of Linear Feedback Controls, Wiley, 1957

139. Niven, J. E., Hixson, W. C., and Correia, M.J., "An Experimental Approach to the Dynamics of the Vestibular Mechanisms," NASA Symposium on the Role of the Vestibular Organs in Space Exploration, NASA SP-77, January 1965

140. Niven, J. I., and Hixson, W. C., "Frequency Response of the Human Semicircular Canals: Steady-State Ocular Nystagmus Response to High-Level Sinusoidal Angular Rotations," Bureau of Med. and Surgery, Rept. No. 58

141. Nuttall, J.B., "The Problem of Spatial Disorientation," JAMA, 155:5, February 1958

142. Roman, J. A., Warren, B. H., and Graybiel, A., "The Sensitivity to Stimulation of the Semicircular Canals During Weightlessness," USAF School of Aerospace Medicine, Rept. No. SAM-TDR-62-148, 1963

143. Schlichting, H., Boundary Layer Theory, McGraw-Hill Book Co., 4th Edition, 1960

144. Schmalz, Proc. Roy. Soc. Med., 25:359, 1932

145. Schone, H., "On the Role of Gravity in Human Spatial Orientation," Aerospace Med., 35:764-772, 1964

146. Steer, R. W., Li, Y. T., Young, L. R., and Meiry, J. L., "Physical Properties of the Labyrinthine Fluids and Quantification of the Phenomenon of Caloric Stimulation," Third Symposium on the Role of the Vestibular Organs in Space Exploration, January 1967

147. Steinhausen, W., Pflug. Arch. ges. Physiol., 229:439, 1931, and 228:322, 1931

148. Stone, R. W., Letko, W., "The Effects of the Plane of Vestibular Stimulation on Task Performance and Involuntary Eye Movement," Third Symposium on the Role of the Vestibular Organs in Space Exploration, January 1967

149. Stone, R. W., and Letko, W., "Some Observations During Weightlessness Simulation with Subject Immersed in a Rotating Tank of Water," NASA TN D-2195, September 1964

150. Tardov, V. M., Ustgushin, B. V., Orlov, S. F., "The Problem of Human Resistance to Short-Term Angular Accelerations of Large Magnitudes," NASA TT F-368, Problems of Space Biology, USSR-1965

151. Van Egmond, A. A. J., Groen, J. J., and Jongkees, L. B. W., "The Mechanics of the Semicircular Canal," J. Physiolog., 110:1-17, 1949

152. Vinacke, E. W., "Aviator's Vertigo," J. Aviation Med., 19:158-170, June 1948

153. Vinnikow, Y. A., "Structure and Function of the Vestibular Apparatus Under Conditions of an Altered Gravitational Field," NASA TT F-278, November 1964

154. Weaver, R. S., "Theoretical Aspects of the Role of Angular Acceleration in Vestibular Stimulation," Acta Oto-Laryng., Supp. 205, 1965

155. Weiss, A. D., Personal communication, May 1967

156. Wendt, G. R., "The Nature of Adaptation to Oscillatory Rotation," Symposium on the Role of the Vestibular Organs in Space Exploration, NASA SP-77, January 1965

157. Wersall, J., and Flock, A., "Physiological Aspects of the Structure of Vestibular End Organs," Acta Oto-Laryng., Supp. 192

158. Woellner, R. C., "The Perception of Vertical in the Presence of Increased Accelerative Forces," Bureau of Medicine and Surgery, Rept. No. 45, October 1957

159. Young, L. R., Meiry, J. L., Li, Y. T., "Control Engineering Approaches to Human Dynamic Space Orientation," Second Symposium on the Role of the Vestibular Organs in Space Exploration, NASA SP-115, January 1966

160. Young, L. R., "A Model for Linear Acceleration Effects on the Vestibular Nystagmus," Third Symposium on the Role of the Vestibular Organs in Space Exploration, January 1967

161. Young, L. R., and Meiry, J. L., "A Revised Dynamic Otolith Model," Third Symposium on the Role of the Vestibular Organs in Space Exploration, January 1967

162. Young, L. R., Stark, L., Taub, K., Taub, A., and Katona, P., "Biological Control Systems - A Critical Review and Evaluation," NASA CR-577, 1966

163. Young, L. R., and Li, Y. T., "Studies of Human Dynamic Space Orientation Using Techniques of Control Theory," Status Rept. on NASA Grant NsG-577, June 1966

164. Yuganov, Y. M., "The Problem of Functional Characteristics and Interaction of the Otolithic and Cupular Portions of the Vestibular Apparatus under Conditions of Altered Gravity," NASA TT F-368, Problems of Space Biology, USSR-1965

BIOGRAPHICAL SKETCH

Robert Wilson Steer, Jr., was born on April 1, 1939 in Haverhill, Massachusetts. He entered Merrimack College in North Andover, Massachusetts in 1956 and graduated Magna Cum Laude in 1960 with a B.S. in Electrical Engineering.

After graduation he joined the staff at the M.I.T. Instrumentation Laboratory and simultaneously worked toward a S.M. in Electrical Engineering at M.I.T. which he was awarded in January 1963.

From 1963 to 1964 he was a Sperry Rand Fellowship student, and from 1964 to 1965 he was a Teaching Assistant under Professor Yao Tzu Li in the Department of Aeronautics and Astronautics at M.I.T.

From 1965 to 1967 he has been a Research Assistant in the Man-Vehicle Control Laboratory where he carried out the research which generated this thesis.